STUDIES ON THE EFFECTS OF PERSISTENT RNA PRIMING ON DNA REPLICATION AND GENOMIC STABILITY

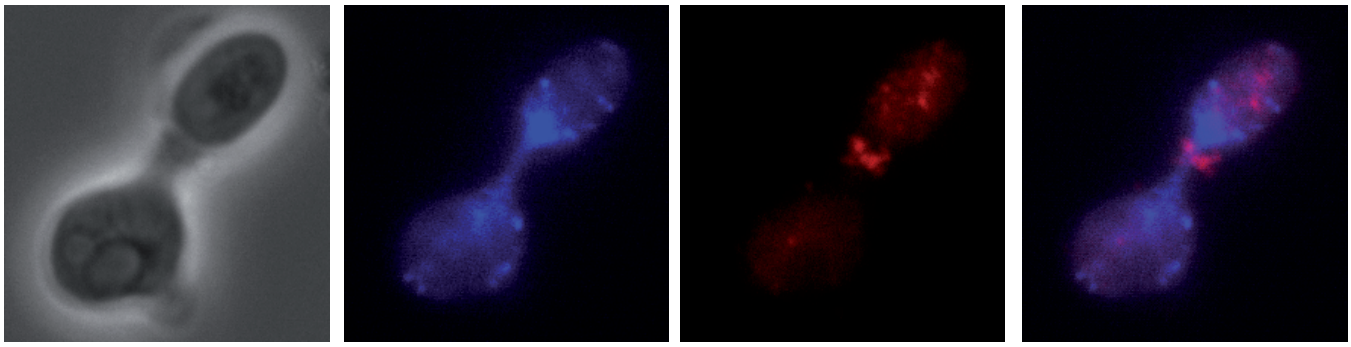

RUTH STUCKEY

June 2014

Tesis Doctoral
Universidad de Sevilla

STUDIES ON THE EFFECTS OF PERSISTENT RNA PRIMING ON DNA REPLICATION AND GENOMIC STABILITY

Trabajo realizado en el Departamento de Genética, Facultad de Biología, Universidad de Sevilla y en el Departamento de Biología Molecular, CABIMER, para optar al grado de Doctor en Biología por la Licenciada

RUTH STUCKEY.

SEVILLA, 2014

La doctoranda

Ruth Stuckey

El director de tesis

Ralf Erik Wellinger

SUMMARY

DNA replication and transcription take place on the same DNA template, and the correct interplay between these processes ensures faithful genome duplication. DNA replication must be highly coordinated with other cell cycle events, such as segregation of fully replicated DNA in order to maintain genomic integrity. Transcription generates RNA:DNA hybrids, transient intermediate structures that are degraded by the ribonuclease H (RNaseH) class of enzymes. RNA:DNA hybrids can form R-loops, three-stranded, thermodynamically stable forms of the RNA:DNA hybrid, which have been shown to challenge replication and genome integrity.

Replication is initiated during S phase from defined replication origins and requires the activity of specialized DNA "primases" to provide the RNA to prime DNA synthesis. However, it has been shown that RNA:DNA hybrids can function to initiate replication in bacteriophage T7, *E.coli* plasmids, or mitochondrial DNA, Here we describe, for the first time in a eukaryotic genome, the formation of replication intermediates that are indicative of RNA:DNA hybrid-mediated replication in the ribosomal DNA of *S. cerevisiae.* These unscheduled replication events were transcription dependent and induced by increased torsional stress due to the elimination of Top1 activity. We named this process "transcription-initiated replication" (TIR) and suggest that it may have important roles in genetic diseases and evolution.

By genetic dissection we demonstrate that cells lacking RNaseH activity depend on homologous recombination and post-replicative repair pathways in order to deal with the deleterious impact of R-loops. Special emphasis is given to the observation that the *MRC1*-complex, considered as a mediator of the replication checkpoint, is very important to tolerate the lack of RNaseH activities. Our data indicate that replication bypass of R-loops may rely on the Mrc1-dependent but Rad53-independent stabilization of replication forks, or suggest that the *MRC1*-complex has a yet to be defined role in genomic stability.

Finally, we show that R-loops constrain chromosome segregation and nucleolar organisation. As a consequence, the action of the phosphatase Cdc14 (a key player in mitotic exit) is constrained and accordingly, we observe a misregulation of B-type cyclins. Thereby, R-loops lead to premature entry into S-phase and promote apoptotic events.

The absence of RNaseH activity had previously been linked to embryonic lethality in mice lacking RNaseH1 activity, and the neurological disorder Aicardi-Goutieres syndrome (AGS) in humans lacking RNaseH2 activity. The findings presented in this thesis extend these observations and highlight the importance of proficient R-loop processing in genome stability and evolution.

RESUMEN

La replicación y la transcripción del ADN suceden al mismo tiempo y en la misma molécula de ADN de modo que su correcta interacción asegura la duplicación precisa del material genético. La replicación del ADN se debe también coordinar con otros eventos del ciclo celular, como la segregación de los cromosomas replicados para, de este modo, mantener la estabilidad del genoma. La transcripción forma híbridos de ARN:ADN, estructuras intermediarias transitorias que son degradadas por unas enzimas denominadas ribonucleasas H (RNasaH). Los "*R-loops*" de triple hebra son formas termodinámicamente estables de los híbridos de ARN:ADN cuya acumulación puede comprometer la replicación e integridad del genoma.

La replicación del ADN se inicia durante la fase S a partir de orígenes de replicación bien definidos y requiere la actividad de *primasas* especializadas para generar cebadores de ARN para la síntesis del ADN. No obstante en procariotas como el bacteriófago T7 o plásmidos de *E.coli*, y en el ADN mitocondrial, los híbridos ARN:ADN pueden iniciar replicación fuera del origen. En esta tesis, describimos por primera vez en un genoma eucariota la formación de intermediarios de replicación que indican una iniciación de replicación mediada por híbridos ARN:ADN en el ADN ribosómico de *S. cerevisiae*. Estos eventos de replicación no programadas son dependientes de la transcripción e inducidos por el aumento de estrés torsional como consecuencia de la eliminación de la actividad de Top1. Nombramos este proceso *replicación iniciada por transcripción* (TIR pos sus siglas en inglés) y sugerimos que estos eventos pueden ser altamente mutagénicos siendo de particular relevancia en enfermedades genéticas así como para la evolución.

Mediante análisis genético demostramos que las células que no poseen actividades RNasaH depende de las vías de reparación de daño en el ADN de la *recombinación homologa* y la

reparación post-replicativa para enfrentarse a los impactos perjudiciales de los *R-loops.* De particular importancia es el hecho que el complejo *MRC1,* un mediador del *checkpoint* replicativo, es fundamental para tolerar la falta de actividad de RNasaH. Nuestros datos indican que el "bypass" replicativo de los *R-loops* podría depender de la estabilidad de las horquillas de replicación mediada por Mrc1 pero independiente de Rad53 o puede apuntar a un papel novedoso y sin definir del complejo *MRC1.*

Por último, demonstramos que los *R-loops* provocan dificultades en la segregación de los cromosomas y la organización nucleolar. Como consecuencia, decrece la acción de la fosfatasa Cdc14 (un factor clave en la salida de mitosis) y, en concordancia, observamos un misregulación de las ciclinas de tipo B. Así, la acumulación de *R-loops* lleva a una entrada prematura en la fase S y promueven eventos apoptóticos. En estudios previos se ha relacionado la ausencia de la actividad RNasaH con mortalidad embrionaria en ratones que no poseen RNasaH1 y la enfermedad neurológica del síndrome de Aicardi-Goutières (AGS) en humanos que no poseen RNasaH2. Los hallazgos presentados en esta tesis amplían este conocimiento y destacan la importancia del procesamiento de los *R-loops* en la estabilidad del genoma y la evolución.

ACKNOWLEDGEMENTS

I´d like to express my gratitude to many special people for helping me achieve this thesis and for their support during my time spent both in- and outside of Cabimer.

First and foremost I would like to express my sincere gratitude to Ralf for all his guidance and wise words, for his continual patience, encouragement and never-ending scientific ideas.

To my surrogate mother, Mª Carmen (Vicky), for teaching me everything she knows. To Marta (Cristina), who has been my rock in so many ways…os quiero.

To Néstor, for accompanying me on adventures in the lab and in los jereles. To Román, for his constant good mood and entertainment. To "las burbujitas" Marina and Mª Jóse, I couldn't have got through the days without you. To Hayat and Migue, for keeping me company and keeping me sane. To "las madres" Ana and Macarena, for all the advice. To RW past and present – Julia (come back!), Elena, April, Nabila, Sergio and Eli. I must also thank Hélène for all her help over the years.

To my adoptive family los Clemente-Ruiz. And a huge thank-you to my "real" family, the Stuckeys. Thank you doesn´t seem sufficient to express my gratitude for everything you´ve done for me over the years, for your unconditional love and support, and for always believing in me. I truly owe you so much.

A mi jerezano favorito, Bito. Perdóname todas las noches que llegaba tarde a casa, todas las veces que estabas esperándome fuera en el coche, y los "tengo que pasar por Cabimer". Pero sobre todo, gracias por aguantarme y quererme…sin ti nada tiene sentido.

I´d like to dedicate this doctoral thesis to my son, Eidan.

This work was supported by a JAE-Predoc grant from CSIC.

"If you don´t ask, you don´t get".
Paul Vincent Stuckey

INDEX

1. ABBREVIATIONS

2D-gel	two-dimensional agarose gel electrophoresis
4NQO	4-nitroquinoline 1-oxide
AGS	Aicardi-Goutières syndrome
AID	auxin-inducible degron
ALF	a-like faker
AMP	ampicillin
APC/C	anaphase-promoting complex/cyclosome
ARS	autonomously replicating sequence
BER	base excision repair
BIR	break induced replication
CDK	cyclin dependent kinase
CPT	camptothecin
CSR	class switch recombination
DAPI	4´,6-diamidino-2-phenylindole
dCTP	deoxycytosine triphosphate
DNA	deoxyribonucleic acid
dNTPs	deoxyribonucleoside triphosphates
DSB	double-strand break
ERC	extrachromosomal rDNA circles
EtBr	ethidium bromide
FACS	fluorescence-activated cell sorting
FRDA	Friedrich´s ataxia
GCRs	gross chromosomal rearrangements
GEN	geniticin
GFP	green fluorescent protein
HR	homologous recombination
HU	hydroxyurea
HYG	hygromycin
IAA	indole acetic acid
Kb	kilobase

LOH	loss of heterozygosity
MCM	minichromosome maintenance complex
MMS	methyl methanosulphonate
mRNA	messenger RNA
mRNP	messenger ribonucleoprotein particles
NAT	nourseothricin (clonNAT)
NER	nucleotide excision repair
NHEJ	non-homologous end joining
OD	optical density
ORF	open reading frame
PCR	polymerase chain reaction
PFGE	pulsed-field gel electrophoresis
Pol	polymerase
pre-IC	pre-initiation complex
pre-RC	pre-replication complex
PRR	post-replication repair
rDNA	ribosomal DNA
RDR	recombination-dependent repair
RF	replication fork
RFB	replication fork barrier
RFP	replication fork pausing
RI	replication intermediate
RNA	ribonucleic acid
RNaseH	Ribonuclease H endonuclease
rNMP	ribonucleotide monophosphate
RNR	ribonucleotide reductase
rNTP	ribonucleoside triphosphates
ROS	reactive oxygen species
rRNA	ribosomal RNA
SCA1	spinocerebellar ataxia
SGD	*Saccharomyces* Genome Database
SSB	single-stranded DNA
TAR	transcription-associated recombination

TLS	translesion synthesis
TNR	trinucleotide repeat
Top1cc	Top1-DNA cleavage complex
tRNA	transfer RNA
UV	ultraviolet radiation
YFP	yellow fluorescent protein
WT	wild-type

2. LIST OF FIGURES AND TABLES

Materials & Methods

3. INTRODUCTION

DNA replication and the cell cycle

DNA replication is a highly regulated process responsible for the accurate duplication of a cell´s genetic material once per cell cycle, which is subsequently segregated into an identical daughter cell. The mechanisms controlling this process are described by the four stage cell cycle, in which the two major events of DNA replication (S phase) and chromosome segregation and cytokinesis (M phase), are separated by two gap phases, known as G1 and G2. In eukaryotes, DNA synthesis occurs during the S phase of the cell cycle.

DNA replication requires the action of DNA polymerases, to synthesize a new DNA strand complementary to the original template strand. This mechanism is conserved from prokaryotes to eukaryotes and is known as semi-conservative DNA replication. DNA replication initiation must be highly coordinated with other cell cycle events, including the repair of damaged DNA and segregation of fully replicated DNA to the daughter cell, to maintain genomic integrity.

Origins of replication and replication initiation

DNA replication is initiated at specific sites, known as origins of replication (*ori*), throughout the genome. Initiation from multiple origins allows eukaryotes to multiply their large chromosomes in an appropriate time (for a review see (1)). The yeast *Saccharomyces cerevisiae* (*S. cerevisiae*), a unicellular fungal eukaryote, has a genome of approximately 12.1Mb with over three hundred origins of replication, referred to as *a*utonomously *r*eplicating *s*equences (ARS), and a doubling time in rich media of approximately 90 minutes (2). ARSs consist of a short consensus sequence that acts as a site of recognition and assembly for the Origin of Replication Complex (ORC). The ORC is associated with the ARS throughout the cell cycle, and acts as a platform for sequential recruitment of the pre-replicative complex (pre-RC)

components Cdc6, Cdt1 and the Mcm2-7 helicase complex, a process known as replication licensing (Figure 1). Once the pre-RC is assembled, the Mcm2-7 helicase complex is activated by Cdc7 phosphorylation and can unwind DNA, converting the pre-RC into a pre-initiation complex (pre-IC) and the origin is fired. The activity of the major cyclin dependent kinase (CDK), Cdc28, directs the formation of pre-RCs. In G1 phase, Cdc28 activity is absent, permitting the formation of pre-RCs but these are not competent to fire (3). Cdc28 then blocks the formation of new pre-RCs until cells have passed through the G2 and M phases of the current cell cycle (4). This Cdc28 control acts to regulate replication initiation, ensuring that each origin is activated, or fired, just once per cell cycle.

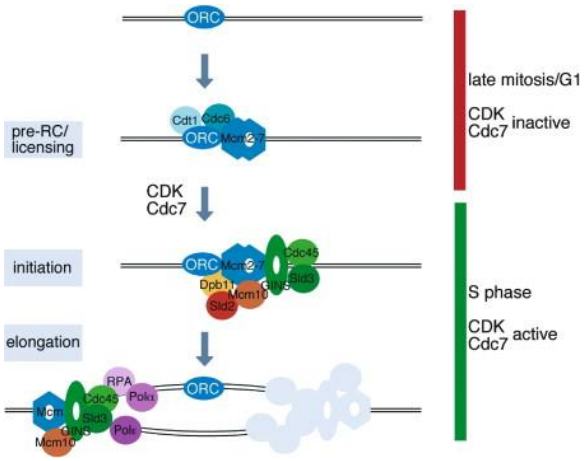

Figure 1. Schematic representation of origin firing. ORC is bound to replication origins throughout the cell cycle. During G1 phase of the cell cycle, Cdc6 binds to ORC-DNA. Cdc6 and Cdt1 bring MCM complexes to the origin, promoting the opening of the MCM ring, so it can encircle DNA. Cdc6 ATP hydrolysis promotes closing of the MCM ring and the release of Cdt1 and Cdc6. Orc1 ATP hydrolysis promotes release of ORC from the MCM2-7 complex. Cdc6 and Cdt1 are no longer required and are removed from the nucleus or degraded. Cdc7 phosphorylates MCM2-7 that can now slide on DNA, and MCMs (and associated proteins, GINS and Cdc45) unwind DNA to expose template DNA. At this point replisome assembly is completed and replication in initiated. Schematic taken from (5).

Replication priming

Following origin firing, the two strands are separated and factors required for DNA synthesis, such as the yeast replicative polymerases alpha (α), delta (δ) and epsilon (ε), now have access to the template DNA and can undertake DNA synthesis. However, the replicative polymerases

need a 3′-hydroxyl group to extend from and require the prior production of RNA primers by specialized polymerases known as primases. This necessity means that the replicative polymerases can only advance in a 5′ to 3′ direction along a template strand. As such, the leading strand is synthesized in the same direction as the movement of the *r*eplication *f*ork (RF) in a continuous manner, by DNA Polymerase (DNA Pol) ε (6). The lagging strand, however, is synthesized in the opposite direction to the movement of the RF as discrete segments of replicated DNA, known as Okazaki fragments of approximately 150 nucleotides in eukaryotic cells (Figure 2). The primase synthesizes an RNA primer, of approximately 10-12 nucleotides, and DNA Polα then adds some 20 nucleotides of DNA, allowing the lagging strand polymerase DNA Polδ to extend from the primers formed and produce an Okazaki fragment. The RNA primers must subsequently be removed before the fragments of replicated DNA can be joined by the action of DNA ligase into a continuous fully replicated complementary strand.

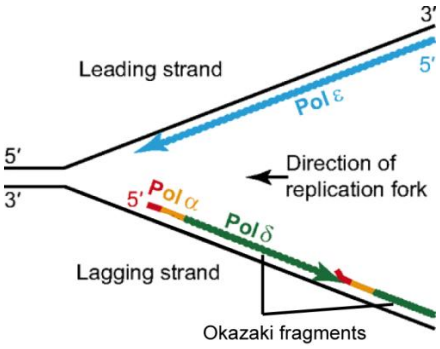

Figure 2. Schematic representation of a replication fork. . DNA Polε (blue) synthesizes the leading strand in the 5′to 3′direction in a continuous manner. For the lagging strand, DNA Polα-primase first synthesizes an RNA fragment of about 10 nt (red) and then extends that with 20–30 nt of DNA (orange). DNA Polδ extends the primer to a length of 200–300 nucleotides (green) until it reaches the already synthesized fragment downstream. Joining of the Okazaki fragments involves additional enzymes, such as FEN1 and DNA ligase. Adapted from (7).

RNA:DNA hybrids

RNA:DNA hybrids are frequently occurring intermediate structures, formed by base pairing between a ssDNA and its complementary RNA strand. Such hybrids exist transiently during normal replication, as part of the primers for DNA synthesis (as Okazaki fragments), and are

also formed during telomere elongation and transcription. For example, during transcription, the two strands of the DNA double helix are separated to form a transcription bubble and the synthesizing RNA forms a short-lived RNA:DNA hybrid of 8bp with the template DNA strand, leaving the non-template DNA to loop out as single-stranded DNA behind the elongating RNA polymerase (8). Under normal conditions this hybrid is a temporary structure and the RNA transcript is removed and further processed and packaged into a ribonucleoprotein particle. However, in some cases the nascent RNA can reanneal to its DNA complement, and form an R-loop (Figure 3). R-loops are a three-stranded, thermodynamically stable form of the RNA:DNA hybrid, formed by base pairing between the hybrid and the displaced ssDNA strand. Certain conditions can favour the formation of R-loops. For instance, negatively supercoiled DNA (9) and G-rich sequences (10) are more prone to form R-loops since both facilitate the opening up of the DNA double helix.

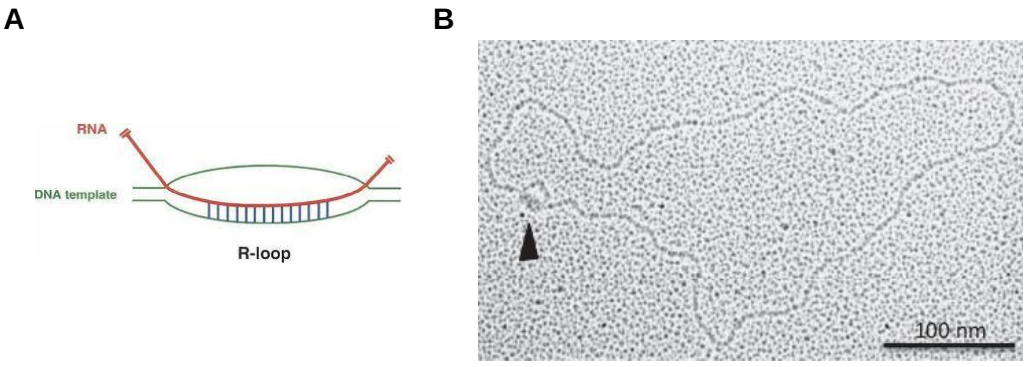

Figure 3. Schematic (A.) and electron micrograph (B.) of an R- loop. Electron micrograph taken from (11). R-loop is indicated by arrowhead.

RNaseH enzymes

Ribonuclease H endonucleases (RNaseH) specifically hydrolyze the RNA moiety when annealed to a complementary DNA. All living organisms possess at least one RNaseH activity to remove RNA:DNA hybrids (reviewed in (12)). *S. cerevisiae* possess two RNaseHs: the monomer Rnh1 (encoded by *RNH1*) and the heterotrimeric protein complex Rnh2 (formed by the gene

products of *RNH201,* the catalytic subunit, and *RNH202* and *RNH203* accessory subunits) (13). Although they seem to have some overlapping functions, Rnh1 specifically recognises RNA:DNA hybrids with stretches of 4 or more consecutive ribonucleotides (rNMPs), whereas Rnh2 can remove hybrids and has an additional activity capable of removing rNMPs covalently attached to DNA, such as those misincorporated into DNA during replication of the genome (14). For instance, DNA Polα lacks 3´-5´exonuclease proofreading activity and includes an average of 1 rNTP per 625 bases of replicated DNA (15).

What happens if R-loops are not removed?

Persistent R-loops have been linked to various forms of genomic instability (for a review see (16)) and may be lethal if not resolved. The looped out ssDNA of the R-loop structure is exposed and more susceptible to damage than dsDNA. For this reason, R-loops have been referred to as "fragile" sites, since they are more likely to suffer base lesions, such as deamination (17), which may lead to mutations or strand breaks (18); R-loop forming regions have also been linked to hyper-recombination (19,20).

Mutations in genes that are involved in the packaging of nascent RNA into a ribonucleoprotein particle increase the likelihood of R-loop formation (21,22), and include genes with roles in transcription and RNA processing and export, such as THO/TREX (19), and the ASF/SF2 splicing factor (20). Mutations in these genes are associated with transcription-dependent genomic instability phenotypes, such as transcription-associated recombination (TAR) (23), and such instability can be suppressed by the overexpression of Rnh1 (19,21), demonstrating that the instability is due to the presence of RNA:DNA hybrids. Furthermore, the R-loop structures themselves may hinder DNA metabolism, blocking transcription elongation (24) or RF progression (25,26).

R-loops have been associated with the instability of trinucleotide repeat (TNR) sequences (27,28). Their formation has been demonstrated *in vitro* at the disease-associated TNR $(CAG)_n$,

(28) in spinocerebellar ataxia disease (SCA1), and $(GAA)_n$, in Friedrich´s ataxia (FRDA) (11), and thus R-loops have been linked to these and other TNR diseases, including myotonic dystrophy (DM1) and fragile X type A (FRAXA) (11,28).

Despite their detrimental consequences to genomic stability, R-loop structures also play some important physiological roles. For instance, they promote transcription termination of RNA PolII genes, such as the human β-actin gene (29), and aid class switch recombination (CSR) of immunoglobulin (Ig) genes, responsible for the diversification of Ig isotypes in mammalian B lymphocytes (30). The looped out ssDNA of the R-loop at the highly repetitive switch regions is specifically attacked by activation-induced cytidine deaminase (AID), an enzyme that deaminates cytidine residues (31), and leads to the formation of DSBs (32) necessary for CSR to take place.

There is also growing evidence associating R-loops with epigenetic modifications and control of gene expression. For example, R-loops may protect against DNA methylation and have been shown to form at CpG islands (CGI) in gene promoters (33). Interestingly, AID-mediated demethylation of DNA has been shown to be important for epigenetic reprogramming of mammalian cells (reviewed in (34)) and linked to the pluripotency of stem cells (15,35). Furthermore, R-loops may favour chromatin accessibility through a reduced affinity for histones (36) and recently, R-loop formation has also been shown to trigger histone 3 S10 phosphorylation (H3S10P) and linked to chromatin compaction (37).

RNA:DNA hybrid-primed replication

In eukaryotes, DNA Polα and its´ intrinsic primase activity initiates RNA-primed DNA synthesis. However, in the case of prokaryotic and mitochondrial DNA, RNA Pol transcripts existing as stable R-loops can function as primers for the extension of DNA synthesis. For example, R-loops can function as origins of replication for T4 and T7 bacteriophages (38), and for ColE1-type plasmids in *E.coli* (39), where replication is sensitive to rifampcin, an RNA Pol inhibitor.

Mitochondrial DNA is a good example of a transcription-primed DNA replication mechanism (for a review see (40)). Replication origins in mtDNA are highly conserved from yeast to humans and consist of a promoter for the initiation of transcription by RNA Pol and a high GC content downstream. In the case of mammalian mtDNA, transcription from the light-strand promoter (LSP) opens up the heavy-strand origin (O_H) (41) and produces a stable and persistent RNA:DNA hybrid (42) (Figure 4), that once processed, can be used as a primer for extension by DNA Polγ (43).

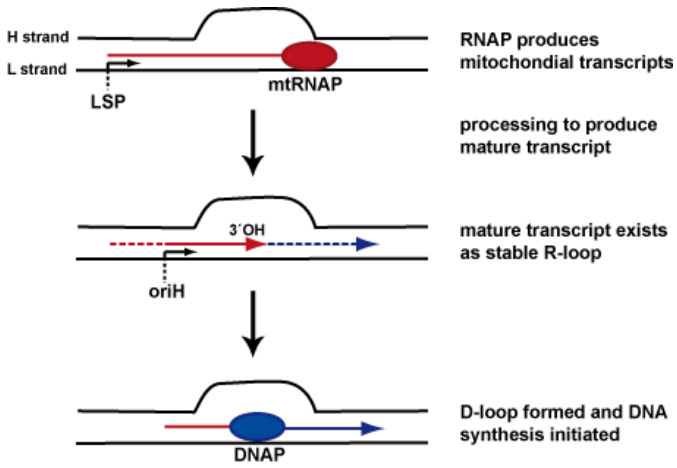

Figure 4. Schematic representation of mtDNA replication, as an example of transcription-primed DNA replication. Transcription from the light-strand promoter creates an RNA:DNA hybrid, which acts as a primer for the initiation of DNA replication of the mitochondrial genome.

Apart from RNA:DNA-primed replication, transcription has also been shown to bypass the need for replication initiation factors in *E.coli* (44). Under normal conditions, *E.coli* chromosomal DNA replication is initiated from one specific origin (*oriC*), whose opening up is essential for the assembly of the replisomes and depends on the replication initiation factor DnaA. However, mutants capable of initiating constitutive stable DNA replication in the absence of DnaA were identified (44) and the mutation was mapped to the RNH locus (*rnhA*) (45). *oriC* independent replication was transcription-dependent suggesting that stabilized R-loops provided access for factors needed for replication initiation. Importantly, *rnhA* mutants

cannot bypass the growth defect of primase deficient *dnaG* mutants (46), indicating that replication has to initiate from a primase generated RNA primer.

Importance of RNA:DNA hybrid removal by RNase H enzymes

The RNaseH enzymes specifically remove RNA:DNA hybrids. Eukaryotic RNases H1 and H2 are important participants in maintaining genome stability by resolving R-loops that form during transcription, and in the case of RNase H2, by initiating the removal of rNMPs in DNA, making an excision on the 5′ side of the rNMP. Misincorporated rNTPs must be removed by DNA repair pathways, since they are more mutagenic than mispaired dNTPs due to the reactive hydroxyl 2′group on the ribose ring (47), and their presence in the template strand can cause the RF to stall *in vitro* (6,48) and sensitize the DNA backbone to spontaneous breaks (49).

The importance of RNaseH activity is exemplified by the fact that deletion of RNaseH1 in drosophila and mice results in embryonic lethality due to the inability to amplify mitochondrial DNA (mtDNA) (50). Furthermore, deletion of RNaseH2B in mice causes embryonic lethality with an observed accumulation of single ribonucleotides in the DNA (51). Mutation in any of the subunits of the human Rnh2 complex can lead to Aicardi-Goutieres syndrome (AGS) (52), a severe but rare autosomal recessive neurological disorder (Figure 5). Patients manifest basal ganglia calcification, cerebral atrophy (loss of tissue), chronic cerebrospinal fluid lymphocytosis (increase of lymphocytes in the cerebrospinal fluid), and characteristic chilblains of fingers, toes and ears. AGS can also be caused by mutations in other enzymes with roles in the removal of nucleic acid species, such as SAMHD1 that reduces dNTP pools and TREX1 (53), a 3′ to 5′ DNA exonuclease, deletion of which leads to the accumulation of fragments of ssDNA of 60-65bp in the endoplasmic reticulum (ER). The accumulation of nucleic acids can trigger the inappropriate activation of the innate immune system (IFNα response) (for a review see (54)), with the body responding as if to a viral infection, and many of the clinical features of AGS parallel those for a viral infection.

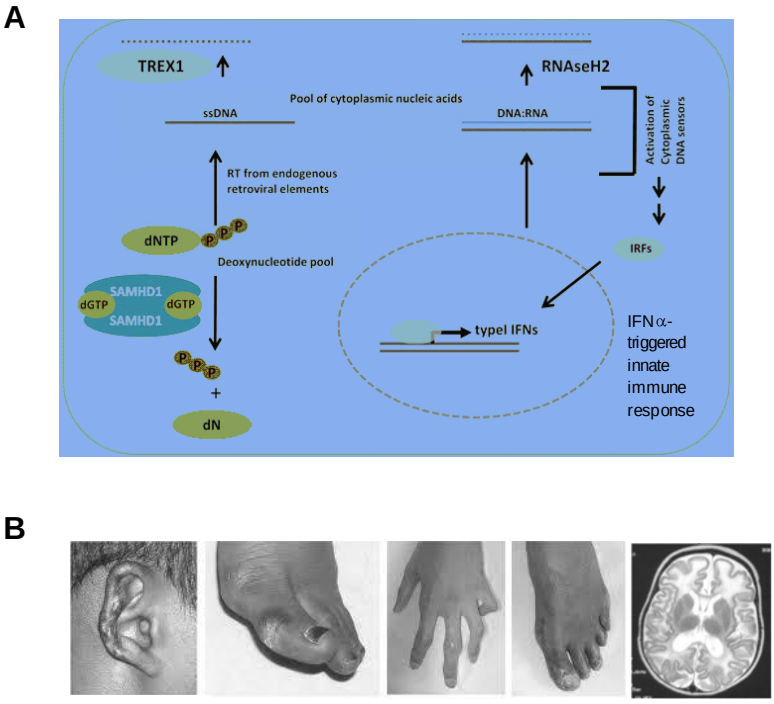

Figure 5. Mutations in nucleic acid removing enzymes can cause Aicardi-Goutieres syndrome. A. Loss of AGS-related protein activity leads to nucleic acid accumulation, which triggers an innate immune response. TREX1 – human exonuclease; degrades ss- and dsDNA. SAMHD1 – converts dNTP to a nucleoside and a triphosphate. Schematic adapted from (55)**. B.** Characteristic phenotypes of AGS patients include chilblains of the ears, toes and fingers (photos taken from www.aicardi-goutieres.org.), and calcification of the basal ganglia. The MRI scan shows rarified white matter, characteristic of neonatal AGS (56).

Other means of removing RNA:DNA hybrids

Since R-loops are a threat to genomic integrity, bacteria and eukaryotic cells possess different mechanisms to prevent the formation of R-loops (Figure 6). Yeast *RNH* double deletion mutants are viable, indicating that cells have other means of processing RNA:DNA hybrids. These may include helicases such as the yeast (and mammalian) Pif1, which has been shown to unwind RNA:DNA hybrids *in vitro* (57), and the yeast Sen1 (known as Senataxin in mammals), whose absence has been shown to result in an accumulation of RNA:DNA hybrids downstream of the poly(A) signal (58).

Figure 6. Schematic of RNA:DNA hybrid removal/avoidance mechanisms in yeast.

Additionally, R-loop formation is promoted when genes are transcribed at high rates (59): with the introduction of positive supercoiling ahead of, and negative supercoiling behind the passing transcriptional machinery. As previously mentioned, negatively supercoiled DNA is more prone to R-loop formation because nascent RNA can anneal to the underwound DNA. Such supercoiling is resolved by the type 1B topoisomerase (Top1), which plays an important role in preventing the formation of RNA:DNA hybrids during transcription. In *E.coli* the lack of Top1 results in R-loop formation (59), and in yeast the combination of loss of Top1 and RNaseH functions leads to a hyper-accumulation of R-loops and subsequent lethality (60).

Topoisomerase 1 activity and inhibitors

Topoisomerases (Top) are important enzymes found in both prokaryotes and eukaryotes, which act to relieve the torsional stress of nuclear and mitochondrial DNA (for a recent review see (61)). Torsional stress is introduced by repair, replication and transcription machineries, and Top1-type topoisomerases relax supercoiling by transiently nicking the DNA, staying covalently bound, and enable the broken strand to rotate (61). In this manner the stress on the helical backbone is released and the covalent phosphodiester bond is reformed. In the absence of Rnh2 and when transcription rates are high, an alternative mechanism can act to remove rNMPs from the DNA, which requires the activity of Top1. However, the Top1-dependent back-up pathway is not particularly efficient, since in the absence of Rnh2 many rNMPs still remain, and is a mutagenic process, introducing short deletions of 2-5bp (14). For these reasons, the removal of misincorporated rNMPs is not believed to be the normal function of Top1.

Incomplete Top1 action has been shown to be a natural source of DNA damage, such as DNA single strand breaks (SSBs), which can be converted to DSBs during replication (62). Camptothecin (CPT) is a Top1 specific inhibitor that acts by trapping the Top1 after nick formation on the DNA as a cleavage complex (Top1cc; Figure 7A), binding at the Top1-DNA interface, and thus impedes religation of the nick (Figure 7B) (63). Water-soluble derivatives of CPT are commonly employed as anti-tumour drugs, such as topotecan for the treatment of ovarian cancer (64).

The CPT sequestered, covalently bound, 90kDa Top1 must be removed from the 3´ end before the DSB can be repaired and replication resumed. Specialized enzymes, such as the tyrosyl-DNA phosphodiesterase, Tdp1 (65), as well as the Rad1-Rad10 and Mus81 endonucleases (66), can remove Top1cc. In addition, the homologous recombination machinery has been reported to be involved in the repair of Top1-mediated lesions (67).

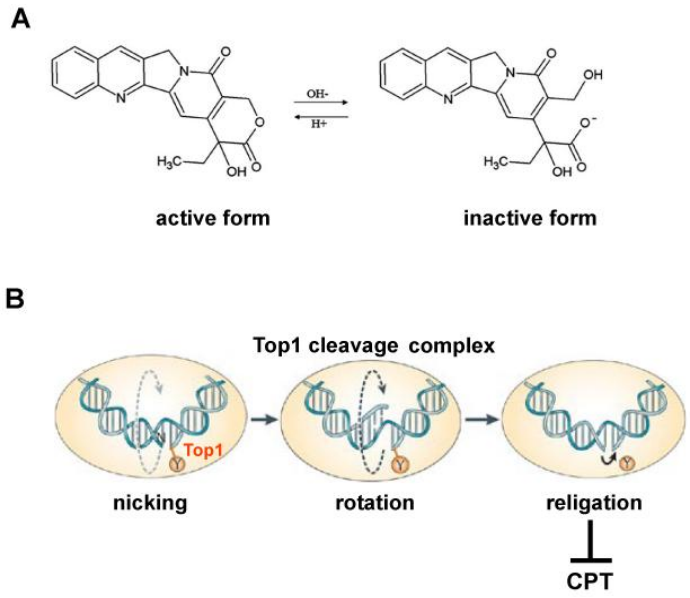

Figure 7. Camptothecin (CPT) is a Top1 specific inhibitor. A. Molecular structure of CPT. The lactone ring in CPT is important for the drug's biological activity, active as a "closed" α-hydroxylactone form and inactive as the "open" carboxylate form. The lactone ring can rapidly open at physiological (or higher) pH. **B.** Schematic of CPT mode of action. Under normal conditions, the covalent Top1cc, formed in the action of nicking, are short-lived and reversible. However, under some circumstances, such as upon treatment with CPT and deriviatives, the Top1cc is stabilized and the ligation stage is impaired, leading to the introduction of a SSB. Adapted from (64).

Organisation of Ribosomal DNA

The ribosomal DNA (rDNA) is compartmentalized within the nucleolus, a crescent-shaped sub-compartment of the nucleus (Figure 8A), which is the site of rDNA transcription and ribosome assembly, essential processes for the cell since cell growth is directly dependent on the rate of protein synthesis (68). Top1 is enriched at the nucleolus (69), and Top1´s activity at this site is particularly important to relieve torsional stress, since rDNA transcription by RNA PolI can account for approximately 80% of the total transcription in yeast (68). The highly transcribed rDNA is more prone to RNA:DNA hybrid formation, and accordingly R-loop formation in the rDNA have been shown to be enhanced in *top1* mutants in yeast (60).

The ribosomal locus of *S. cerevisiae* consists of a single array of 150-200 copies of a 9.1kb repeat unit located in the middle of chromosome XII (Figure 8B). In contrast to yeast, the rDNA repeats of higher eukaryotes are located in multiple nucleolar organizing regions (NORs). One yeast repeat unit consists of the RNA PolI transcribed 35S gene that encodes the 35S precursor rRNA, which is processed into the mature 18S, 5.8S and 26S rRNAs, and the RNA PolIII transcribed (in opposite direction) 5S gene, respectively. Two non-transcribed intergenic spacers (NTS1 and NTS2) separate the 35S and 5S rRNA sequences. The NTS regions contain *cis*-regulatory elements for the control of DNA replication, which include a *r*eplication *f*ork *b*arrier (RFB) and an origin of replication (ARS), respectively (for a review of the rDNA organisation, see (70)). The RFB is polar, allowing RFs to pass if moving in the same direction as transcription of the 35S gene, but blocks over 90% of advancing forks from opposing direction (71). RFBs appear to be a highly conserved feature of rDNAs, confirmed in a number of other organisms, including humans (72).

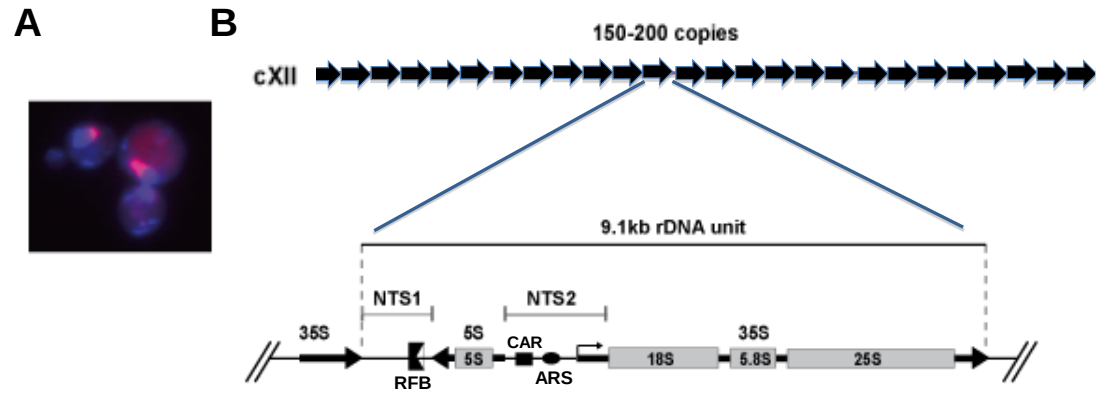

Figure 8. A. Fluorescent microscopy image to show the nucleolus. The nucleolus is seen in red (Nop1-mRFP), and the nucleus in blue (DAPI stain). **B.** Schematic representation of the rDNA locus of *S.cerevisiae*. A single rDNA unit measures 9.1kb and contains two transcribed genes – 35S transcribed by Pol I, processed to mature 18S, 5.8S and 25S species, and 5S by Pol III. NTS, non-transcribed spacer; RFB, replication fork barrier; ARS, origin of replication; CAR, cohesion attachment region.

In addition, each rDNA repeat contains a cohesion attachment region (CAR) located proximal to the 5S gene in the NTS2 (73). Cohesion is an evolutionarily conserved complex that contains several members of the Smc (structural maintenance of chromosomes) family. The association of cohesion is thought to hold sister chromatids together during S phase, to regulate recombination between repeats, until their controlled separation and segregation during mitosis (74). Smc proteins are also found in condensin complexes, and there is an intimate relationship between cohesin and condensin functions (cohesin and condensin are reviewed in (74)), both of which are important for the correct segregation of the rDNA array (75). The presence of cohesion within the tandem repeated rDNA array may limit the template available for recombinational repair of a DNA break (73) and therefore is important for maintaining rDNA repeat stability (75).

The replication-transcription conflict

The polarity of the ribosomal RFB allows the replication and transcription machineries to move in the same direction. However, in other regions of the genome, this is not the case such that replication and transcription machineries can collide (76,77) leading to RF stalling or

arrest (reviewed in (78,79)). It has been suggested that head-on collisions are more detrimental than co-directional collisions (80), and consequently, highly expressed genes tend to be transcribed with the same polarity as RF progression (71,81). For example, RFs were shown to pause at tRNA genes when the direction of transcription was opposite to the direction of RF progression (82). Therefore, eukaryotes have evolved mechanisms to help prevent head-on collisions (for a recent review see (83)), explaining the presence of RFBs in the highly transcribed rDNA (71).

Pathways that resolve constrained replication

In addition to transcription-induced impediments, the RF must deal with other DNA-bound proteins, secondary structures, and frequently occurring DNA lesions caused by various exogenous and endogenous sources, which can cause RF stalling. Blocks to replication can lead to RF collapse if not resolved and result in DNA strand breaks. As such, a plethora of repair factors and pathways exist to remove DNA lesions and facilitate RF progression, in order to maintain genomic integrity. The choice of which repair system to use depends on both the type of lesion and on the cell-cycle phase (reviewed in (84)).

Continuously produced *r*eactive *o*xygen *s*pecies (ROS), a by-product of normal cellular metabolism, can modify bases by oxidation, and such oxidative base lesions can block the progress of DNA and RNA polymerases (85,86). The *B*ase *E*xcision *R*epair (BER) pathway acts to repair damage to individual bases, including methylation, deamination and depurination/depyrimidation (for a review of BER see (87)). In contrast, *N*ucleotide *E*xcision *R*epair (NER) acts to remove bulky DNA adducts that cause a structural deformation of the DNA helix, such as DNA intrastrand and interstrand crosslinks, and pyrimidine dimers that can be produced by *u*ltra*v*iolet (UV) radiation (for a review of NER see (88)). A specific sub-pathway of NER can repair lesions that impede RNA Pol progression through transcribed

genes. A stalled RNA Pol at the lesion, for example helix-distorting lesions, appears to be the signal for *T*ranscription-*c*oupled *r*epair (TC-NER) (reviewed in (89)).

However, the most commonly formed lesions resulting from stalled or collapsed RFs are *d*ouble-*s*trand *b*reaks (DSBs). The two major pathways for repair of DSBs are *n*on-*h*omologous *e*nd *j*oining (NHEJ) and *h*omologous *r*ecombination (HR). NHEJ is error-prone, ligating together the broken DNA ends with little or no homology, often resulting in loss or gain of sequence at the site of repair (reviewed in (90)), while HR repairs the DSB with high fidelity, using the sister chromatid or homologous chromosome as template. NHEJ has been shown to be active throughout the cell cycle, although it is particularly active in G1 (91), whereas HR is restricted to the S and G2 phases, when the sister chromatid is available to act as the template for this mode of repair (reviewed in (92)).

The Mre11/Rad50/ Xrs2 (MRX) complex functions in both HR and NHEJ, where Rad50 holds DSB ends together to favour NHEJ (93). In yeast, HR is initiated with processing of the ends of the break by the MRX complex to generate 3′-ssDNA. Rad51 then searches for the homologous sequence and facilitates strand invasion of the ssDNA at the homologous sequence, allowing the DNA Pol to extend the 3´ end using the homologous sequence as a template.

There are at several different mechanisms of homologous recombination that can be used to repair a chromosomal DSB in yeast cells, including *d*ouble *s*trand *b*reak *r*epair (DSBR), *s*ynthesis-*d*ependent *s*trand *a*nnealing (SDSA), *s*ingle-*s*trand *a*nnealing (SSA) and *b*reak-*i*nduced *r*eplication (BIR) (see Figure 9) (reviewed in (94)).

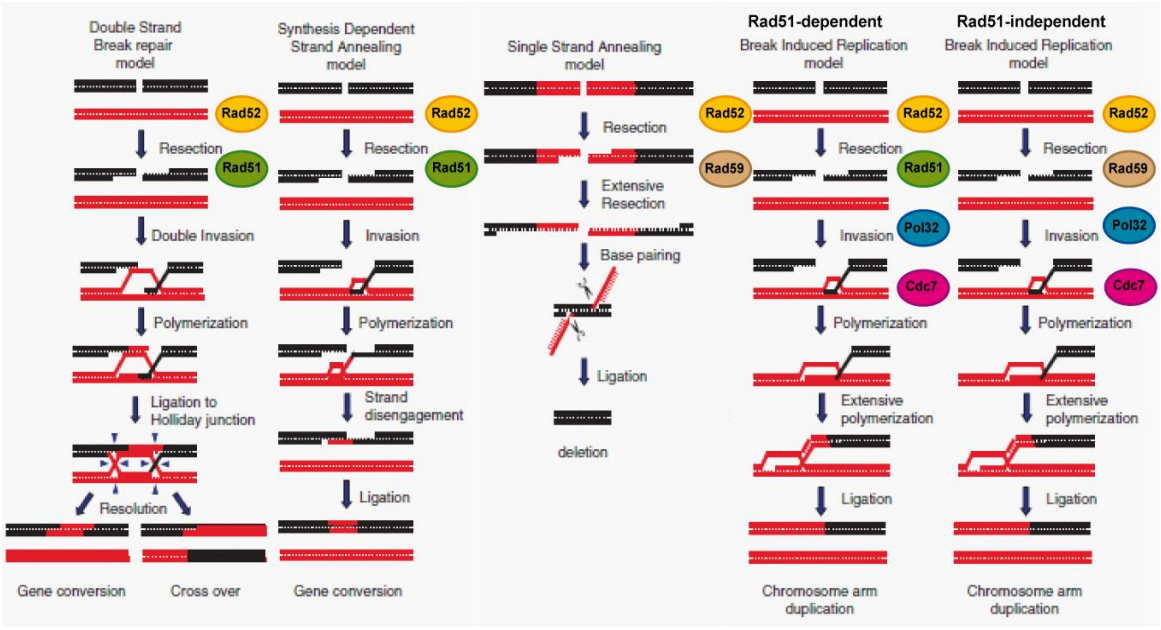

Figure 9. . Recombinational repair pathways. Schematic highlighting key factors in double-strand break repair (DSBR), synthesis-dependent strand annealing (SDSA), single-strand annealing (SSA) and break-induced replication (BIR) homology-dependent recombinational repair pathways. Adapted from (34).

Eukaryotic cells also possess two damage tolerance mechanisms that depend on the activities of Rad6 and Rad18 to allow the RF to by-pass blocking lesions (95,96). Damage tolerance can be mediated by the error-prone TLS, where a specialized polymerase can replicate across the DNA lesion (97), or the error-free Rad5-dependent pathway, that uses the undamaged sister chromatid via template switching (98) to re-prime replication downstream of the lesion. The deletion of both template switch and TLS pathways were shown to be essential to tolerate misincorporated rNMPs in the DNA of yeast lacking RNaseH activity upon replicative stress (99).

Cell cycle checkpoints

Surveillance mechanisms known as checkpoints exist, which act to detect problems that may arise during eukaryotic DNA replication and respond by eliciting a signalling cascade (100). Checkpoints contain sensor proteins that can detect stretches of ssDNA, an indication of stalled forks or DNA damage, incorrect attachment of sister chromatids to the mitotic spindle, cell size,

or cellular conditions such as protein and nutrient levels. Depending on the stimulus, the checkpoint can activate signal transducers, protein kinases that transmit the checkpoint signal to induce the expression of specific downstream target genes that act to maintain the stability of the RF and/or facilitate repair, in the case of damage (101), and in all cases, delay cell cycle progression to allow time for the problems to be resolved (100). Loss of checkpoint function results in genomic instability (102) and has been implicated in the evolution of normal cells into cancer cells (103,104).

In *S. cerevisiae* there are three checkpoint pathways that recognize the presence of damaged DNA at the G1/S transition, during the S-phase (Intra-S), and at the G2/M cell cycle phases (see Figure 10). The G1/S cell cycle checkpoint, also known in yeast as START (for a review see (105)), ensures there is no damaged DNA before transition into S phase (106). Additionally, START acts as a decision point to confirm that all conditions required for DNA synthesis, including a minimum cell size and sufficient nutrient and enzyme levels, before committing to a cell division cycle. Alternatively, cells arrest at START and enter a resting state called G0.

The S-phase checkpoint senses both DNA damage and replication stress, caused by stalled or broken RFs, which result in stretches of ssDNA (for a review see (107)). The Mec1 checkpoint sensor is recruited to the RPA-bound ssDNA and activates the downstream effector kinases that include Rad9 and Mrc1 ((108) and (109), respectively). The phosphorylation of either Mrc1 or Rad9 recruits and activates Rad53 (110). In addition to *RAD9*, the checkpoint genes *RAD17* and *RAD24* are also required for the intra-S and G2/M damage checkpoints and function upstream of Rad53. Rad53 activation stabilizes the RF (111), induces damage-responsive genes via its downstream paralogue kinase Dun1 (112), and slows down DNA replication, by the inhibition of late origin firing (113).

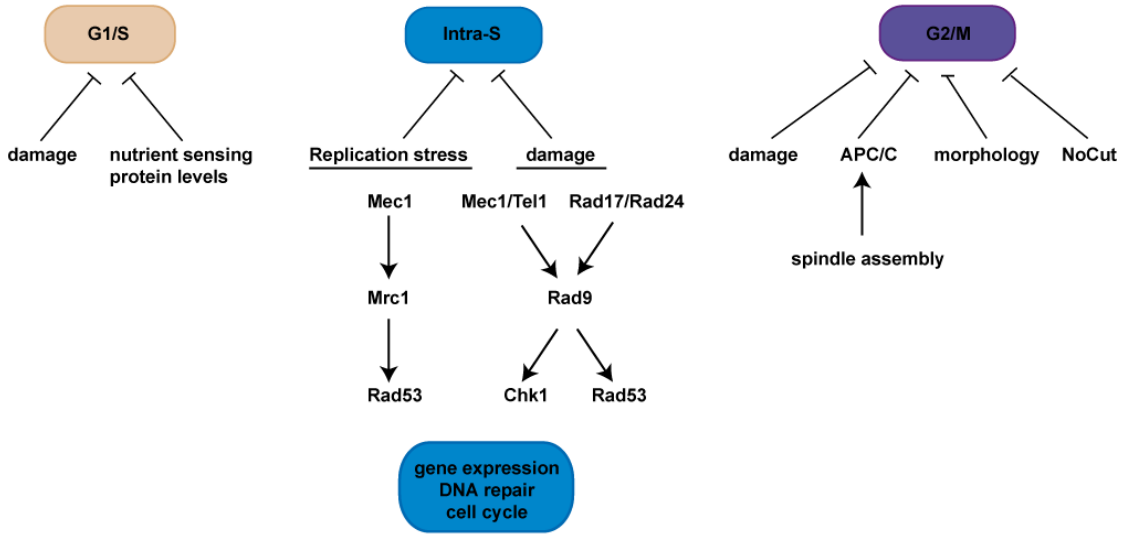

Figure 10. The G1/S, intra-S, and G2/M checkpoint responses. Schematic representation of the key factors involved in the checkpoint pathways.

Any unrepaired damage in the newly synthesized DNA will trigger the G2/M damage checkpoint, which prevents cells from entering mitosis until the DNA damage has been resolved, to prevent the segregation of damaged chromosomes (114). Other G2/M checkpoints include the morphogenesis checkpoint, which delays cells at the G2/M transition in response to problems that delay bud formation (115), and the *s*pindle-*a*ssembly *c*heckpoint (SAC) that monitors attachment of replicated chromatids to the microtubules to achieve spindle connection (for a review see (116)). SAC activation achieves G2/M arrest by inhibiting the *a*naphase *p*romoting *c*omplex/*c*yclosome (APC/C) specificity factor Cdc20, delaying exit from mitosis [22]. The APC/C is an E3 ubiquitin ligase that regulates the metaphase/anaphase transition through the ubiquitin-mediated proteolysis of various substrates (117), including mitotic cyclins and the sister chromatid separation inhibitor securin/Pds1 (118). When the kinetochores are attached to microtubules the APC/C^{Cdc20} ubiquitinates securin and cyclin B and thereby activates the protease separase and inactivates the cyclin-dependent kinase-1 (Cdk1). Separase can cleave the cohesin complexes that are holding sister chromatids together and separate sister chromatids. The activated SAC inhibits the capability of APC/C^{Cdc20} to ubiquitinate securin and cyclin B and thereby prevent anaphase and mitotic exit. As such, the

SAC ensures a correct chromosome segregation and is a key mechanism to prevent aneuploidy, a contributory factor of cancer (119).

4. OBJECTIVES

RNA:DNA hybrids are transient structures generated during DNA replication, transcription and telomere elongation and can lead to R-loop formation. R-loops may physically interfere with transcription elongation (24) or cause replication fork blockage (25,26). As such, persistent R-loops are detrimental to the cell and have been linked to various forms of genomic instability (for a review see (16)). All eukaryotes and bacteria possess at least one enzymatic activity to specifically remove RNA:DNA hybrids. The human disease AGS and embryonic lethality in mouse (and *Drosophila*) caused by the lack of RNaseH2 and RNaseH1 respectively, demonstrate the important contributions of the RNaseH enzymes to global DNA metabolism (50,52). Furthermore, recent studies have shown that R-loops are linked to disease-associated alterations in trinucleotide repeat sequences, supporting the need for further investigation of the cellular roles of the RNaseHs and the consequences when their activity is compromised.

Using *Saccharomyces cerevisiae* as a model organism, this thesis aims to explore the contributions of RNaseH activity to faithful DNA replication, genomic stability and cell cycle control.

The objectives of this thesis are:

1. To categorize the replication/recombination intermediates formed in RNaseH$^-$ cells.

2. To identify factors and pathways, that interact with RNaseH enzymes by genetic analyses.

3. To dissect the impact of R-loop formation on cell cycle progression.

5. RESULTS

CHAPTER 1 - Transcription-initiated DNA Replication in Yeast

Yeast lacking RNaseH activity are sensitive to the Top1 inhibitor CPT

The yeast *S. cerevisiae* possess two RNaseH activities, Rnh1 and Rnh2, which can act to remove RNA:DNA hybrids and have been suggested to have some redundancy in functions (120). Deletion of the *RNH201* gene, coding for the catalytic subunit of Rnh2, eliminates yeast Rnh2 activity, and deletion of both *RNH1* and *RNH201* abolishes all RNaseH activity in yeast cells. Double mutants *rnh1Δ rnh201Δ* (referred to herein as *rnh1Δ rnh2Δ*) are viable, suggesting that this activity in dispensable for viability or that yeast have other means of removing RNA:DNA hybrids. However, yeast cells lacking RNaseH activity have been shown to be more sensitive to the DNA damaging agent *e*thy*m*ethyl*s*ulfanate (EMS), the checkpoint inhibitor caffeine and the ribonucleotide reductase inhibitor *h*ydroxy*u*rea (HU) (120). To confirm and extend these observations, we performed drop test analyses using HU; the DNA alkylating agent *m*ethyl *m*ethane*s*ulphonate (MMS); and the Topoisomerase 1 (Top1) specific inhibitor *c*am*p*to*t*hecin (CPT; Figure 11A). Cells lacking either RNaseH activity were not sensitive to genotoxic agents, but we noted that the *rnh1Δ rnh2Δ* double mutant became hypersensitive to HU, MMS, and CPT; suggesting that although each RNaseH enzyme has a specialized role, they can substitute for each other (Figures 11A and B). We found the CPT sensitivity of the *rnh1Δ rnh2Δ* double mutant particularly interesting, because *rnh1Δ rnh2Δ* has been shown to be synthetic lethal in the absence of the CPT target, Top1 (60). Top1 is crucial during transcription to relieve the accumulation of torsional stress associated with the formation of negative supercoils behind the transcription machinery (121). Negative supercoils in the DNA can enhance RNA:DNA hybrid formation (59), and consequently Top1 plays an important role in preventing R-loop formation. CPT sequesters Top1 via the formation of a covalently bound Top1 *c*leavage *c*omplex (Top1cc) Top1-DNA complex (reviewed in (122)), so that it cannot act elsewhere in

the genome, analogous to a depletion of Top1. A recent report of Marinello *et al.* has shown that CPT treatment of human cells leads to an increase in R-loops at highly transcribed regions, such as ribosomal genes, due to an increased negative torsion (123). Thus, CPT treatment of *rnh1Δ rnh2Δ* mutants can be used as a tool to chemically induce and maximize RNA:DNA hybrid formation in yeast.

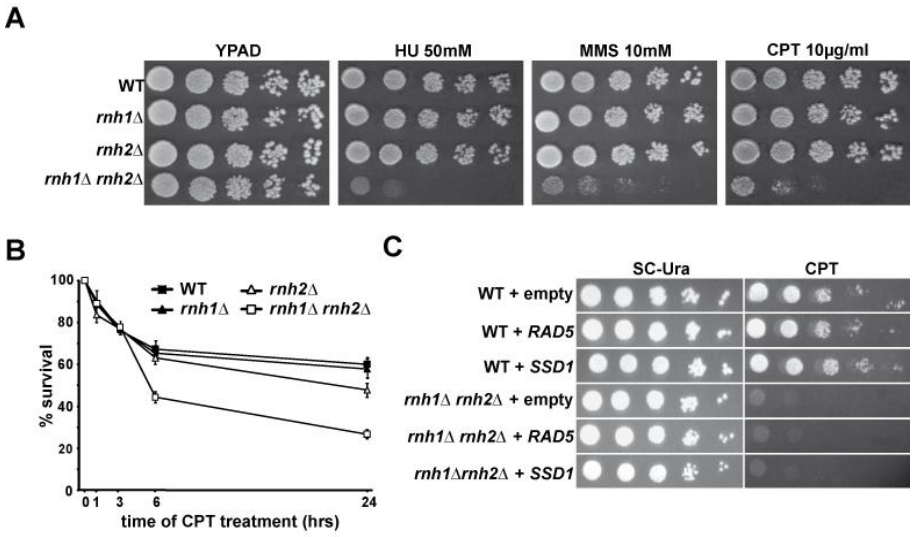

Figure 11. Yeast lacking RNase H activity are sensitive to replication stress and DNA damage independent of proficient Rad5 and Ssd1 activity. **A.** Analysis of sensitivity to genotoxic agents. 10-fold serial dilutions of cells grown for 3 days on YPAD or YPAD-containing HU (50mM), MMS (10mM), or CPT (10µg/ml). **B.** Cell survival after prolonged incubation with CPT. Data is shown as the mean ± standard deviation. **C.** 10-fold serial dilutions of cells containing an empty (control), or the *RAD5*-expressing (pBJ6) or *SSD1*-expressing (pLO92) plasmids grown on SC-Ura or SC-Ura-containing CPT (5µg/ml).

The YKL83 strains used in this study are derivatives of W303-1A (124) (a complete list of strains used in this thesis can be found in Table 2). However, genetic alterations in the W303-1A strain include a mutation in the *RAD5* (*rad5-535* (125)) and *SSD1* genes (*ssd1-1* (126)). *RAD5* codes for a factor with both DNA helicase and ubiquitin ligase activities that functions in postreplicative repair (PRR), and the *rad5-535* mutation has been associated with a slight increase in UV and MMS sensitivity (125), while *SSD1* codes for a translational repressor with roles in polar growth, TOR signalling and cell wall integrity (126,127). To determine whether the *rad5-535* or *ssd1-1* mutations contribute to the CPT sensitivity of the *rnh1Δ rnh2Δ* mutant,

strains were transformed with the *RAD5*- or *SSD1*- expressing plasmids (a list of plasmids included in this thesis can be found in Table 3). *RAD5* or *SSD1* expression from low copy number plasmids did not alleviate the *rnh1Δ rnh2Δ* CPT sensitivity (Figure 11C), supporting the idea that CPT sensitivity is due to the lack of RNaseH activities.

Yeast lacking RNaseH activity suffer from increased genome instability

CPT damages DNA by trapping the Top1-DNA cleavage complex (Top1cc) such that it cannot ligate the single-strand nick made by Top1 (128,129). Such Top1cc can be processed by the action of Rad1 and Tdp1, which form part of redundant DNA damage repair pathways (66). Tdp1 is a tyrosyl-DNA phosphodiesterase, capable of hydrolyzing the covalent link between Top1 and DNA, while Rad1 acts in conjunction with Rad10, as a structure-specific endonuclease during nucleotide excision repair (NER). The *rad1Δ tdp1Δ* double mutants are themselves very CPT sensitive due to accumulation of Top1-mediated DNA damage (Figure 12A; note the drop test analysis was performed at the lower CPT concentration of 1µg/ml due to the elevated sensitivity of the strain). To test if the RNaseHs contribute to the Rad1 or Tdp1-dependent CPT-repair pathways, we therefore generated *rnh1Δ rnh2Δ* mutants lacking only Rad1, Tdp1 or both activities (Figure 12A). The *rnh1Δ rnh2Δ* mutants were further sensitized to CPT in the absence of both *rad1* and *tdp1* (see the quadruple mutant), but not in the absence of either repair protein. The enhanced CPT sensitivity of the quadruple but not the triple mutants indicates that it is unlikely that RNase H enzymes are involved in the repair of Top1-mediated DNA damage but rather, DNA damaging events might be more frequent in these mutants.

Next, we examined if *rnh1Δ rnh2Δ* mutants suffer from a general increase in genome instability. Genetic alterations can be detected as events that lead to a loss of heterozygosity (LOH) in yeast cells, where a cell only contains a single copy of an allele due to loss or inactivation of the second copy. LOH can become critical when the sole remaining allele contains a point

mutation that renders the gene inactive. For example, LOH is a common occurrence in cancers where a tumor suppressor gene is inactivated (130,131). We measured the frequency of LOH in yeast cells by monitoring the formation of "a-like faker" cells (ALF, (132); Figure 12B), resulting from loss or inactivation of the *MATα* locus leading to the default *MAT***a** mating type in yeast. *MAT* allele disruption can be due to chromosomal rearrangement or gene conversion of the silent mating type locus *HMRa*, and more frequently, due to loss of chromosome III, that hosts the mating cassette. ALF cells can be detected by the selection of mated products, since ALFs will mate as **a**-type cells. In wild-type yeast, ALF mitotic segregants are generated at a rate of approximately 10^{-6} (133). The *rnh1Δ rnh2Δ* double mutants exhibited a frequency of ALF formation about 10-fold increased, as compared to the WT, suggesting that cells lacking RNaseH activity have chromosome instability.

To further monitor genomic instability, mutation frequencies in *rnh1Δ rnh2Δ* mutants were detected by measuring the frequency of Ura$^-$ mutations (selected in medium containing FOA; Figure 12B), using the pCM184-LAUR plasmid system ((134), see Materials & Methods for details). We found that cells lacking RNaseH activity had a 12-fold increase in the frequency of Ura- mutators as compared to the WT, suggesting that loss of RNaseH activity is associated with a hypermutator phenotype. In addition, we measured forward mutation rates by monitoring the spontaneous appearance of colonies in a medium supplemented with the toxic compound L- canavanine (Can). *S. cerevisiae* take up arginine and canavanine by means of a specific permease, and resistance to Can is associated with a loss of arginine permease function encoded by the *CAN1* locus. We observed an increase in Can resistant cells of over 6-fold in the *rnh1Δ rnh2Δ* double mutant (Figure 12B). Notably, in order to perform the *CAN1* forward mutation assay we had to use strains in the BY background, since YKL83 strains are mutated in the *CAN1* gene (*can1-100).* Taken together, these results indicate that RNaseH double mutants are prone to genomic instability.

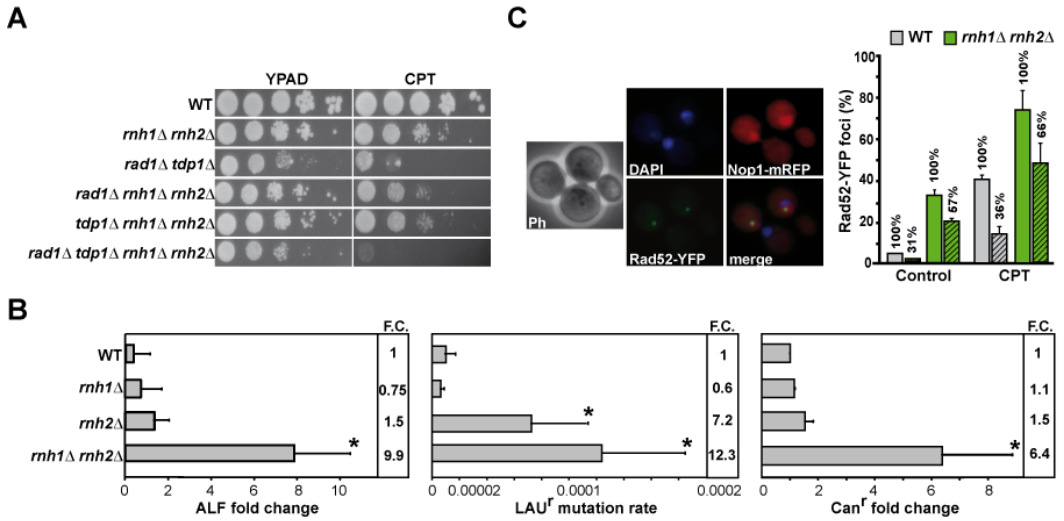

Figure 12. Loss of RNaseH activity contributes to genome instability. A. Drop test analysis of genetic interaction between RNaseH activity and CPT repair pathways. 10-fold serial dilutions of cells grown for 3 days on YPAD or YPAD-containing CPT (1μg/ml). **B.** Rate of *MAT*α conversion to a-mating type. ALF frequency values (mated products/total cells) shown as fold change (F.C.) relative to WT (left panel). Mutation rates as determined by the pCM184-LAUR plasmid mutation system (middle panel) and by canavanine resistance (right panel). Data represent the mean ± standard deviation obtained from the mean of three fluctuation tests of four independent colonies each. Differences between mutants and the WT were examined by Student's *t*-test and were considered statistically significant for p-values<0.05 (asterisks). **C.** Representative image of Rad52-YFP foci co-localized with the nucleolar periphery (left). Percentage of Rad52-YFP foci counted in exponentially growing cells growing with or without the presence of CPT (10μg/ml, 3hr treatment). Nuclear versus nucleolar Rad52-YFP foci were determined according to co-localization with the nucleolar Nop1-mRFP marker. Data represent mean ± SD from at least three independent experiments. Differences between mutants and the WT were examined by Student's *t*-test and were considered statistically significant for p-values<0.05.

Subsequently, we asked whether *rnh1Δ rnh2Δ* yeast were also more susceptible to spontaneous DNA lesions and we tested for this by analysing the formation of Rad52-YFP foci. Rad52 is a key player in repair by homologous recombination (HR); when assembled at a DSB, the clustering of Rad52-YFP proteins can be seen as an intense focus, such that foci are representative of sites of DNA repair (135). Interestingly, we observed a statistically significant increase of Rad52-YFP foci formation in *rnh1Δ rnh2Δ* cells (5-fold with respect to the WT), and an even greater increase upon the addition of CPT (Figure 12C). Notably, the Top1 specific inhibitor CPT introduces single-stranded nicks that can be converted into DSBs by collision of the replication or transcription machineries with the covalently bound Top1cc

(136,137), and so we questioned whether we would observe an even greater frequency of Rad52-YFP foci formation in a highly transcribed region of the genome. The nucleolus is ideal to test for this possibility because it hosts the highly transcribed ribosomal genes. Ribosomal genes are needed for the synthesis of rRNA by RNA PolI accounting for about 80% of the total transcription in yeast (68). High rRNA levels are achieved by transcription of approximately 100-200 identical repeats of the yeast ribosomal genes, organized into the rDNA locus on chromosome XII. Cells were co-transformed with Rad52-YFP- and Nop1-mRFP-expressing plasmids to compare the localization of Rad52 foci with the Nop1 nucleolar stain (Figure 12C). We observed that 31% of Rad52-foci colocalized with the nucleolar periphery in WT cells following CPT treatment. Strikingly, some 66% of the Rad52-YFP foci in the *rnh1Δ rnh2Δ* double mutant appeared to be associated with nucleolar DNA following CPT treatment. In fact, an already significant proportion of *rnh1Δ rnh2Δ* cells (57%) had foci that co-localized with the nucleolar periphery in logarithmically growing cells under normal conditions. Extensive work by the groups of Michael Lisby and Luis Aragon using 3D reconstruction, demonstrated that Rad52 is excluded from the nucleolus and damaged rDNA relocates to the nucleolar periphery to interact with the recombinational repair machinery (138). Collectively our results suggest that RNaseH activities contribute to the maintenance of genomic stability, and are particularly important for preserving rDNA genome stability.

Genome stability of the rDNA is particularly affected in RNH$^-$ mutants

Chromosome XII (cXII) is approximately 2.5Mb in length, being one of the largest yeast chromosomes. From sequence information, non-rDNA regions on the chromosome account for approximately 1.1Mb, and therefore, the remaining 1.4Mb are made up of rDNA repeats, constituting some 150 copies of the rDNA repeat in a control strain. The repetitive nature of the rDNA locus makes this region of the genome particularly unstable. Changes in rDNA repeat length can occur in response to repair processes initiated at stalled replication forks within the rDNA array (139-141). Homologous recombination-mediated invasion of an rDNA repeat with

a complementary sequence can lead to expansion - a gain in copy number, or contraction - resulting in copy number loss - of the rDNA array; such events being related to genome instability. The mobility of chromosome XII can be easily visualized by CHEF analysis, and provides a direct measurement of rDNA repeat length. We investigated whether the repeat length of the rDNA array was altered in mutants lacking RNaseH activity. CHEF analysis showed that the regulation of rDNA repeats was significantly affected in yeast lacking RNaseH activity (Figure 13A). We observed a substantial decrease in rDNA copy number for the *rnh2Δ* mutant as compared to the WT, related to a loss of rDNA repeats. The cXII signal for *rnh1Δ* cells and the double mutant was observed as an intense band just below the wells. For the *rnh1Δ* simple mutant, cXII migrates in a higher intense band, however, a second band corresponding to cXII can be observed just below the WT band. This result would indicate a population of *rnh1* cells with a strongly enhanced repeat expansion phenotype and a second sub-population with a shorter rDNA array. In the case of cells lacking both RNaseH activities, cXII was always detected as a diffuse signal, and generally the cXII signal seemed reduced in the double mutant. A diffuse signal represents a dispersed population that has undergone larger expansions of the rDNA array (142), and such copy number heterogeneity would reflect a particularly unstable rDNA array in the *RNH* double mutant.

Ribosomal repeat stability can also be monitored by the pop-out of rDNA repeats from cXII by intra-chromatid recombination (143), and consequently, the formation of extrachromosomal rDNA circles (ERCs) (Figure 13B). ERCs are maintained in the cell as plasmid-like circular DNA, since they can replicate autonomously (144). It has been proposed that the accumulation of ERCs is an aging factor in yeast, and the "rDNA theory" directly relates rDNA stability with longevity in yeast (145). As we had observed considerable fluctuations in rDNA repeat length in the *RNH-* mutants we questioned whether we could associate this with changes in the levels of ERCs. ERCs were separated from logarithmically growing yeast by gel electrophoresis, followed by Southern blot and hybridization with an rDNA probe. The number of ERCs was increased 4-fold in *rnh2Δ* cells yet reduced in the *rnh1Δ* as compared to the WT (Figure 13B),

which complements the previously observed decrease and increase in rDNA copy number, respectively. The double mutant has an increased number of ERC pop-outs compared to the WT further demonstrating ribosomal repeat instability.

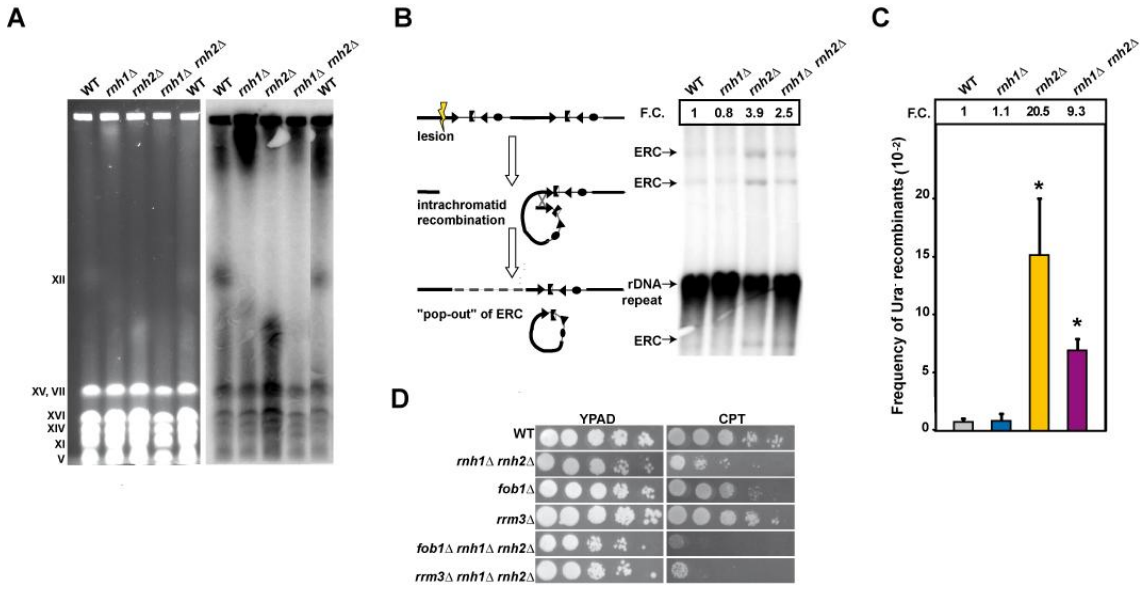

Figure 13. Lack of RNase H activity specifically affects genome stability of the rDNA array. **A.** CHEF analysis to measure rDNA repeats. Left panel EtBr-stained gel, right panel following hybridization with rDNA probe. **B.** Schematic of how a copy of the rDNA repeat can be lost when a broken end recombines with its own chromatid (intrachromatid recombination), with subsequent pop-out of an ERC (left); adapted from (143). *Bam*HI digested genomic DNA separated by gel electrophoresis (right). The strongest band observable corresponds to chromosomal rDNA (rDNA repeat); monomeric and dimeric ERC bands are observed below, and larger multimers above the chromosomal rDNA band. The three ERC signals were quantified relative to the rDNA repeat signal. Fold change relative to the WT is indicated. **C.** Recombination frequencies of strains containing the *leu2-k::ADE2-URA3::leu2-k* recombination system (146). Data represent the mean ± SD of three independent fluctuation tests, each fluctuation test representing the median value of 6 independent colonies. Fold change (F.C.) relative to WT is indicated. Differences between mutants and the WT were examined by Student's *t*-test and were considered statistically significant for p-values<0.05 (asterisk). **D.** 10-fold serial dilutions of *fob1Δ* and *rrm3Δ* strains on YPAD or YPAD-containing 5µg/ml CPT for 3 days.

Next, we measured recombination frequency within the rDNA repeats. Using an intra-chromosomal recombination system (*leu2-k::ADE2-URA3::leu2-k*) (146), loss of a functional copy of the *URA3* gene inserted into the rDNA repeats can be measured by 5-FOA resistant colony formation. We observed a 20-fold increase in FOA resistant colonies in the *rnh2Δ*

mutant, and a 9-fold increase in the double mutant (Figure 13C), corroborating the observed increase in ERC levels. Collectively these results confirm that RNaseH activities are important for normal rDNA repeat number maintenance. In RNase H lacking cells, the rDNA array undergoes higher rates of recombination with associated fluctuations in length, and reveals the rDNA array as a hot-spot for genome instability in *RNH-* mutants.

Finally, to further substantiate the importance of RNaseH in rDNA stability, we investigated whether alterations in the structural integrity of rDNA constrains the viability of *rnh1Δ rnh2Δ* mutants. To do so, we generated triple mutants lacking either Fob1 or Rrm3 activities. Fob1 codes for a replication fork blocking protein, which is important for rDNA copy number regulation (140) and is also needed to prevent collision between RNA PolI and the replication machinery (71,143); while the helicase Rrm3 is needed for the RF to bypass protein-DNA complexes formed during rDNA replication (147). Interestingly, while the *fob1Δ* and *rrm3Δ* single mutants themselves are not CPT sensitive, CPT sensitivity of both respective triple mutants was increased as compared to the *rnh1Δ rnh2Δ* double mutant (Figure 13D). This result indicates that RNaseH activities are important for unperturbed rDNA replication.

Impaired R-loop processing leads to aberrant DNA replication fork progression

To further investigate DNA replication in the *rnh1Δ rnh2Δ* double mutants and the impact of CPT on rDNA maintenance, we monitored the fate of replication intermediates (RIs) at the molecular level by 2D agarose gel electrophoresis (2D-gel) (71). 2D-gel RI separation is a powerful technique that allows one to investigate the structural properties of replicating DNA fragments, and to localise and characterise origins of replication and fork progression (see Materials & Methods for a more detailed explanation of the 2D-gel technique).

In order to address the fate of RFs, we monitored S-phase transition of α-factor synchronized cells upon release into CPT-containing medium (Figure 14A). Interestingly, in contrast to CPT treated WT cells, S/G2 progression was impaired in *rnh1Δ rnh2Δ* mutants. This finding

corroborates the previously described cell-cycle delay of *rnh1Δ rnh2Δ* cells in G2/M (99). Next, we monitored by formation of Rad52-YFP foci whether DNA damage increases during S-phase progression (Figure 14B). This was indeed the case for the WT and *rnh1Δ rnh2Δ* mutants, but importantly, only in cells devoid of RNaseH activities was DNA damage massively induced upon CPT treatment, with a peak of Rad52-YFP foci observed at the timepoints corresponding with late S/G2 phases of the cell cycle.

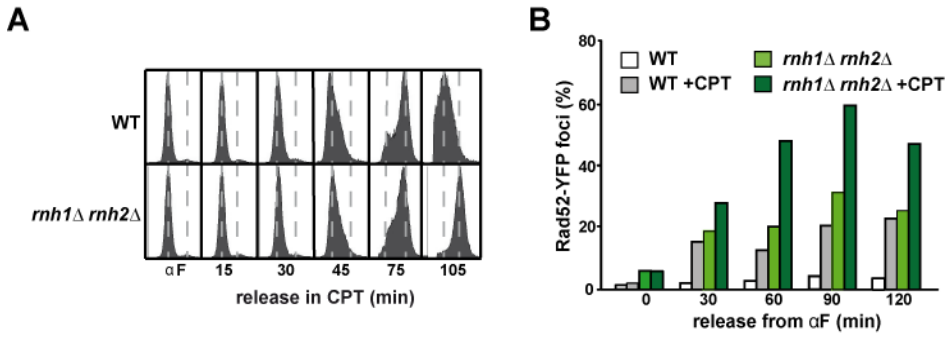

Figure 14. CPT treatment of *rnh1Δ rnh2Δ* mutant cells causes an increase of DNA damage at late S-phase. **A.** Flow cytometry analysis of strains grown in the presence or absence of 10μg/ml CPT following release from α-factor. **B.** Time-course analysis of Rad52-YFP foci appearance following release from α-factor in the presence or absence of CPT. Data represent mean from two independent experiments.

Genomic DNA was isolated and cut with *Bgl*II, which gives rise to two fragments of approximately 4.5kb, encompassing the 35S transcribed region or the non-transcribed intergenic region (which includes the ARS and RFB) and RIs were separated by 2D-agarose gels. We first probed against the non-transcribed intergenic region of the rDNA locus (Probe A, Figure 15A, top left). As replication starts bi-directionally at the ribosomal ARS, the leftwards-moving RF will be paused at the replication fork barrier (RFB), while the rightwards moving fork will proceed until it meets a RF stalled at the downstream RFB. Accordingly, the expected 2D-gel pattern corresponds to simple Y-shaped molecules (simple Y arc), an accumulation of stalled molecules at the RFB, revealed as a discrete spot on the Y-arc, and recombination intermediates that migrate along the 2n spike (Figure 15A, top right, expected RIs represented

in gray). This was indeed the case for WT cells, where such RIs increased within 45 min upon release from α-factor and then decayed towards the end of S-phase.

During the first 45 min, the S-phase specific patterns were very similar, however at late S/G2 phase we monitored a dramatic difference between the 2D-gel patterns of RIs isolated from WT and *rnh1Δ rnh2Δ* cells. Firstly, the 2n spike, representative of increased recombination intermediates, persists in *rnh1Δ rnh2Δ* mutants, as does the RFB signal. It´s interesting to note the stronger RFB signal for the *RNH* double mutant at all time points, suggesting an increase in the number of rDNA replication origins fired or a delay in the advance of the rightwards-moving replication fork needed for replicon fusion and RFB resolution (see RFB quantification, Figure 15B). Secondly, we found that *RNH-* mutants exhibited an increase in Y-arc RIs and noted the appearance of additional replication fork pausing sites (RFPs), observed as distinct spots along the Y-arc (shown with the white arrows, 105 min time point) in the non-transcribed spacer region. Thus the *RNH* double mutants are still replicating rDNA at 105 minutes post-release, when replication would normally be completed (compare to the WT).

We also observed a novel, cone shaped signal above the inflection point (indicated by the black arrow). Interestingly, Daalgard *et al*. had identified a similar intermediate in this position in *Schizosaccharomyces pombe* (*S. pombe*) (148). This cone signal in *S. pombe* was caused by the specific incorporation of two ribonucleotide residues into the lagging stand at the *mat1* locus, acting to initiate a replication-coupled recombination that leads to mating type switching (reviewed in (149)). The authors state that this cone signal is characteristic of a chicken foot structure, representative of regressing RFs, signifying that the imprint causes a programmed RF block.

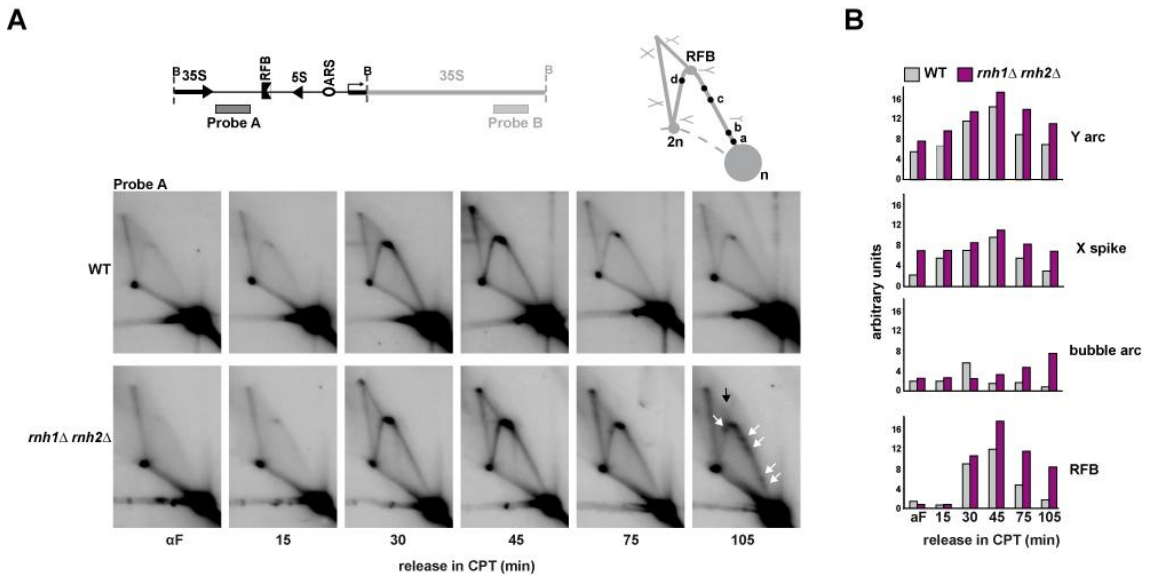

Figure 15. CPT treatment of *rnh1Δ rnh2Δ* mutant cells provokes replication fork pausing. A. Schematic representation of the rDNA locus (top left). *Bgl*II restriction sites (B) are indicated. Predicted (gray) and novel (black) replication intermediates following hybridization to the non-transcribed ribosomal spacer region (NTS; probe A; top right)**.** 2D-gel analysis of *Bgl*II-digested replication intermediates at the rDNA locus in WT versus *rnh1Δ rnh2Δ* mutants following release from α-factor in the presence of CPT (bottom left); hybridization with probe A. RFPs represented by white arrows. **B.** Quantification of RIs. Quantifications are relative to the "n" spot intensity.

Impaired R-loop processing leads to origin independent replication initiation

To continue, the 2D-gel membranes were hybridized with a second probe (Probe B), corresponding to the 35S rRNA gene (Figure 16A, left). Because the 35S rRNA gene does not contain an origin of replication, it must be replicated by RFs that enter the fragment from either direction, leading to Y-shaped molecules (Figure 16A, right). For the WT, the Y arc signal increases following release from the G1 block, peaking at 45 minutes and then the signal diminishes as replication is completed. In contrast, persistence of the Y arc and X spike signals was apparent throughout the time-course in the *rnh1Δ rnh2Δ* mutants. A particular accumulation of Y-structures towards the end of the descending Y-arc (to the right of the inflection point) was evident for the double mutant, and confirmed by quantification of right versus leftwards Y-arc signal (Figure 16B). This result is consistent with a slowdown of RFs through this highly transcribed gene region and would suggest that RF progression through the 35S rRNA gene was affected in the *RNH*-mutant.

Surprisingly, for the *rnh1Δ rnh2Δ* double mutant we noted the appearance of bubble-shaped molecules, most clearly seen at 105 minutes (indicated by blue arrow, Figure 16A; quantified in Figure 16B), but arising 75 minutes after release from CPT treatment.

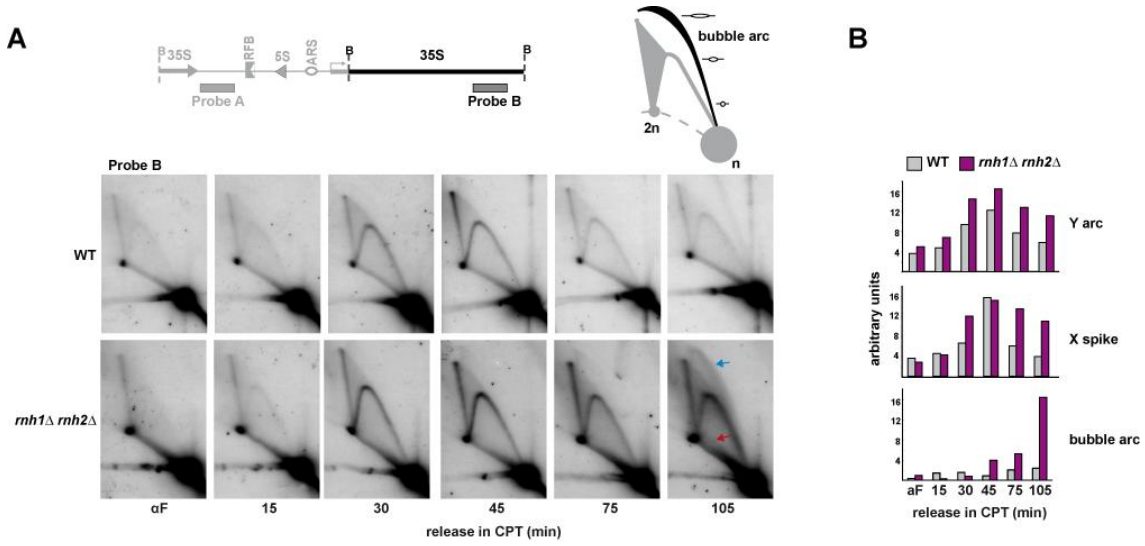

Figure 16. CPT treatment of *rnh1Δ rnh2Δ* mutant cells provokes rARS-independent replication initiation at late S-phase. A. Predicted (gray) and novel (black) replication intermediates (right) following hybridization to the transcribed 35S gene (probe B). 2D-gels as for **Figure 15.** but hybridized with probe B (left). Blue arrows represent bubble arcs; red arrows represent sub-Y arcs. **B.** Quantification of RIs for CPT treated samples. Quantifications are relative to the "n" spot intensity.

A bubble arc is indicative of active replication from an origin within this fragment, since only active replication within a fragment leads to the formation of replication bubbles in 2D-gel. Additional signals resembling Y-arcs were observed in the 2D-gels of the *RNH* double mutants, which were not observed in the WT and were dependent upon CPT treatment (Figure 17). These signals, apparent from 45 minutes, have been denominated sub-Y arcs (150), as they migrate below the standard Y-arc, (indicated by red arrows, Figure 16A).

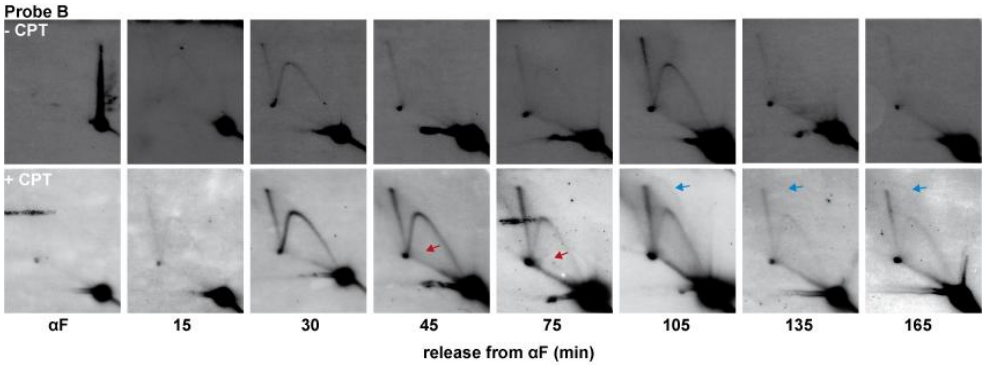

Figure 17. rARS-independent replication initiation is only observed in *RNH-* mutants following CPT treatment. 2D-gels as for Figure 6.

We wished to characterize these interesting 2D-gel results further. Firstly, in order to classify the pausing sites more precisely they were compared to the pause sites of a *fob1Δ rrm3Δ* mutant (Figure 18A). Work by Virginia Zakian´s group has described known pausing sites for the *rrm3Δ* mutant (147), a helicase needed to allow RF passage through protein-DNA interactions. We chose to use a *fob1Δ rrm3Δ* double mutant, to additionally remove the strong pause signal caused by the RFB, as RF blocking activity at the RFB is dependent upon the activity of Fob1. The majority of the pausing sites identified in the *RNH-* mutant in response to CPT treatment overlapped with those previously described for DNA helicase-deficient *rrm3Δ* mutants (147). Consequently, the RFPs, (labelled **a** to **e**, Figure 18A), correspond to sites of protein barriers provided by the ribosomal ARS (sites **a**/**b**), or the RNA PolIII transcribed 5S gene (site **c**) or the 3' end of RNA PolI transcribed 35S gene (site **d**). Notably one RFP was exclusively observed in the *rnh1Δ rnh2Δ* mutants (depicted by an arrow). The novel spot observed in *rnh1Δ rnh2Δ* cells (adjacent to pause site c, depicted by arrow) corresponds to a RFP in the region between the ARS and 5S rRNA gene, and could possibly correspond to the region rCNS3. rCNS3 was identified in the rDNA (151) as corresponding to a previously identified bidirectional RNA PolII promoter (152). No specific function has been attributed to this element, although it seems to play a key role in the regulation of recombination in the rDNA (151). Another important difference is the lack of pausing site **e** in *rnh1Δ rnh2Δ* mutants; according to the work of the Zakian group (153), spot **e** corresponds to RIs stalled at the

ribosomal ARS. The lack of this pausing site might be explained by the temporal appearance of pausing sites in the *RNH*- mutants. In *rrm3Δ* mutants, replication pausing sites coincide with ongoing DNA synthesis, while *rnh1Δ rnh2Δ* mutant-dependent pausing sites are restricted to late S/G2, at which time the ribosomal ARS might be devoid of origin interacting proteins that are needed to impair fork progression.

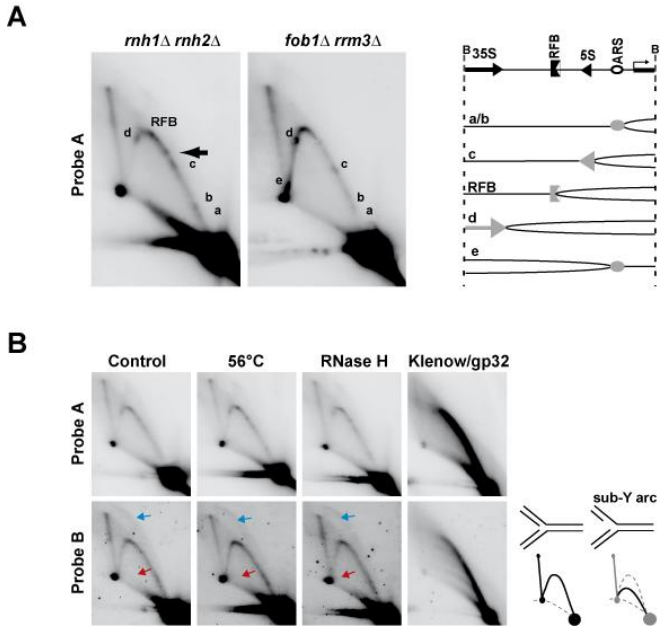

Figure 18. A. Characterization of RFP sites in the NTS region in *rnh1Δ rnh2Δ* as compared to *fob1Δ rrm3Δ* mutant strain. Pausing sites are labelled a-e; black arrow represents unique RFP site. **B.** Prior to 2D-gel, RIs isolated from CPT-treated *rnh1Δ rnh2Δ* cells at 105 minutes were subjected to heat or enzymatic treatments as indicated. Blue arrows represent bubble arcs; red arrows represent sub-Y arcs. Schematic representation of species that would migrate as sub-Y arcs (right). 2D-gel analyses shown were performed by Nestor García Rodríguez.

To address whether these bubble-shaped intermediates consist of extensive R-loops, after restriction digestion we performed *in vitro* RNaseH digestion of the genomic DNA from *rnh1Δ rnh2Δ* yeast cells at the 105 min time point prior to 2D-gel (Figure 18B). RNaseH would digest regions of RNA hybridized to DNA, and therefore if the bubble-shaped molecules simply corresponded to extended RNA:DNA hybrid regions the bubble arcs should collapse upon RNA degradation. This, however, was not the case, as the bubble-shaped molecules were resistant to *in vitro* RNaseH treatment (Figure 18B, blue arrows). Furthermore, the sub-Y arcs, consistent with the presence of segments of ssDNA, were equally unaffected by RNaseH treatment (Figure 18B, red arrows). Secondly, we questioned whether such molecules contained a 3' extendable DNA polymerase substrate. Prior to 2D-gel, RIs were subjected to *in vitro* treatment with the exo- Klenow Polymerase, gp32 single-stranded DNA binding protein

and nucleotides (154) (Figure 18B). The disappearance of bubble-shaped molecules suggests that these intermediates are a substrate for the DNA polymerase and indicates that they contain an extendable 3´ hydroxyl group. Together our results open the possibility that the bubble signals were not made up of an RNA:DNA hybrid, but rather have all of the features of replicating molecules, and thus represent origin-independent replication initiation events.

Lack of Top1 is crucial for origin-independent replication initiation events

The bubble arcs detected in the *RNH* double mutant were only evident following growth in the presence of CPT. CPT stabilizes a Top1-DNA complex and results in nicked DNA by a so-called Top1 cleavage complex (Top1cc). This kind of DNA damage or the sequestering of Top1 could be critical for bubble arc formation. To distinguish between these two possibilities, we decided to employ the conditional protein degradation system, or "Degron", as a tool to rapidly deplete Top1 proteins from yeast cells. Consequently, we constructed an auxin-inducible Top1 degron (Top1AID-9Myc) in *rnh1Δrnh2Δ* yeast expressing the SCF^{TIR1}. The auxin-inducible degron (AID) system acts to proteolytically remove the target protein upon addition of the plant auxin-like pheromone, indole acetic acid (IAA) to the growth media (see Materials & Methods for details) (155).

Firstly, we confirmed that Top1AID-9Myc protein levels were reduced in response to auxin. G1-synchronized cells were incubated for 30 minutes in the presence of 1mM IAA to induce degradation of the aid-tagged protein, prior to release into fresh YPAD containing IAA, and samples were collected at the indicated timepoints for western blot analysis (Figure 19A). After 30 minutes, Top1AID-9Myc protein levels were significantly down-regulated. In line with the rapid degradation of Top1AID-9Myc, growth of the *rnh1Δ rnh2Δ* Top1AID-9Myc strain was severely impaired in the presence of IAA (Figures 19B and 19C), thus resembling synthetic lethality observed for the *top1Δ rnh1Δ rnh2Δ* triple mutant (60).

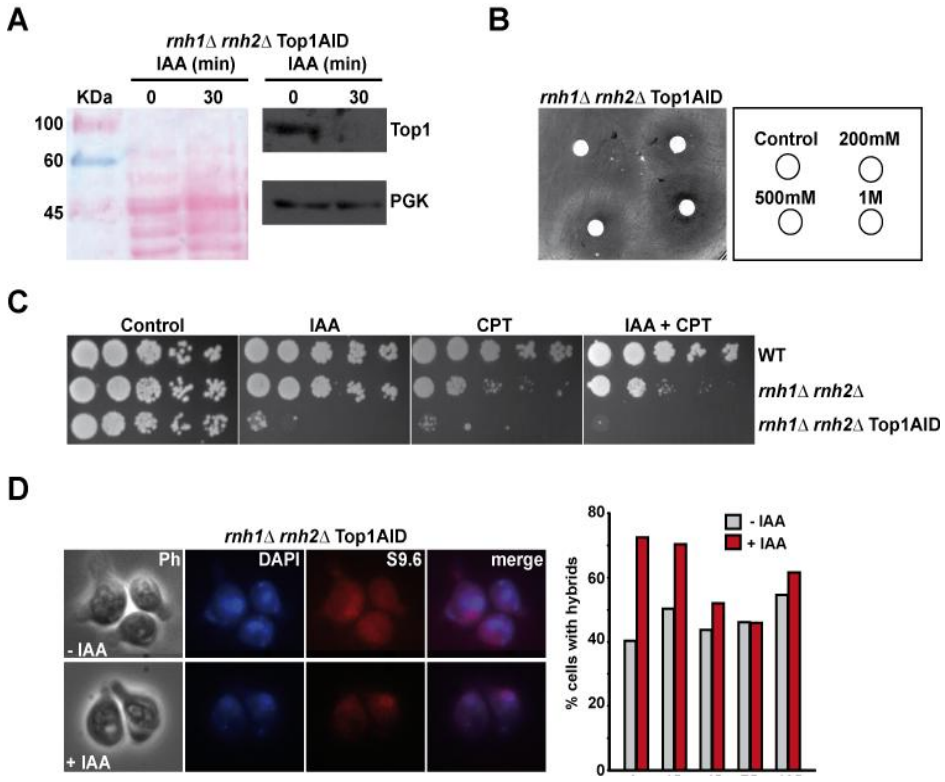

Figure 19. Confirmation of functionality of the 9Myc-Top1AID degron in *rnh1Δ rnh2Δ* TIR1-expressing yeast. **A.** Western blot analysis against the Myc tag to confirm degradation of Top1AID protein in response to 1mM IAA. Ponceau stained membrane (right panel); Western with α-Myc and α-PGK loading control (left panels). **B.** Halo assay with increasing concentrations of IAA. **C.** Drop test analysis on YPAD plates containing 1mM IAA in the presence or absence of 5μg/ml CPT. **D.** Immunofluorescence analysis of RNA:DNA hybrids with S9.6 antibody in the Top1AID degron in *rnh1Δ rnh2Δ* yeast in the absence or presence of 1mM IAA for 30 minutes. Representative images (left) of RNA:DNA hybrids (S9.6; red) and co-localisation with DAPI nuclear strain (blue); photos taken with the same settings for comparison of signal intensity. Quantification of cells with RNA:DNA hybrid and DAPI co-localising signals.

Furthermore, formation of RNA:DNA hybrids was significantly increased (Figure 19D), as determined by immunofluorescence using the S9.6 antibody that recognizes RNA:DNA hybrids (156). Importantly, the signal for RNA:DNA hybrids co-localized in its majority with DAPI-stained nuclear material, although some additional foci could be observed, indicative of mitochondrial RNA:DNA hybrid detection.

Next, we examined the fate of DNA replication of the auxin-inducible *rnh1Δ rnh2Δ* Top1AID-9Myc strain. Monitoring cell cycle progression following release from α-factor in the presence of IAA (Figure 20A) the conditional triple mutant was able to pass through and complete S

phase by 45 minutes. However, up to 165 minutes post-release the mutant remained in G2/M phase. As for CPT treated *rnh1Δ rnh2Δ* mutants, 2D-gel analysis confirmed the formation of RFPs with probe A (Figure 20B upper panels), and sub Y-arcs (blue arrows) and bubble arc signals with probe B (red arrows, Figure 20B lower panels). Interestingly, in contrast to the CPT treated *RNH* double mutant, only the RFP site labelled as **d** (white arrows) was prominent upon induction of the conditional *rnh1Δ rnh2Δ top1Δ* triple mutant.

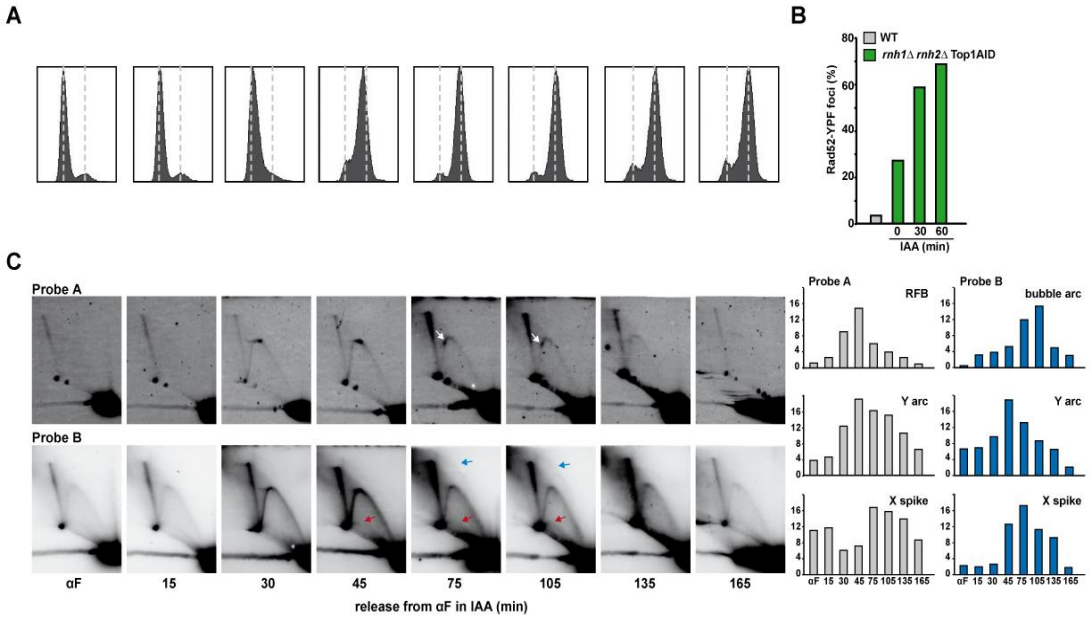

Figure 20. Absence of Top1 activity in *RNH-* mutant cells leads to RF pausing and replication re-initiation. Flow cytometry (top panels) and 2D-gel analysis of Top1AID *rnh1Δ rnh2Δ* strain grown in the presence of 1mM IAA following release from α-factor. Gels were hybridized with probe A and probe B, and quantified (right panels) as previously described.

Both CPT treatment and Top1 depletion could induce the formation of novel RFP sites and the formation of bubble like structures with some exceptions. In contrast to CPT treatment, only pausing site **d**, which corresponds to pausing at the 3' end of the highly transcribed 35S rRNA gene was clearly evident in Top1 depleted cells. These results indicate that it is not the nicking activity of CPT, but rather the down-regulation of Top1 activity that leads to the formation of these replication intermediates.

Unscheduled replication initiation events at rDNA are RNA PolI transcription-dependent

Because the bubble-shaped replication intermediates were restricted to the RNA PolI-transcribed 35S rRNA fragment, we asked whether their appearance was dependent on transcription. To specifically reduce transcription of the rDNA locus we took advantage of temperature sensitive RNA PolI mutants for alleles of Rpa190 (*rpa190-3*), which is the largest and catalytic core component of RNA PolI, and Rrn3 (*rrn3-8*), which recruits RNA PolI to the 35S rRNA gene promoter. Transcription of the rDNA array occurs normally when the temperature sensitive RNA PolI mutants are grown at permissive temperatures (23ºC), but growth of these mutants at higher restrictive temperatures (34-37ºC) impairs transcription and leads to cell death due to impaired ribosome biogenesis (157). These mutants are viable at semi-permissive temperatures (30ºC), although rDNA transcription by RNA PolI is reduced. Interestingly, growth of the *rpa190-3* (and to a lesser extent, *rrn3*-8) triple mutant at semi-permissive temperatures suppressed the CPT-sensitivity of the *RNH-* mutants (Figure 21A), suggesting a link between RNA PolI transcription and CPT toxicity.

It´s tempting to speculate that highly transcribed genes are more prone to DNA damage formation, perhaps caused by increased RF stalling at RNA:DNA hybrids or by collision with the transcription machinery. To test for this possibility we assayed the RNA PolI-dependent formation of Rad52-YFP foci formation. Interestingly, a down-regulation of RNA PolI transcription reduced the formation of nucleolar DNA repair centres (Figure 21B). Raising the temperature from 23º to 30ºC (permissive to semi-permissive conditions), caused a general increase in the number of Rad52-YFP foci in the *rpa190-3 rnh1Δ rnh2Δ* triple mutant, however, the number of foci that localize to the nucleolar periphery was significantly decreased in the triple mutant at the semi-permissive temperature of 30ºC. These experiments suggest that rDNA transcription by RNA PolI has a major impact on the formation of CPT induced rDNA lesions in the *RNH* double mutant. To gain insight into this possibility, we determined the

recombination frequency within the rDNA repeats (Figure 21C). Indeed, and in accordance with a previous study (143), down-regulation of RNA PolI transcription at the semi-permissive temperature reduced the recombination frequency within the rDNA repeats.

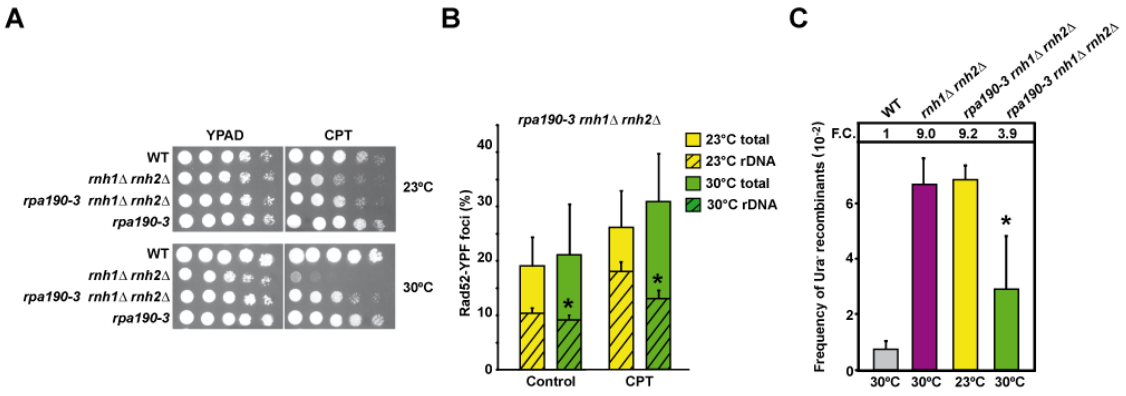

Figure 21. CPT sensitivity of *rnh1Δ rnh2Δ* is related to rDNA transcription by RNA PolI. **A.** 10-fold serial dilutions of the temperature-sensitive conditional RNA PolI subunit mutant *rpa190-3* grown on YPAD or YPAD-containing 5μg/ml CPT for 3 days at permissive (23ºC) or semi-permissive (30ºC) temperature. **B.** Reduced RNA PolI transcription in *rpa190-3 rnh1Δ rnh2Δ* triple mutants correlates with a reduced amount of nucleolar DNA damage. Percentage of nuclear versus nucleolar Rad52-YFP foci (determined by co-localization with the Nop1-mRFP) at permissive (23ºC) or semi-permissive (30ºC) temperature with or without the presence of 10μg/ml CPT (3hr treatment). Data represent mean ± SD, from at least three independent experiments. The p-value for 23°C rDNA versus 30°C rDNA was 0.0053 without and 0.001 with CPT. **C.** Recombination frequencies of strains containing the *leu2-k::ADE2-URA3::leu2-k* recombination system. Data represent the mean ± SD of three independent fluctuation tests, each fluctuation test representing the median value of 6 independent colonies. Fold change relative to WT is indicated. The p-value for *rpa190-3 rnh1Δ rnh2Δ* at 30°C versus 23°C was 0.0361. Differences were examined by Student's *t*-test and were considered statistically significant for p-values<0.05 (asterisks).

Subsequently we examined the fate of replication in *rpa190-3 rnh1Δ rnh2Δ* mutants by 2D-gels, to test if the previously observed origin-independent replication re-initiation requires active transcription of the rDNA unit by RNA PolI (Figure 22A). Triple mutant *rpa190-3 rnh1Δ rnh2Δ* yeast were grown at 26°C, prior to synchronization with α-factor and release into CPT containing media at permissive (23°C) or semi-permissive (30°C) temperatures. As expected, upon hybridization with probe B against the transcribed 35S rRNA gene, we observed bubble arcs in the *rpa190-3* triple mutant at the permissive temperature when RNA PolI transcription

is most active. Strikingly, bubble-shaped molecules were barely detectable at the semi-permissive temperature when RNA PolI transcription is down-regulated (Figure 22B).

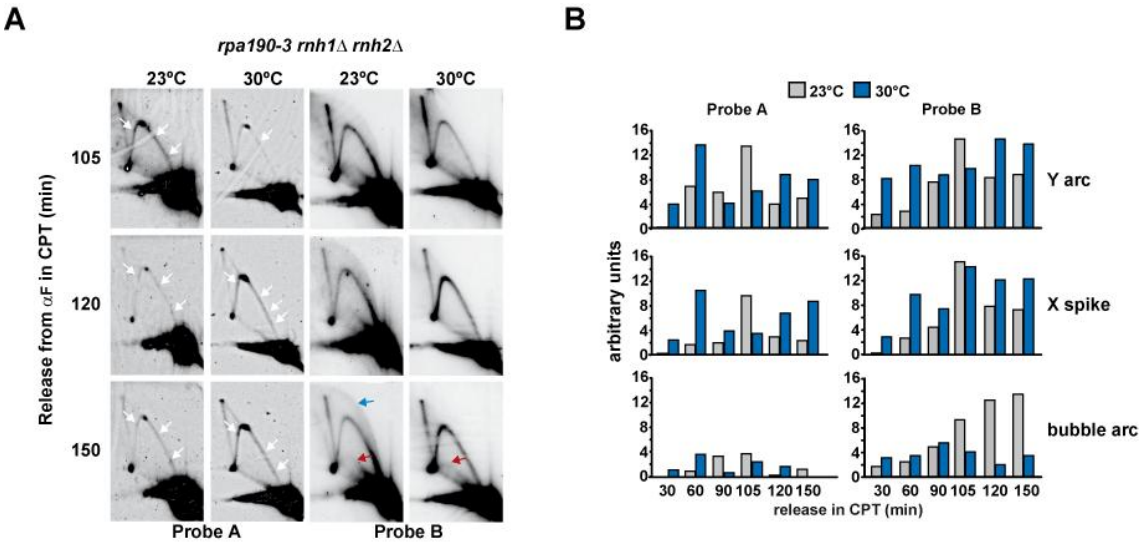

Figure 22. ARS-independent replication initiation is dependent on 35S rDNA transcription by RNA PolI. A. Analysis of replication intermediates of *rpa190-3 rnh1Δ rnh2Δ* triple mutant by 2D-gel. Strains grown under permissive or semi-permissive conditions following release from α-factor in the presence of 10μg/ml CPT. Gels were hybridized with probe A and probe B as before. **B.** Quantification of replication intermediates relative to n spot intensity.

In addition, the sub-Y arcs (red arrows, Figure 22A), previously observed in the *RNH-* mutant were observed at both 23º and 30ºC for the *rpa190-3* triple mutant, whereas bubble arcs were only seen at the permissive temperature. We can conclude, therefore, that the formation of replication bubbles does not depend on the formation of the sub-Y arcs, and that these structures are two independent intermediates. Furthermore, as the sub-Y arcs were observed at permissive and semi-permissive temperatures, formation of these structures does not appear to be affected by RNA PolI transcription of the rDNA.

Re-hybridization of the 2D-gels with probe A against the non-transcribed ribosomal spacer region (Figure 22A, left panels) revealed some RFPs in the *rpa190-3* triple mutant at both permissive or semi-permissive temperatures (indicated by white arrows; see Figure 18A for explanation of pausing sites). The RFP corresponding to the RNA PolI transcribed 35S gene (site **d**) was especially prominent at both temperatures. The RNA PolIII transcribed 5S gene

pause site (site **c**) was also observed in both conditions as would be expected, since the down-regulation of RNA PolI would not necessarily affect the transcription of RNA PolIII. These results indicate that even with the down-regulation of RNA PolI activity, replication forks have problems to progress through the rDNA locus, and in particular the 35S rRNA gene.

Taken together, our results reveal that the CPT sensitivity and instability of the rDNA array of *rnh1Δ rnh2Δ* yeast are linked to the transcriptional activity of rDNA. We propose that the absence of RNaseH activity, in combination with a reduction in Top1 activity (either by reducing protein levels or by CPT sequestering) leads to an accumulation of RNA:DNA hybrids, particularly across highly transcribed regions such as the rDNA locus. These hybrids can interfere with ongoing replication, lead to replication fork blockage or even initiate unscheduled replication (see Figure 23 for hypothetical model). We infer from our results that RNA:DNA hybrids provide the nucleation point for the assembly of a non-canonical replication machinery and are able to initiate origin-independent DNA replication in a eukaryotic genome.

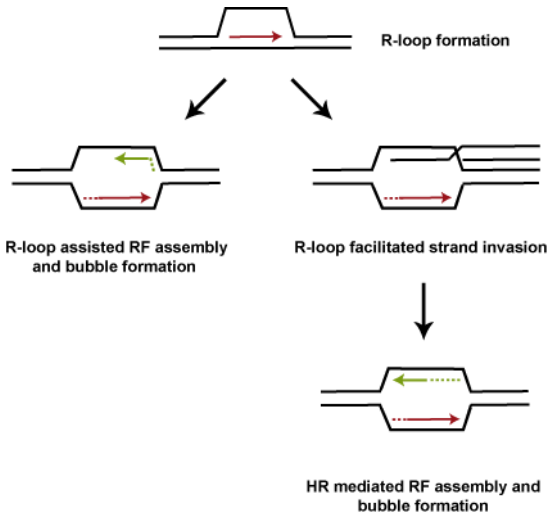

Figure 23. Model for Transcription Initiated Replication in Yeast Ribosomal DNA.

DISCUSSION for CHAPTER 1

Consequences of Persistent R-loops

Persistent R-loops have previously been linked to genomic instability ((16) and references within), including mutations and hyper-recombination. This thesis confirms the critical role of the RNaseH enzymes in removing R-loops for the maintenance of genome integrity, and extends these findings, highlighting in particular the ribosomal DNA array as a hot-spot for R-loop mediated genome instability. Furthermore, we reveal a novel impact of R-loops as sites of replication initiation in a eukaryotic genome, which we refer to as "transcription-initiated replication" or TIR.

R-loops Promote Origin-Independent Replication

DNA replication is normally initiated at determined origins of replication throughout the genome and requires the function of DNA Polα-primase to initiate DNA synthesis. Furthermore, origin firing follows a strict temporal control, with replication initiated specifically during S phase of the cell cycle (reviewed in (158)). However, we show that the origin-independent replication initiation observed in the highly transcribed 35S rRNA occurs outside of the normal program of origin firing, both spatially (not at a defined ori) and temporally (the replication initiation occurs in late S/G2 phase of the cell cycle, when replication would normally be completed).

The function of RNA:DNA hybrids as "origins of replication" has been well documented in prokaryotic plasmids, bacteriophages and mitochondrial DNA. In these cases, transcription produces an RNA:DNA hybrid that can subsequently prime replication initiation. In fact, an origin-independent replication initiation was observed in *dnaA* mutants of *E.coli* over 40 years ago (44). DnaA is a replication initiation factor that promotes the unwinding and strand separation of DNA at the bacterial origin (*oriC*), essential for the assembly of the replisome

(159). Mutants capable of initiating DNA replication in the absence of DnaA were mapped to the RNH locus (*rnhA*) (45) encoding the bacterial RNaseH. RNA:DNA hybrids are thermodynamically stable structures, where the two strands of the DNA duplex are open. Therefore, the persistence of such structures could by-pass the need for DnaA or strand separation activity. However, mutants in *rnhA* are unable to suppress the need for DnaG, the bacterial primase (46), suggesting that this mode of replication initiation is not sufficient for replication of the complete genome.

Various alternatives could account for the R-loop-mediated replication observed in the yeast genome. These could include the direct assembly of the replisome at the open and stable R-loop, with the RNA moiety acting as a primer for extension by a DNA Pol (with or without processing to generate a 3′end), analogous to the replication initiation of the multi-copy plasmid ColE1 (160). Another possibility may be that an R-loop could be a suitable substrate for a specialized polymerase such as the recently characterized human PrimPol (161). PrimPol could re-prime with dNTPs to re-initiate DNA synthesis downstream of hybrid-stalled RFs (162), although such an activity has not been identified in yeast to date. On the other hand, the R-loop structure could facilitate strand invasion for a recombination-dependent assembly of the replisome. An ongoing canonical RF may stall at the R-loop creating a break, and the processed 3' single stranded end could invade a homologous template, promoting RF assembly. The repetitive nature of the rDNA array, and subsequent ease of homology search, might make this mechanism of replication initiation particularly favourable. This mode of origin-independent replication would be similar to the recombination-dependent replication mechanism of *E. coli* and bacteriophage. This possible mechanism of TIR will be investigated in more detail in Chapter 2 of this thesis. An alternative hypothesis, not explored further in this thesis, would be the possibility that TIR events are restricted to ERCs. Yeast lacking RNaseH activities exhibited copy number heterogeneity and concomitant increase in the number of ERCs (see Figure 13) and interestingly, *top1* mutants were also reported to have more ERCs (163). ERCs are maintained in the cell as plasmid-like circular DNA (145), and can replicate

autonomously (164). One could presume that an rDNA repeat-containing ERC could replicate by an R-loop mediated mechanism analogous to ColE1 plasmid replication. However, investigating this possibility is hampered by the fact that the DNA sequences that constitute ERCs and the genomic rDNA are identical. Therefore, ERCs would have to be separated from genomic DNA to distinguish between an rDNA 9.1kb repeat unit located on chromosome XII or found on an ERC by 2D-gel and subsequent probe hybridization.

Persistent R-loops Particularly Affect the Stability of rDNA

The accumulation of ERCs has been shown to be toxic and has been linked to a decreased lifespan (senescence) in yeast (145). However, in the case of the *hpr1* mutant, shown to accumulate R-loops (19), no increase in ERCs was observed despite an increased rate of recombination within the rDNA array (165). In this case the reduced life span was associated with increased genomic instability, and over time a revised "rDNA instability" theory of aging has been proposed (142). In fact, in aging mammalian cells changes in nucleolar morphology have been detected (166), and the tumour suppressor protein RB, an important regulator of senescence (167), has been shown to accumulate in the nucleolus and repress PolI transcription (168,169). Due to the increased production of ERCs in yeast lacking RNaseH activities, and the increased genomic instability of the rDNA locus, it would be interesting to investigate whether the lifespan of the *RNH-* mutants is affected.

DNA damaging events were found to be particularly frequent in the rDNA locus in yeast lacking RNaseH activities (see Figure 12). We found that the down-regulation of RNA PolI could suppress the CPT sensitivity of the *RNH-* mutants (see Figure 21), suggesting that the majority of the DNA lesions were mediated by rDNA transcription. A recent study demonstrated that Top1ccs are specifically enriched and stabilized at the RFB of the yeast rDNA (170), and the formation of these targeted Top1cc complexes would explain the previously reported occurrence of DSBs near the RFB (63,64). Consequently, we were very interested to note that there is a Top1 binding site near the 35S promoter, at approximately 180bp upstream of the

35S rRNA transcriptional start (171). This specifically located Top1 binding site may reflect the importance of the action of Top1 to prevent RNA:DNA hybrid formation across this highly transcribed active gene, and thus repress R-loop assisted RF assembly. An alternative explanation may be that programmed RF pausing at the 35S promoter, due to the presence of a Top1 cleavage complex, is necessary for subsequent DSB formation and recombination-mediated replication fork re-start. Interestingly, TIR was only observed upon the down-regulation of Top1 activity (by protein depletion or CPT treatment). This would indicate that the action of Top1 for the avoidance of the formation of RNA:DNA hybrids is normally sufficient to suppress TIR in the absence of RNaseH activity.

Origin-Independent Replication Outside of S-phase

As seen by our immunofluorescence timecourse, RNA:DNA hybrids were present in yeast from G1 synchronization and throughout S phase (see Figure 19), and therefore replication initiation could have occurred at any stage during the cell cycle. However, the appearance of the RF pause sites and the transcription dependent replication bubbles were only observed when cells were held in late S/G2 phases of the cell cycle. Perhaps TIR can only occur in late S/G2 phase, since this is when an enzymatic activity needed for the formation of a replication bubble is available. For example, an enzymatic activity that could liberate a free 3´OH end to allow strand invasion, such as the nucleases Mus81, Yen1, or Slx1-4, may be necessary for R-loop assisted RF assembly. The highly redundant activities of the 3´end resection factors make it difficult to study the contributions of each individual factor but it would be interesting to investigate the impact of these nucleases on TIR.

R-loops Provoke Replication Fork Pausing

The progression of both transcription (24) and replication machineries (25,172) can be blocked by R-loops and our results confirm that yeast cells lacking RNaseH activity have an impaired ability in replication progression. The majority of the pausing sites identified in this study corresponded to sites of protein barriers provided by the ribosomal ARS, or the RNA

PolIII transcribed 5S- or RNA PolI transcribed 35S genes (see Figure 18). However, we suggested that one novel pause site corresponded to rCNS3 (151), a bidirectional RNA PolII promoter (152) of dubious function. It´s interesting to note that the *RDN1* (rDNA) locus contains some RNA PolII transcribed units, including the gene *TAR1*, encoding a mitochondrial protein, found on the opposite strand to the 25S rRNA gene (173). Furthermore, as we observed common pausing sites between yeast lacking RNaseH activity and those published for the *rrm3Δ* mutant, we can reason that the replisome assembled for TIR missed some factors necessary to move through protein-DNA interaction sites. Our findings predict a non-canonical replication machinery is involved in TIR. A future challenge will be to determine the molecular composition of such a replication machinery e.g. by selective immunoprecipitation against factors that may interact with TIR intermediates.

Removal of R-loops Protects Genome Integrity

Our report of a transcription-dependent mechanism of replication initiation reveals a critical interplay between replication and transcription. Both processes must be highly regulated and coordinated in order to occur simultaneously without risking genome integrity. Maintaining the stability of rDNA is vital since cell growth is directly dependent on the rate of protein synthesis and thus on the transcription of rDNA. Interestingly, a common feature of rapidly proliferating cancer cells is an increase in rDNA transcription (reviewed in (174)) and the human prostate cancer line 15PC3 was shown to express RNaseH2 throughout the cell, when it´s expression is usually confined to the nucleus (175). As such, determining how cells activate rDNA transcription and how this can influence DNA replication is important for understanding mechanisms that can lead to tumourigenesis. We reveal TIR at the highly transcribed 35S rRNA gene and one may presume that such a mechanism of R-loop primed replication initiation could occur at other highly-transcribed regions of the genome.

Our work highlights the essential roles of the RNaseH enzymes, and redundant activities, to eliminate RNA:DNA hybrids, and thus repress an inefficient and unregulated origin-

independent mechanism of DNA replication in eukaryotic cells. Unscheduled replication, particularly in regions of repetitive sequences such as the rDNA array, could lead to re-replication, loss of heterozygosity, and the deletion of repetitive sequences or gene amplifications. Such copy number changes are relevant to carcinogenesis, as gene amplification can lead to tumourigenesis, i.e. through the enhanced levels of an oncogene (176,177), and DNA amplification is also one of the key mechanisms by which cells acquire resistance to many cytotoxic compounds, i.e. the overexpression of multidrug transporter proteins has been observed frequently in many types of human tumors (178). However, gene amplification is also an important condition for beneficial adaptation to environmental changes (reviewed in (179)). In some organisms gene amplification is developmentally regulated and is an essential feature of the life cycle, for example for the amplification of chorion gene clusters in *Drosophila melanogaster* follicle cells during oogenesis (180), where gene amplification occurs through repeated initiation of the chorion gene cluster (for a review see (181)). We believe that highly transcribed genes might be more prone to gene amplification events induced by RNA:DNA hybrid-mediated replication. Such events might be more frequent than anticipated and may contribute significantly to genetic alterations in eukaryotic chromosomes, and open the possibility that TIR could present a driving force in evolution.

The RNaseHs have an essential role in the removal of R-loops, whose formation has been linked to genome instability and cancer, neurodegenerative diseases and possibly senescence. Our work adds a new perspective to the critical role of the RNaseH enzymes and Top1 enzymes in eukaryotic genomes to prevent unscheduled TIR mediated by R-loops.

RESULTS

CHAPTER 2 – RNH coding genes: genetic interactions reveal a link to genome stability and nucleolar function

Genetic interactions of RNH enzymes with DNA replication and repair factors

To understand how the RNaseH activities are linked to rDNA replication, stability and organisation, we first conducted a genetic analysis by crossing a selection of non-essential mutants covering representative steps in DNA replication and/or DNA repair with *rnh1Δ rnh2Δ* lacking yeast, then analysing the growth and viability of meiotic segregants (examples are shown in Figure 24A and summarized in Table 1). Triple mutants were classified as synthetic sick if the triple mutants showed a considerably smaller spore size or a slow growth phenotype on rich medium, when compared to the *rnh1Δ rnh2Δ* double mutant. Synthetic sick interactions were obtained as soon as cells were impaired in checkpoint function (e.g. *DUN1* and *RAD24*), DNA repair (e.g. *EXO1, RAD18* and *MUS81*), replication fork stability (e.g. *CSM3* and *RRM3*) or rDNA organisation (e.g. *FOB1* and *HMO1*).

Besides the well-documented synthetic lethal interactions between *RNH-* mutants with *TOP1* and *RAD27 (60,182),* our genetic analyses revealed previously unreported synthetic lethal interactions between *rnh1Δ rnh2Δ* mutants and mutants in *RAD52, SRS2, POL32,* and the MRX complex (*MRE11, RAD50,* and *XRS2*). We confirmed that Rad52 activity is essential in *RNH-* mutants by expressing *RAD52* under control of a galactose-inducible promoter (from plasmid pMDL5 (183)) in the double mutant, and crossed with a *rad52* mutant (Figure 24A). The *rad52Δ rnh1Δ rnh2Δ* (*GAL1p-RAD52-URA3*) triple mutant was subsequently streaked onto S-Ura galactose (plasmid inducing conditions) or SC-Ura glucose-containing plates (plasmid expression repressed). The *rad52Δ rnh1Δ rnh2Δ* (*GAL1p-RAD52-URA3*) triple mutants were unable to grow on medium containing glucose, indicating that the *RNH* double mutant cannot

survive without *RAD52* expression. Therefore, the action of Rad52 and/or HR is essential for *rnh1Δ rnh2Δ* viability.

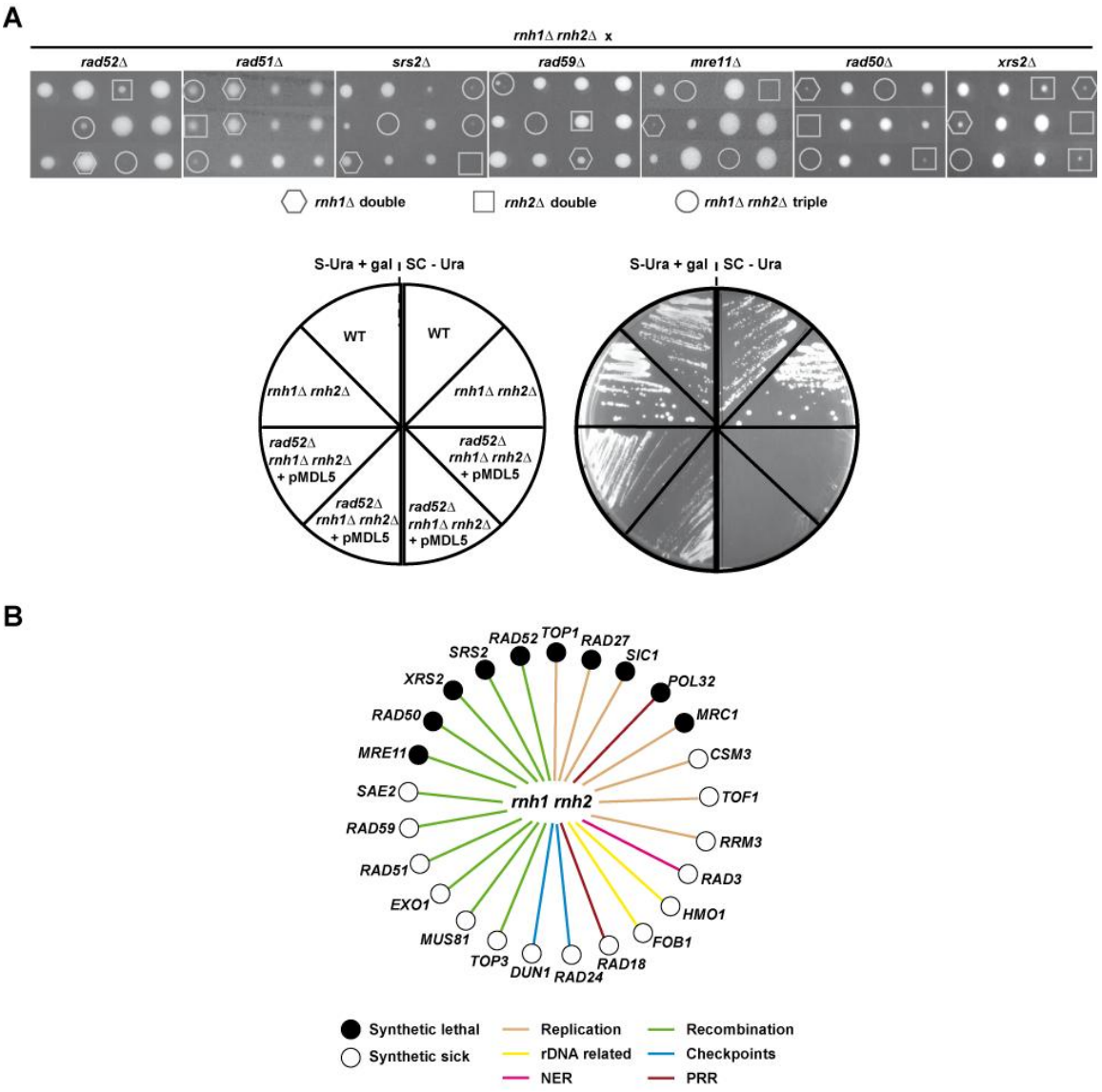

Figure 24. Synthetic lethal and synthetic sick interactions with the *RNH* mutants. A. Tetrad analysis of *rnh1Δ rnh2Δ* in combination with null mutations of *rad52, rad51, srs2, rad59,* and the MRX complex members *mre11, rad50* and *xrs2* (top panel). Rad52 activity is essential in *RNH* double mutants (lower panel). Yeast transformed with *GAL1p-RAD52-URA3* were streaked onto SC-Ura and SC supplemented with 500mg/ml of 5-Fluorotic acid (5-FOA). **B.** Diagram of synthetic lethal and synthetic sick interactions with the *rnh1Δ rnh2Δ* double mutant. Filled circles represent synthetic lethal, and open circles represent synthetic sick interactions. The mutants were broadly grouped according to gene function, as indicated by the different coloured connecting lines. PRR, post-replicative repair; NER, nucleotide excision repair. Note that the synthetic lethal interactions between the *rnh1Δ rnh2Δ* double mutant, *SIC1, MRC1* and other checkpoint genes will be further explored in Chapter 3 of this thesis.

TIR is Rad51 independent

Our genetic analyses revealed that homologous recombination is a critical pathway in yeast lacking RNaseH activity, because Rad52 activity became essential even in the absence of exogenous DNA damage. Rad52 is a key factor for the repair of single-strand and double-strand DNA breaks, and is required for the homology search and strand invasion steps of all homology-dependent repair pathways (reviewed in (184)). For example, Rad52 acts in both the Rad51-independent pathways: single-strand annealing (SSA) and break-induced replication (BIR), (185) and the Rad51-dependent DSBR and synthesis-dependent strand annealing (SDSA) pathways (as summarized in Figure 9). In contrast to the synthetic lethal interaction with *RAD52* and the synthetic sick genetic interaction with *RAD59,* the *rad51Δ rnh1Δ rnh2Δ* triple mutants were viable and did not manifest a significant growth defect when compared to the *RNH* double mutant. The *rad51Δ* simple mutant itself is very CPT sensitive (drop tests carried out with 0.1μg/ml CPT), and the *rad51Δ rnh1Δ rnh2Δ* triple mutant is even more sensitive to CPT (Figure 25A). This result indicates different constrains mediate CPT sensitivity in the absence of Rad51 or RNaseH activities.

HR may drive the formation of bubble shaped replication intermediates in CPT-treated *rnh1Δ rnh2Δ* mutants. Given that *rad51Δ rnh1Δ rnh2Δ* triple mutants are viable we intended to test for this possibility by 2D agarose gel analysis of replication intermediates (Figure 25B). Interestingly, bubble shaped replication intermediates were present in CPT-treated *rad51Δ rnh1Δ rnh2Δ* triple mutants. However, we cannot rule out that Rad51, but not HR, is dispensable for the formation of bubble shaped RI because melting of the DNA double helix by RNA:DNA hybrids may provide sufficient single-stranded DNA in order to bypass the need for Rad51 activity during HR. As HR is stimulated in the absence of Srs2 (186,187), we questioned whether we would see more TIR events in the absence of Srs2 activity. We were interested to find that the s*rs2Δ rnh2Δ* double mutant is synthetic lethal, and only 31% of s*rs2Δ rnh1Δ rnh2Δ* triple mutants were viable (Figure 24A). Viable triple mutants were very small and sensitive to

CPT, suggesting that Srs2 is an important factor when RNaseH activity is absent, particularly in the case of Rnh2. However, we were still able to observe bubble arcs in the *srs2* triple mutant (Figure 25B). Therefore, although the activity of Srs2 is important in response to CPT and for survival of the RNaseH$^-$ yeast, it does not contribute to the R-loop dependent replication initiation. In this manner, we demonstrate that neither Rad51 nor antagonistic Srs2 activity is required for TIR.

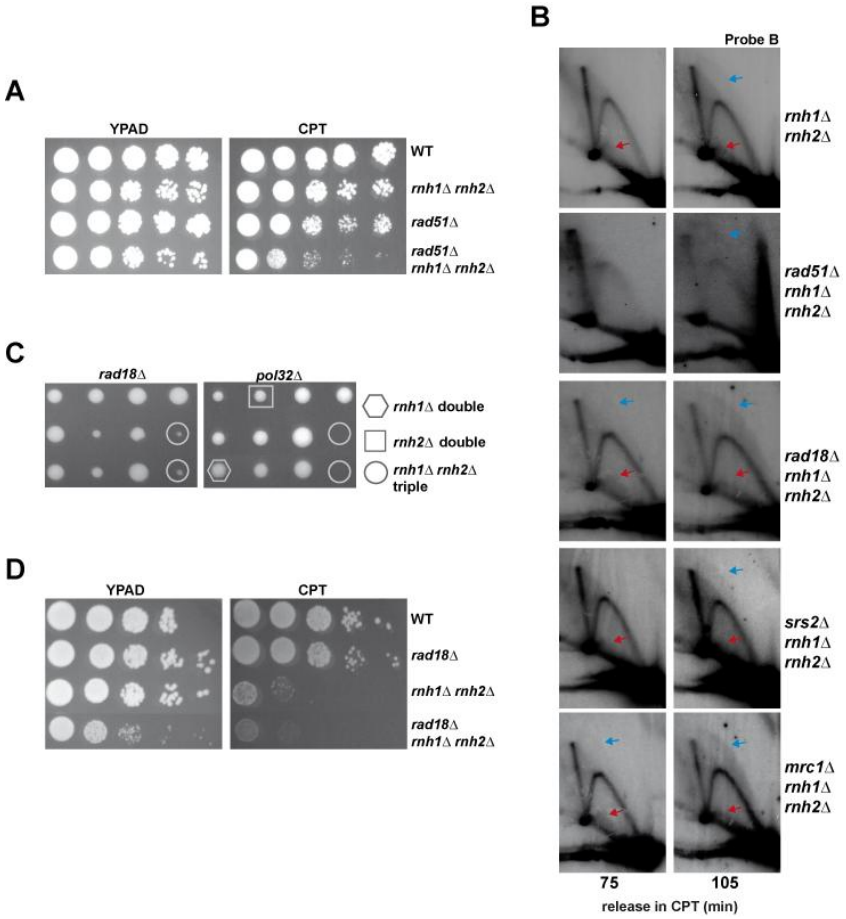

Figure 25. Rad51 is not needed for the formation of replication bubbles by TIR. **A.** Drop test analysis of CPT sensitivity of *rad51*. **B.** 2D-gel analysis of *rad51, rad18, srs2* and *mrc1* triple mutants following release from α-factor in the presence of CPT, as previously described. **C.** Tetrad analysis of *rnh1Δ rnh2Δ* in combination with null mutations of the PRR factors *rad18* and *pol32*. **D.** Drop test analysis of CPT sensitivity of *rad18* triple mutants.

PRR, NER but not NHEJ is required for the repair of CPT mediated DNA damage

For viable triple mutants, we performed a more extensive analysis of how the formation of CPT-mediated DNA damage or Top1-depletion would affect the viability by drop test analysis.

Classification was carried out according to the following categories; as additive – the triple mutant was more sensitive than the double mutant; epistatic – the triple mutant has the same sensitivity as the double mutant; or suppressive – the triple mutant is less sensitive than the double mutant, or the triple mutant has an intermediate CPT sensitivity, between the double mutant and the single mutant (in the case of an exceptionally sensitive simple mutant). The results are summarized in Table 1.

The NHEJ-member triple mutants showed no synthetic sick interaction with the *RNH-* mutant and behaved differently upon treatment with CPT, e.g. the triple mutant with *ku70* showed an additive CPT sensitivity whilst the triple mutant with *lig4* suppressed to some extent the CPT sensitivity of the *RNH* double mutant (data not shown). This difference may be due to the additional role of Ku70 in telomere maintenance (for a review see (188)). However, we can conclude that NHEJ, in contrast to HR, is not an essential process in yeast lacking RNaseH activity.

Genetic analyses revealed that homologous recombination is a critical pathway in yeast that lack RNaseH activity, even in the absence of exogenous damage. The structure-specific endonuclease Mre11 plays an important role in the repair of DSBs by HR. As a component of the MRX complex (Mre11-Rad50-Xrs2), it is responsible for processing of the ends of the break to produce a free 3´ ssDNA end, which is essential for strand invasion and for subsequent extension by a DNA Pol. Mre11 has also been reported to be a specialized nuclease capable of removing bulky adducts from DNA ends (67,189), and may be able to cleave the Top1 tyrosyl-DNA bond (190). Therefore, Mre11 could play a role in the repair of CPT-induced damage in yeast (67). Therefore, we were particularly interested to identify a synthetic lethal interaction of the *rnh1Δ rnh2Δ* double mutant with *mre11Δ* (Figure 24A). Subsequently, we crossed *rnh1Δ rnh2Δ* cells with *rad50Δ* and *xrs2Δ,* and identified synthetic lethal interactions with all the members of the MRX complex (Figure 24A).

	YPAD	CPT
WT	+++++	+++++
rnh1Δ rnh2Δ	+++++	+++

Replication

sic1Δ	+++++	ND
sic1Δ rnh1Δ rnh2Δ	SL	ND
clb5Δ	+++++	+++++
clb5Δ rnh1Δ rnh2Δ	+++	++++
rad27Δ	+++++	+++++
rad27Δ rnh1Δ rnh2Δ	SL	ND
mrc1Δ	+++++	+++++
mrc1Δ rnh1Δ rnh2Δ	+++	++
csm3Δ	+++++	+++++
csm3Δ rnh1Δ rnh2Δ	++++	++
tof1Δ	+++++	+++++
tof1Δ rnh1Δ rnh2Δ	++++	+++
top1Δ	+++++	++++
top1Δ rnh1Δ rnh2Δ	SL	ND
rrm3Δ	+++++	+++++
rrm3Δ rnh1Δ rnh2Δ	++++	++

rDNA related functions

fob1Δ	+++++	++++
fob1Δ rnh1Δ rnh2Δ	++++	++
hmo1Δ	+++++	++++
hmo1Δ rnh1Δ rnh2Δ	++++	++
rpa190-3	+++++	++++
rpa190-3 rnh1Δ rnh2Δ	+++++	++++
tof2Δ	+++++	+++++
tof2Δ rnh1Δ rnh2Δ	+++++	+++
rrn3-8	+++++	++++
rrn3-8 rnh1Δ rnh2Δ	+++++	++++
tdp1Δ	+++++	++++
tdp1Δ rnh1Δ rnh2Δ	+++++	++
nsr1Δ	+++++	+++++
nsr1Δ rnh1Δ rnh2Δ	+++++	+++
rpa12Δ	+++++	++++
rpa12Δ rnh1Δ rnh2Δ	+++++	++++
rpa49Δ	+++++	++++
rpa49Δ rnh1Δ rnh2Δ	+++++	++++
uaf30Δ	++++	++
uaf30Δ rnh1Δ rnh2Δ	++++	+++

Telomere related functions

rif2Δ	+++++	+++++
rif2Δ rnh1Δ rnh2Δ	+++++	++++
pif1-m2	+++++	+++++
pif1-m2 rnh1Δ rnh2Δ	+++++	+++++

NER

rad16Δ	+++++	+++++
rad16Δ rnh1Δ rnh2Δ	+++++	++
rad3-2	+++++	+++++
rad3-2 rnh1Δ rnh2Δ	+++++	++
rad1Δ	+++++	+++++
rad1Δ rnh1Δ rnh2Δ	++++	++

Checkpoints

rad9Δ	+++++	+++++
rad9Δ rnh1Δ rnh2Δ	+++++	++
chk1Δ	+++++	+++++
chk1Δ rnh1Δ rnh2Δ	+++++	++
tel1Δ	+++++	+++++
tel1Δ rnh1Δ rnh2Δ	+++++	++
rad24Δ	+++++	+++
rad24Δ rnh1Δ rnh2Δ	++++	++
dun1Δ	+++++	+++++
dun1Δ rnh1Δ rnh2Δ	++++	+++
mec1Δ sml1Δ	+++++	+++
mec1Δ sml1Δ rnh1Δ rnh2Δ	++++	++
sml1Δ	+++++	++++
sml1Δ rnh1Δ rnh2Δ	+++++	+++
swe1Δ	+++++	+++++
swe1Δ rnh1Δ rnh2Δ	+++++	++++
mad1Δ	+++++	+++++
mad1 Δrnh1Δ rnh2Δ	+++++	+++

PRR

pol32Δ	+++++	+++++
pol32Δ rnh1Δ rnh2Δ	SL	ND
rad18Δ	+++++	++++
rad18Δ rnh1Δ rnh2Δ	+++	++
shu1Δ	+++++	+++++
shu1Δ rnh1Δ rnh2Δ	+++++	++

NHEJ

ku70Δ	+++++	+++
ku70Δ rnh1Δ rnh2Δ	+++++	++
lig4Δ	+++++	+++++
lig4Δ rnh1Δ rnh2Δ	+++++	++++

Recombination

rad52Δ	+++++	+++
rad52Δ rnh1Δ rnh2Δ	SL	ND
rad51Δ	+++++	++
rad51Δ rnh1Δ rnh2Δ	++++	+
exo1Δ	+++++	++++
exo1Δ rnh1Δ rnh2Δ	++++	+
rad59Δ	+++++	++
rad59Δ rnh1Δ rnh2Δ	++++	+
mus81Δ	+++++	++
mus81Δ rnh1Δ rnh2Δ	++++	+
mre11Δ	+++++	+
mre11Δ rnh1Δ rnh2Δ	SL	ND
srs2Δ	+++++	+++
srs2Δ rnh1Δ rnh2Δ	+++	+
sgs1Δ	+++++	+++++
sgs1Δ rnh1Δ rnh2Δ	+++++	++
top3Δ	+++++	++
top3Δ rnh1Δ rnh2Δ	++++	++
sae2Δ	+++++	++
sae2Δ rnh1Δ rnh2Δ	++++	+
siz1Δ	+++++	+++++
siz1Δ rnh1Δ rnh2Δ	+++++	++

Table 1. Analysis of the CPT sensitivity of *rnh1Δ rnh2Δ* triple mutants. Triple mutants were obtained by genetic crosses and tested for sensitivity to CPT by drop test assay. Sensitivity was scored as SL synthetic lethal/unviable; + severe growth defect/ very CPT sensitive; +++ moderate CPT sensitivity; +++++ normal growth, as WT; ND not determined. Growth of the triple mutants was compared to growth of the *rnh1Δ rnh2Δ* double mutant, whose CPT sensitivity was scored as +++. Light gray shading represents an additive effect and dark gray shading represents suppression of CPT sensitivity. PRR, post-replicative repair; NER, nucleotide excision repair, NHEJ, non-homologous end joining.

100% of *mre11Δ* and *xrs2* triple mutants were lethal, and 86% of *rad50* triple mutants. In addition, 39% of *mre11Δ rnh2Δ*, 50% of *rnh2Δ rad50Δ* and 33% of *rnh2Δ xrs2Δ* were synthetic lethal, revealing important interactions of the RNaseH enzymes with the MRX end-processing complex under normal conditions. Mre11 is believed to be recruited to DSBs by the endonuclease Sae2. Sae2 itself possesses endonuclease activity and is thought to be involved in processing of 3´ends for ssDNA tail generation (191). In a yeast deletion screen, Deng *et al.* identified deletion of *sae2* as one of the most CPT sensitive (ranked 6th out of the 4728 deletion strains tested) and suggest that Sae2 acts in a pathway redundant to Tdp1 or Rad1 to repair CPT-induced lesions. In fact, it has been reported that Sae2 is able to cleave off by endonucleolytic action the Top1 enzyme covalently bound at the 3´ end of the SSB, to create an appropriate end for repair and/or strand invasion (192). The structure-specific endonuclease Mus81 (acting with Mms4) has also been implicated in repairing the Top1-DNA complex by resecting the DNA ends where Top1 is covalently attached (66). Additionally, Exo1 has been shown to perform 3´end resection roles (193-195). We identified interesting interactions with the end-processing factors Mus81, Exo1, and Sae2 (Figure 24B), with roles in recombinational repair. The single mutants were already extremely sensitive to CPT, suggesting that these factors play a role in the processing of CPT damage, compatible with the published data for these mutants. However, the triple mutants were even more CPT sensitive in combination with the *RNH* double mutant and showed a synthetic sick interaction with the RNH enzymes (data not shown). Together these results highlight a key role for end-processing factors, and the recombinational repair machinery in general, in yeast cells lacking RNaseH activity under normal growth conditions as well as for the repair of CPT-induced lesions.

Additionally, we observed that mutants affected in PRR (*rad18Δ* and *shu1Δ*) became highly sensitive to CPT treatment. The PRR pathway allows the bypass of DNA lesions so that DNA replication can resume, through an error-prone translesion synthesis (TLS) or error-free template switch mechanism (196,197). Both pathways are controlled by Rad6 and Rad18 (95,96) and mediated by the mono- or poly-ubiquitination of PCNA, respectively (198). We found a major interaction with the E3 ubiquitin ligase Rad18. The *rad18Δ rnh1Δ rnh2Δ* triple mutant had a significant synthetic growth defect, including a slow growth phenotype on rich medium and an increased sensitivity to CPT (Figures 25C and 25D). However, we decided not to investigate interactions with other members of the *RAD6* epistasis group further in this study, since contributions of the template switch and TLS pathways to the genomic stability of *RNH-* mutants had been published recently by another group (99). Nevertheless, we did ensure that the function of Rad18 was not contributing to the origin-independent replication events observed in this study. We demonstrated by 2D-gel that replication bubbles still appeared when the *rad18* triple mutant was released from G1 block in the presence of CPT (Figure 25B, blue arrows). In fact, the replication bubbles increased in intensity during the timecourse, persevering until 180 minutes and possibly longer (data not shown). We conclude that *RAD18-RAD6* mediated PRR is important for the fitness of RNaseH lacking yeast (this study, and (99)), and PRR pathways may play a role in the repair of single-stranded gaps and replication-blocking Top1-DNA lesions introduced by CPT. However, the origin-independent replication initiation observed in the *RNH-* mutants is not dependent on Rad18, and the higher intensity bubble arcs suggest that absence of template switching activity may even channel lesions into an alternative pathway that encourages TIR events.

Break induced replication (BIR) is a PRR pathway capable of repairing collapsed replication forks, where homology only exists on one side of the DSB, or where only one of the two free DNA ends can find homology for strand invasion (for a review see (199)). The non-essential subunit of DNA Polδ, Pol32, has been shown to play an important role in BIR (200), although it is dispensable for normal DNA replication and DSB repair (200). We were unable to recover

any viable *pol32Δ rnh1Δ rnh2Δ* triple mutants (Figure 25C). This result indicates that Pol32 is essential for the survival of yeast cells lacking RNaseH activity, and also implies that BIR may be an important mechanism in the *RNH-* mutants.

It is interesting to note that RNaseH lacking cells became more sensitive to CPT in the absence of the NER factors *rad1, rad3-2* and *rad16*. Rad16 codes for a protein that binds to damaged DNA and is involved in *t*ranscription-*c*oupled *r*epair (TCR), a subpathway of NER mediated DNA repair. Rad16 acts together with Rad7 and TCR-defects can only be detected in the absence of either repair factor (see (89) for a recent review on TCR). TCR has also been shown to be active on ribosomal DNA lesions (201), questioning if NER may facilitate the repair of CPT-mediated DNA lesions in the presence of RNA:DNA hybrids. There are various reports that NER factors can erroneously recognize and bind abnormal DNA structures, including R-loops (202), mistaking these for the intermediate bubble structures formed during NER. For example, the NER nucleases XPF-ERCC1 and XPG can cleave bubble structures at the duplex-single strand junctions, at the 5´side, and 3´side of the junction, respectively. Both XPF-ERCC1 and XPG have been shown to cleave RNA:DNA hybrids formed in the transcribed S regions of the class switch sequences (203).

Nucleolar activity and integrity is linked to CPT sensitivity

We found a rather striking correlation between CPT sensitivity and nucleolar function. Specifically, the lack of factors involved in rDNA replication and organisation (*fob1Δ, rrm3Δ, hmo1Δ* and *siz1Δ)* enhanced CPT sensitivity, while mutants impaired in rDNA/35S transcription (*uaf30Δ*, *rpa190-3, rrn3-8, rpa12Δ* and *rpa49Δ*) alleviated CPT hypersensitivity. The link between impaired RNA PolI transcriptional activity and CPT resistance is given by the fact that: Uaf30 is needed to assist RNA PolI in the initiation of rDNA transcription together with the core factor, the TATA-binding protein and Rrn3, (for a review see (204)); proficient recruitment of the Rrn3-RNA PolI complex to the 35S rRNA gene promoter requires Rpas12 and 49 (205); and mutants affected in Rpa190, the largest and catalytic core component of RNA

PolI, are also more CPT resistant at semi-permissive temperatures, as previously discussed in Chapter 1 (Chapter 1, Figure 21A).

Although the rDNA array on cXII contains approximately 150 repeats of the rDNA locus, under normal conditions only about 50% of the 35S rRNA genes are active (206). Hmo1 is a high-mobility group protein found to bind across the 35S rDNA sequence that has a structural role in the formation of rDNA-specific chromatin (207). In fact, actively transcribed rRNA genes are largely devoid of histone molecules (206,208,209), and instead associate with Hmo1 (210), although not all studies concur on this matter (211). Work by Takehiko Kobayashi´s group has shown that inactive ribosomal genes are necessary since transcription by RNA Pol I blocks binding of cohesin and condensin (75), important for chromosome segregation and chromosome condensation, respectively (212). In combination with the *rnh1Δ rnh2Δ,* the *hmo1* triple mutant showed a synthetic sick phenotype and an additive CPT sensitivity. Therefore, as previously described for Fob1 and Rrm3 (Chapter 1, Figure 13), the role of Hmo1 in maintaining the structural integrity of the rDNA locus seems to be an important contributory factor to the sensitivity to CPT of the *rnh1Δ rnh2Δ* mutants.

In chapter 1 we described that the regulation of rDNA repeats was significantly affected in yeast lacking RNaseH activity (Chapter 1, Figure 13). The lack of factors involved in rDNA repeat stability (*mus81Δ, tof2Δ, sgs1Δ* and *top3Δ*) had an additive effect such that the corresponding triple mutants were further sensitized to CPT. Mus81 has key roles both in the quality control of replication forks at the rDNA and in the maintenance of rDNA repeat number (213), and from our genetic analyses we observed that the *mus81* triple mutant was synthetic sick and extremely CPT sensitive. Furthermore, interactions with *tof2,* required for rDNA silencing, and *sgs1-top3,* needed to maintain the integrity of rDNA repeats (214) and prevent rDNA recombination (215), both led to an increased CPT sensitivity.

The synthetic growth defect of *fob1Δ rnh1Δ rnh2Δ* mutants is especially interesting, because it suggests that collision of the replication and transcription machineries could increase torsional

stress in the absence of the replication fork blocking activity (143). Sogo and co-workers have shown that the number of active copies can be influenced by temperature, growth media, and growth phase (216). For example, the transcription of rRNA and ribosomal proteins coding genes increases after yeast are shifted to rich medium (217). A temperature shift from 30º to 37ºC also causes an increase in growth rate, and silencing of rDNA copies is reduced, leading to more actively transcribed 35S genes to deal with the increased demand for ribosome biogenesis, with a subsequent increase in negative supercoiling (218). To see if growth conditions affect CPT sensitivity, we therefore incubated *rnh1Δ rnh2Δ* yeast cells in the presence of CPT at different temperatures (Figure 26A) and observed an increase in the CPT sensitivity of the *RNH-* mutant with increased temperatures. This experiment relates the CPT sensitivity of the *RNH-* mutants to rDNA transcription suggesting that increasing the number of transcribed 35S genes increases sensitivity to CPT.

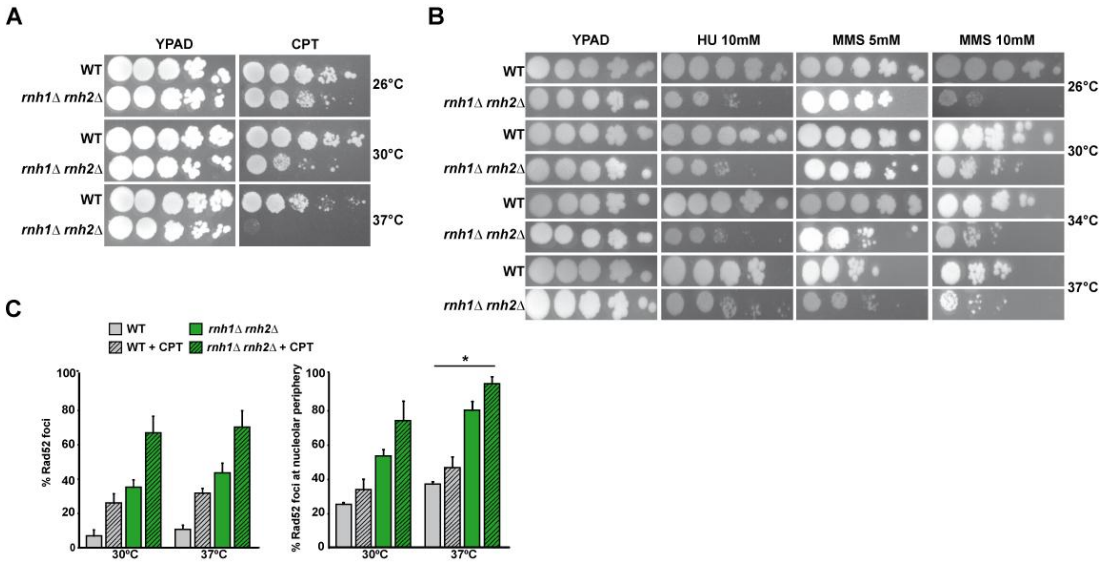

Figure 26. Growth at higher temperatures further sensitizes *rnh1Δ rnh2Δ* mutants to CPT. A. 10-fold serial dilutions of cells grown for 3 days on YPAD or YPAD-containing 5µg/ml CPT at the indicated temperatures. **B.** 10-fold serial dilutions on plates with 10mM HU, 5mM MMS or 10mM MMS at the indicated temperatures. **C.** Percentage of Rad52-YFP foci counted in exponentially growing cells growing at 30º or 37ºC with or without the presence of 10µg/ml CPT (3hr treatment) (above). Nuclear versus nucleolar Rad52-YFP foci were determined according to co-localization with the nucleolar Nop1-mRFP marker. The proportion of rDNA-associated foci in the *RNH-* mutant upon CPT treatment increased significantly from 30º to 37ºC (p=0.0166). Data represent mean ± SD, from at least three independent experiments.

To study whether the increase in CPT sensitivity with higher temperature was specific to CPT or a general effect, similar drop test analyses were performed with the genotoxic agents MMS and HU. Raising the temperature from 30º to 37ºC sensitized WT and *rnh1Δ rnh2Δ* mutants to the DNA alkylating agent MMS but not to HU (Figure 26B).

Ide *et al*. previously demonstrated that sensitivity to MMS depends on transcription by RNA Pol I and state that increased rDNA transcription may be toxic due to greater sensitivity to DNA damaging agents (75). Therefore, we can speculate that higher RNA PolI transcription rates are responsible for the increased sensitivity to MMS observed at 37ºC in an RNA:DNA hybrid independent manner. Notably, growth at 30°C or 37°C did not change the number of cells with damaged DNA as determined by Rad52-YFP foci formation in both the WT and *rnh1Δ rnh2Δ* cells (Figure 26C). However, growth at 37ºC caused a marked increase in the proportion of Rad52-YFP foci that co-localized with the Nop1 nucleolar marker protein, suggesting an increase in the proportion of rDNA-associated DNA damage. Thus, it is possible that increased rDNA transcription exacerbates genomic instability of the rDNA locus at the higher temperature.

DISCUSSION for CHAPTER 2

HR and PRR are Critical Pathways in Yeast Lacking RNaseH Activity

In Chapter 1 of this thesis we described how unprocessed R-loops could act as sites of replication initiation, demonstrating a critical role for the RNaseH enzymes and Top1 in preventing unscheduled TIR events and thus maintaining genomic stability. We then sought in this Chapter, by genetic analysis, to identify activities needed for survival in the absence of *RNH*. *RNH* double mutants display negative genetic interactions or increase the CPT sensitivity of mutants affected in genes coding for proteins involved in NER, HR, and PRR pathways. HR was identified as a critical pathway in yeast lacking RNaseH activity, since both Rad52 and *MRX*-complex activity became essential even in the absence of exogenous DNA damage. These observations suggest *RNH-* cells accumulate toxic DNA intermediates that are a substrate for HR. R-loops could also be channeled into repair pathways that convert them into toxic DNA intermediates. Yet, it remains to be determined if TIR-intermediates are HR dependent. HR could contribute to the formation or resolution of TIR-intermediates and it would be interesting to test for this possibility, for example by the use of Rad52- or Rnh2-degron constructs. Surprisingly, *RNH-* cells were still viable in the absence of Rad51 (see Figure 25), the bacterial RecA homologue, which binds to ssDNA and catalyzes the search for and strand invasion of homologous sequences (219). Importantly, we detected bubble-shaped replication intermediates in *rad51Δ rnh1Δ rnh2Δ* mutants suggesting that TIR is Rad51-independent. However, Rad51 seems to be essential in the repair of Top1-mediated DNA lesions, seen by the acute CPT sensitivity of *rad51Δ* mutants (Figure 25 and (66)). It is therefore perhaps surprising that we did not detect more TIR molecules in the *rad51Δ* background. This result would suggest that TIR is not initiated by DNA repair of a Top1cc but rather due to the lack of Top1 activity, perhaps due to an increase in torsional stress.

As described in Chapter 1 (Figure 23) two alternative mechanisms could account for TIR, including a direct assembly of the replication machinery at the R-loop, or by recombination-dependent replication. TIR appears to be a post-replicative event, as bubble arcs were only observed in cells held in late S/G2 phase of the cell cycle, and apart from *RAD52*, genetic analyses revealed that *POL32* is essential for the viability of *RNH-* yeast. Rad52 and Pol32 are required for break-induced replication (BIR), a mechanism of replication-dependent repair (220). BIR was originally studied in prokaryotes (where it is referred to as recombination-dependent repair (RDR)) as a mode of *oriC*-independent chromosomal replication, where the processing of arrested replication forks into a DSB led to replication restart (reviewed in (221)). In the BIR described in yeast, a DSB with only one free end initiates repair by strand invasion of the 3´end into an intact homologous duplex DNA, priming DNA replication to the chromosome end (reviewed in (199)). The complex lesion of a Top1cc bound to the 3´ end of a DSB could potentially explain why there is only one free end available for strand invasion. Rad52-mediated strand invasion could occur by annealing between the single-stranded strand and the open and stable R-loop structure, in the absence of Rad51 (222), perhaps assisted by Rad59 activity (223). According to Lydeard *et al.*: "*Two of the major questions regarding the DNA synthesis steps of BIR are: 1. What DNA helicases are responsible for unwinding the template DNA? 2. How is the replication fork established in the absence of an origin?*" (220). In our opinion, R-loops could open up the DNA, particularly in combination with a loss of Top1 activity and associated increase in torsional stress, and provide a starting point for replication, as described for prokaryotes, thereby offering a solution to both of these questions.

Mrc1 is important for viability in the absence of RNaseH activities

The observation that *RNH-* mutants require a functional *MRC1*-complex to combat CPT toxicity suggests that replication fork stability may be important for the fitness of yeast lacking RNaseH activity. A functional *MRC1*-complex is important for both cell viability and CPT resistance in the absence of RNaseH activities. This was a rather surprising observation given that single

mutants of the *MRC1* complex do not display sensitivity to CPT. Mrc1, together with Csm3 and Tof1, exists as an integral member of the replisome (224), maintaining the stability of stalled RFs and promoting subsequent DNA repair events by activation of Rad53-dependent intra S replication checkpoint (109). These observations made it likely that RNA:DNA hybrids not only constrain genome stability but also interfere with cell cycle progression (for further results and discussion on the *MRC1*-complex see Chapter 3). Importantly, TIR-mediated replication intermediates were evident in CPT treated *mrc1* triple mutants, suggesting that TIR events do not constrain the viability of these cells. R-loops could hinder replication fork progression leading to replication fork break-down. The Sgs1 and RecQ-like helicases have been suggested to play roles in maintaining lagging strand polymerases at stalled forks (225) via interactions with the ssDNA binding complex, RPA (226). The differences observed in the CPT sensitivity between *sgs1* and *top3* triple mutants, may suggest that the Top3-independent RF stability function of Sgs1 may be important in response to CPT treatment in the *RNH-* mutants, however, we have not investigated further the roles of Sgs1 in yeast lacking RNaseH activity. Rrm3 belongs to the Pif1-class of helicases and is needed for the bypass of protein-DNA interaction sites, and whose absence leads to the accumulation of paused replication forks in the rDNA (147). *In vitro* studies showed that Pif1 is able to resolve RNA:DNA hybrids (57), but notably, *pif1-m2* triple mutants are viable and CPT resistant suggesting that, at least for ribosomal DNA, Pif1 is dispensable for RNA:DNA hybrid processing *in vivo*. Interestingly, mutations in the *E.coli* mutation Pif1 homologue *recG* are synthetic lethal in combination with mutation to *rnhA* (46). Recent reports suggest a role for Pif1 in BIR (227), and therefore the difference in the requirement for Pif1 and Pol32 activity may reflect the need for BIR for R-loop tolerance. Mutations to Pol32 specifically affected the rDNA array with no detectable alterations to other chromosomes (228), suggesting that Pif1-independent but Pol32-dependent BIR may be of particular relevance for stability of the rDNA region of the genome.

Loss of Rnh2 Activity is more detrimental than Loss of Rnh1

We find that the absence of Rnh2 activity generally had a greater contribution to viability and CPT sensitivity in combination with DNA replication and/or DNA repair mutants, than the absence of Rnh1. For example 39% of *mre11Δ rnh2Δ*, 50% of *rnh2Δ rad50Δ* and 33% of *rnh2Δ xrs2Δ* mutants were inviable, while 100% of the corresponding *rnh1* double mutants were viable and only affected in growth. The same was true for cells lacking Srs2, where 96% of the *srs2Δ rnh2Δ* double mutants were inviable, but 100% of the *srs2Δ rnh1Δ* double mutants were found to be viable. These results emphasize that although Rnh1 and Rnh2 have overlapping specificities in removing transcription-associated R-loops, Rnh2 has additional functions, including the removal of misincorporated rNMPs that contribute to genomic stability (14). Interestingly, deletion of *RNH1* was reported to be more deleterious than the deletion of *RNH201* in combination with defects on RNA biogenesis factors (21). It may be possible to take advantage of the Rnh201 P45D-Y219A separation-of-function mutant that can remove R-loops but not rNMPs to see if impaired rNMP repair would still constrain viability in the absence of Top1 (229). The lack of Rnh201 may have additive effects, weakening protein interactions of its accessory subunits, Rnh202 and Rnh203, with other factors. For example, Rnh202 has been reported to interact with the cyclin-dependent kinase Cak1, that has roles in passage through the G2/M stages of the cell cycle; and the replication fork clamp, *p*roliferating *c*ell *n*uclear *a*ntigen complex (PCNA) (12), the sliding clamp for DNA Polδ and an interaction site for other replication and repair proteins (for a review see (230)). PCNA itself is responsible for the recruitment of PRR (231), NER (232), and cohesion (233) factors. In addition, PCNA interacts recruits Srs2 (234), playing a role in the repair of replicative damage by directing the repair of stalled RFs away from HR and into *t*rans*l*esion **s**ynthesis (TLS) and template switching pathways, both shown to be important repair pathways for yeast lacking RNaseH activities (99).

Persistent R-loops may impede TCR

Rad16, together with Rad7, has a role in both global genomic repair (GGR) and TCR. TCR-defects can only be detected in the absence of either repair factor (see (89) for a recent review on TCR). Interestingly the *rad16* triple mutant was found to be more sensitive to CPT than the *RNH* double mutant. This result would suggest that yeast have defective TCR in the absence of RNaseH activity, and TCR may be particularly impeded at the rDNA locus. We would like to confirm this observation in a *rad7* triple mutant, as it would suggest that persistent R-loops impede RNA Pol progression through transcribed regions and could lead to more lesions than TCR can deal with.

Nucleolar Function Affects CPT Sensitivity and Viability

Ribosomal DNA function was shown to have a major influence on CPT sensitivity in Chapter 1, and in this chapter we analysed many different factors linked to rDNA organisation and transcription. We observed the reproducible pattern that a disruption of rDNA organisation enhanced CPT sensitivity of *RNH-* mutants, whereas the down-regulation of RNA PolI transcription alleviated CPT sensitivity. Together these results confirm that proficient transcription of the rDNA locus is crucial for CPT-mediated genotoxicity and reveal the rDNA as a major contributory factor of CPT-mediated DNA damage.

As the rDNA constitutes such a large part of the eukaryotic genome, it is perhaps not surprising that RNA PolI-mediated R-loops in the rDNA can have such a major impact on cell viability. In Chapter 3 of this thesis we will investigate in more detail by what means viability is constrained in the *RNH-* mutants.

RESULTS

CHAPTER 3 – Yeast lacking RNaseH activity exhibit altered cell cycle progression

RNH lacking cells suffer from premature S-phase entry

Cell cycle analysis of *rnh1Δ rnh2Δ* yeast revealed that the *RNH* double mutant consistently showed a much faster S-phase transition than the WT following release from α-factor synchronization (Figure 27A, best observed at the 30 minute time point). This highly reproducible, premature progression through S-phase was observed in both *BAR1*$^{+}$ and *bar1Δ* strains, and was CPT independent.

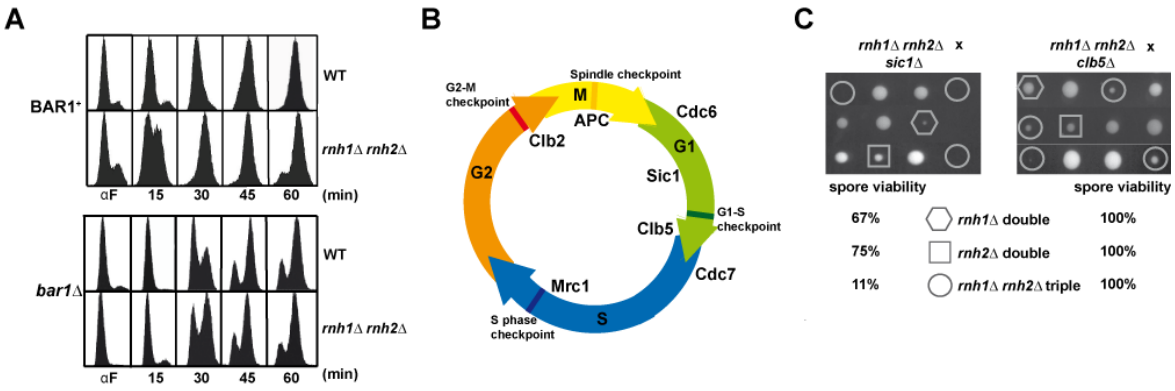

Figure 27. Yeast lacking RNase H activity show a premature S-phase transition. **A.** Flow cytometry analysis of strains following release from α-factor in YPAD. **B.** Representation of the *S.cerevisiae* cell cycle with approximate time of activity for different cyclins and checkpoint factors. **C.** Genetic analysis of *sic1Δ rnh1Δ rnh2Δ* and *clb5Δ rnh1Δ rnh2Δ* tetrads.

An earlier activation of standard origins of replication, leading to a precipitated G1/S transition, would make the S-phase appear "shorter". *CDC28* is an essential gene, encoding the catalytic subunit of the main CDK factor, which acts as the major coordinator of the yeast cell cycle (reviewed in (235)). The activity of Cdc28 is controlled post-translationally via associations with many different regulators throughout the cell cycle. During G1, Sic1 binds to and inhibits the CDK Cdc28 (Figure 27B). Cells are able to enter S-phase and begin DNA

replication by phosphorylating Sic1, which targets it for ubiquitin-mediated degradation (236), thus permitting Cdc28 activity and the G1 to S-phase transition. Mutants in yeast *sic1* exhibit premature entry into S-phase due to unusually high Cdc28 activity (237). We studied the interaction of *RNH-* mutants with the cyclin-dependent kinase inhibitor (CKI) *SIC1* to examine the possibility that yeast lacking RNaseH activity present a faster transition through S phase due to an accelerated entry into S phase. Interestingly, we revealed synthetic lethal interactions between the *RNH* double mutant and *sic1Δ* by genetic analysis (Figure 27C) and furthermore, deletion of *sic1* was lethal in combination with the *rnh1Δ* or *rnh2Δ* simple mutants in 33% and 25% of the cases, respectively. Also of interest was the observation that the *RNH* double mutant is synthetically sick with the B-type cyclin Clb5 (Figure 27C). Like Sic1, Clb5 also acts to regulate Cdc28 levels and promotes the initiation of DNA synthesis, however, contrary to mutation of *sic1,* loss of *clb5* results in an extension of the S-phase due to the inability to activate late origins of replication (238). Collectively, these results suggest that *rnh1Δ rnh2Δ* mutants enter early into S-phase, and the G1 to S-phase transition activity of Sic1, and to a lesser extent Clb5, is essential to maintain the viability of cells in the absence of RNaseH activity.

An earlier activation of standard origins of replication, leading to a precipitated G1/S transition, would make the S-phase appear "shorter". *CDC28* is an essential gene, encoding the catalytic subunit of the main CDK factor, which acts as the major coordinator of the yeast cell cycle (reviewed in (235)). The activity of Cdc28 is controlled post-translationally via associations with many different regulators throughout the cell cycle. During G1, Sic1 binds to and inhibits the CDK Cdc28. Cells are able to enter S-phase and begin DNA replication by phosphorylating Sic1, which targets it for ubiquitin-mediated degradation (236), thus permitting Cdc28 activity and the G1 to S-phase transition. Mutants in yeast *sic1* exhibit premature entry into S-phase due to unusually high Cdc28 activity (237). We studied the interaction of *RNH-* mutants with the cyclin-dependent kinase inhibitor (CKI) *SIC1* to examine the possibility that yeast lacking RNaseH activity present a faster transition through S phase

due to an accelerated entry into S phase. Interestingly, we revealed synthetic lethal interactions between the *RNH* double mutant and *sic1Δ* by genetic analysis (Figure 27C). Deletion of *sic1* was also lethal in combination with the *rnh1Δ* or *rnh2Δ* simple mutants in 33% and 25% of the cases, respectively, indicating a significant interaction between RNaseH activity and Sic1. Also of interest was the observation that the *RNH* double mutant is synthetically sick with the B-type cyclin Clb5 (Figure 27C). Like Sic1, Clb5 also acts to regulate Cdc28 levels and promotes the initiation of DNA synthesis, however, contrary to mutation of *sic1,* loss of *clb5* results in an extension of the S-phase due to the inability to activate late origins of replication (238). Collectively, these results demonstrate that *rnh1Δ rnh2Δ* mutants enter early into S-phase, and the G1 to S-phase transition activity of Sic1, and to a lesser extent Clb5, is essential to maintain the viability of cells in the absence of RNaseH activity.

R-loop formation partially overcomes cdc7-4 temperature sensitivity

The initiation of DNA replication in eukaryotic cells during S phase is regulated by 'origin licensing', and requires the sequential assembly of pre-RC proteins, such as Cdc7 and Cdc6, at the ARS. Cdc6 is an essential component of the pre-RC and acts prior to Cdc7 kinase activation, loading the Mcm2-7 proteins onto the ORC (239,240). Firing from normally inactive origins, or the formation of entirely new sites of replication initiation could account for the completion of DNA synthesis more quickly in the absence of RNaseH activity. We questioned whether the origin-independent, R-loop-mediated replication initiation (see Chapter 1), could by-pass the need for canonical origin firing. To address this question we created a *cdc7-4 rnh1Δ rnh2Δ* triple mutant (Figure 28A). The *cdc7-4* allele permits growth at 23ºC (permissive temperature) but not at 30ºC (4) because the Cdc7 kinase is essential for the opening up and firing of replication origins by phosphorylation of Mcm2-7 proteins (4,241). Notably, restrictive temperature was shifted from 30°C to 37ºC in the *cdc7-4 rnh1Δ rnh2Δ* triple mutant, indicating that R-loops could help to make replication origins more accessible to replication factors. Additionally, the CPT sensitivity of *cdc7-4 rnh1Δ rnh2Δ* mutants was comparable to

rnh1Δ rnh2Δ mutants at 23ºC, but this sensitivity was increased dramatically at 30ºC (Figure 28B). Interestingly, transcription through origins of replication has been shown to inactivate replication firing (242). It is conceivable, that R-loop stabilization within replication origins by CPT could have the same effect.

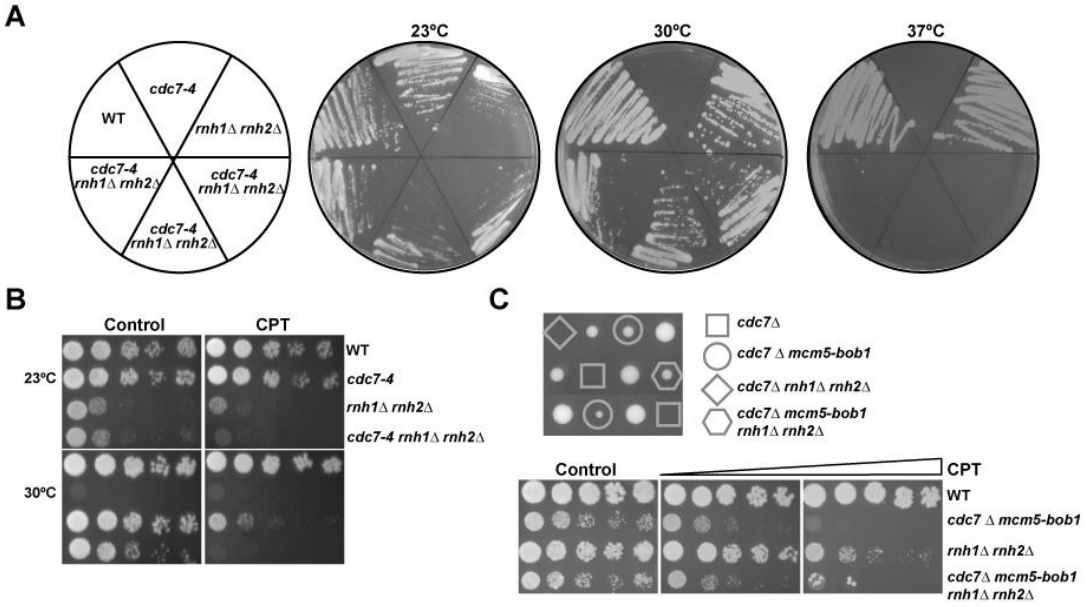

Figure 28. R-loop formation partially overcomes *cdc7-4* temperature sensitivity. A. Viability of *cdc7-4* simple and triple mutants grown at 23º, 30º, or 37ºC. **B.** Drop test analysis of *cdc7-4 rnh1Δ rnh2Δ* at 23º or 30º on YPAD or YPAD-containing CPT (5μg/ml). **C.** Tetrads (top) and drop test analysis for *cdc7Δ mcm5-bob1* quadruple mutant. Plates contained 0.5 or 1μg/ml CPT.

Besides its well-reported roles in replication initiation, Cdc7 also operates in post-replicative repair (PRR). Cdc7 is a member of the DNA damage tolerance *RAD6* epistasis group, associated with the TLS branch (243). It has been proposed that different *cdc7* alleles can result in hyper- or hypo-mutagenic phenotypes (244). To exclude the possibility that the PRR function of Cdc7 was interfering in the analysis of viability of the *cdc7-4 rnh1Δ rnh2Δ* mutant we opted to use a *cdc7Δ mcm5-bob1* strain. The function of Cdc7 in replication initiation is no longer essential in a *mcm5-bob1* (P83L) mutant (245), since presence of the *mcm5-bob1* allele bypasses the need for the phosphorylation and activation of the MCM helicase by Cdc7 kinase (246). Analysing the viable spores from genetic crosses between the *cdc7Δ mcm5-bob1* and *rnh1Δ rnh2Δ* yeast strains, we attained *cdc7Δ mcm5-bob1 rnh1Δ rnh2Δ* quadruple mutant spores (Figure 28B).

We confirmed the *mcm5-bob1* genotype by back-crossing the quadruple spore with a WT yeast strain: the ability to recover viable *cdc7Δ* spores from the back-cross meant that the yeast also carried the *mcm5-bob1* allele, originating from the quadruple spore from the first cross (results not shown). These analyses tell us that *cdc7Δ rnh1Δ rnh2Δ* yeast are inviable without the compensatory *mcm5-bob1* allele, and that Cdc7 kinase activity is essential in the *RNH-* mutant, as for the WT. Therefore, the origin-independent transcription-initiated replication events that we observe in the *RNH* double mutant do not bypass the need for normal replication initiation from origins in S-phase.

RNH- mutants are not held in G2/M in the absence of Mrc1 activity

The synthetic lethal interaction of *RNH-* mutants and *SIC1* suggested that cells may suffer from constrains that may be generated during replication and still be present when cells are in the next G1 phase. To assess for replication-associated DNA damage, we inactivated different S-phase specific checkpoint pathways including *rad9, chk1, tel1*, and *rad24*. No significant differences were observed in the cell cycle progression of the triple mutants tested; all the triple mutants exhibited a similar holding of cells in G2/M phase as per the *RNH* double mutant (data not shown), although they showed an additive CPT sensitivity (see Chapter 2, Table 1). Interestingly, we detected a synthetic lethal interaction of *RNH-* mutants with *MRC1* (see Chapter 2; Figure 24). Mrc1, *m*ediator of the *r*eplication *c*heckpoint, the homologue of human Claspin, associates with replication forks shortly after replication initiation, remaining during elongation as an integral part of the replication machinery (224) and has been shown to have a dual role, acting both as a component of the RF and as a mediator of the S/G2 checkpoint (247). Viable *mrcΔ rnh1Δ rnh2Δ* triple mutants notably manifested a different cell cycle progression profile to that of the *RNH* double mutant. The *mrc1Δ rnh1Δ rnh2Δ* triple mutant was able to re-enter G1-phase of the following cell cycle whilst the *RNH* double mutant remained held in late S/G2 (Figure 29A). Moreover, the *mrc1Δ rnh1Δ rnh2Δ* yeast exhibited an even more accelerated entry into and passage through the S-phase, compared to the *RNH* double mutant.

Furthermore, of significant interest was the finding that Mrc1 is important for cell survival in the absence of RNaseH enzymes. From tetrad analysis we detected that only 33% of triple spores were viable (Figure 29B). Remaining viable triple mutant spores have a growth defect, and interestingly, whilst the *mrc1Δ* itself is not CPT sensitive, elimination of *MRC1* in the *RNH* double mutant resulted in a highly CPT sensitive triple mutant (Figure 29C). These results suggest that Mrc1 activity is crucial in cells lacking RNaseH activity and can protect them from CPT-induced replication stress.

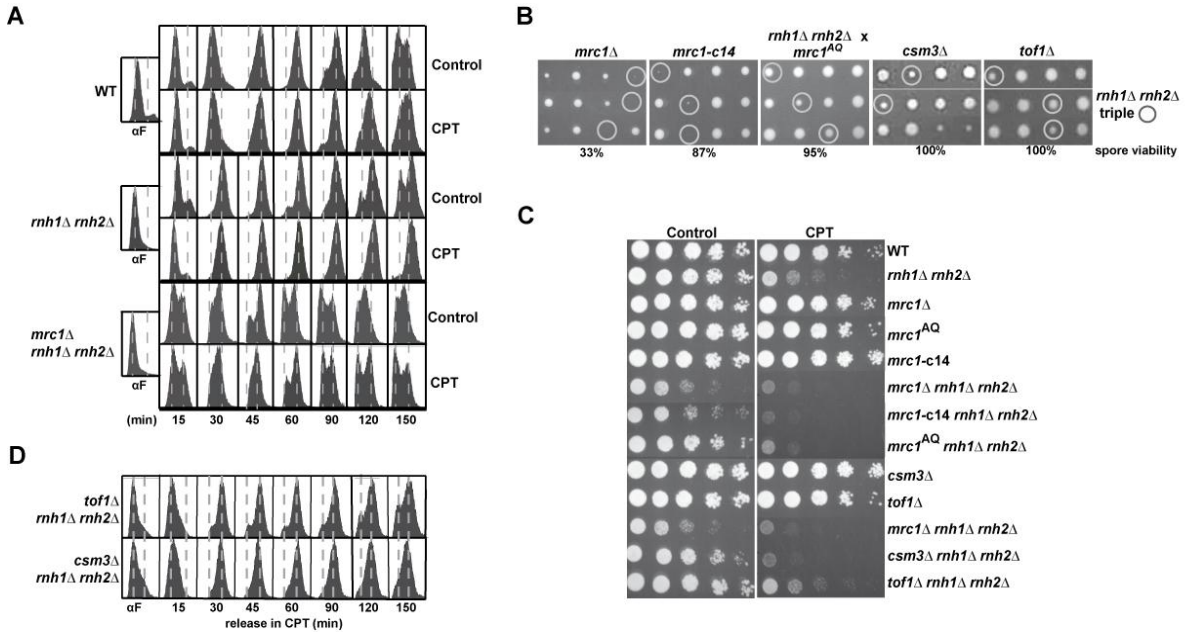

Figure 29. Mrc1 protects cells from CPT-induced replication stress. A. Flow cytometry analysis of *mrc1* triple mutant cells grown in the presence or absence of CPT following release from α-factor. **B.** Tetrad analyses of Mrc1 separation-of-function alleles (top) and Mrc1 mediator complex members (bottom). **C.** Drop test analysis of Mrc1 separation-of-function alleles (top) and Mrc1 mediator complex members (bottom). **D.** Flow cytometry analysis of Mrc1 mediator complex members.

Since *mrc1Δ rnh1Δ rnh2Δ* triple mutants did not arrest in late S/G2-phase in response to CPT (Figure 29A), their increased CPT sensitivity could reflect a problem in S/G2-dependent damage repair or RF stability. To discriminate between these possibilities, we took advantage of the Mrc1 separation of function mutants. Combination of the checkpoint-defective allele *mrc1^{AQ}*, which cannot be phosphorylated by the checkpoint kinases (248), and the RF stability mutant allele, *mrc1-c14* (249), with the *RNH* double mutant, resulted in an increased CPT

sensitivity. These results suggest that both S/G2-checkpoint and RF stability functions of Mrc1 contribute to CPT tolerance in the *rnh1Δ rnh2Δ* background. In contrast, only the triple mutant with the RF stability mutant allele, *mrc1-c14,* closely resembled the growth, CPT sensitivity and spore viability phenotypes of the *mrc1*Δ *rnh1Δ rnh2Δ* mutant (Figures 29B and 29C). The *mrc1-c14* triple mutant spores were affected negatively in growth with some lethality observed in meiotic segregants (87% viability of spores corresponding to triple mutants). Collectively, these results demonstrate that Mrc1 plays an important role in the stabilization of RFs in the *RNH-* mutant, and may be particularly important for the survival of CPT-induced lesions, and that both functions of Mrc1 are indispensable for the viability of yeast lacking RNaseH activity.

Mrc1 exists as an integral member of the replisome (224), with Csm3 and Tof1, as part of the Mrc1-mediator complex. Csm3 and Tof1 are specifically required for the association of Mrc1 with the RF, interacting directly with the MCM helicase, and thus play a central role in RF progression. The complex is also important in maintaining the stability of stalled RFs and promoting subsequent DNA repair events (224,247). Genetic interaction analysis revealed novel functional relationships between the RNaseH enzymes and all members of the Mrc1 mediator complex (Figure 29B). Triple mutants of *rnh1Δ rnh2Δ* with *csm3Δ* and *tof1Δ* were synthetic sick; triple mutants also exhibited extreme sensitivity to CPT, in contrast to the CPT resistant *csm3Δ* and *tof1Δ* single mutants (Figure 29C). Cell cycle progression of the *tof1Δ* triple mutant, upon release from G1 synchronization into media in the presence of CPT, was very similar to that previously observed for the *mrc1*Δ triple mutant (Figure 29D). In contrast, the *csm3Δ* triple mutant remained held in late S/G2, as for the *RNH* double mutant, suggesting a possible difference in functions for individual members of the complex in the absence of RNaseH activity. These results indicate that the replication fork stabilization function of Mrc1 (together with Tof1) is important in protecting cells from R-loop mediated replication constrains and, similar to its role in the response to osmostress (250), support a role for Mrc1 in the co-ordination of transcription and replication events in CPT treated *RNH-* mutants.

G2/M DNA damage- and morphogenesis checkpoints fail to hold RNH- cells in G2/M

The presence of RNA:DNA hybrids caused by the lack of RNaseH activity led to an accumulation of yeast cells in G2/M stages of the cell cycle. A large budded cell arrest can be triggered by the DNA damage checkpoint, or by activation of the morphogenesis or the spindle checkpoints, both of which would cause yeast to arrest as large budded cells with an undivided nucleus. Wee1-related kinases function in the highly conserved morphogenesis checkpoint that coordinates cell size and entry into mitosis. The budding yeast Swe1 kinase accumulates during the S-phase and can inhibit Clb2-Cdc28 (251); it is then targeted for proteasome-mediated degradation in late S/early G2-phase (252). Activation of the morphogenesis checkpoint in response to defects in cytoskeletal function or bud formation blocks Swe1 degradation (253), leading to Swe1-dependent phosphorylation of Cdc28, and delaying entry into mitosis (for review see (115)). Deletion of *SWE1* causes cells to enter prematurely into mitosis before sufficient growth has occurred (253), leading to the formation of abnormally small daughter cells. Conversely, we found that cell size of the *swe1Δ rnh1Δ rnh2Δ* triple mutant was actually increased and no difference was observed in the cell cycle progression of the *swe1* triple mutant compared to the *RNH* double (results not shown). Therefore, it seems improbable that the G2/M phase holding of the *RNH-* mutants is due to the activation of the morphogenesis or size checkpoint. Nevertheless, removal of the morphogenesis checkpoint did slightly favour the survival of yeast lacking RNaseH activity in response to CPT (results not shown).

The S-phase DNA damage and DNA replication checkpoints employ many common factors. The effector kinase, Rad53, becomes hyperphosphorylated in response to replication stress, acting to stabilize stalled replication forks and prevent the activation of later origins of DNA replication. Mrc1 acts by transducing signals from Mec1 to Rad53, activating Rad53 upon fork stalling (109). In response to DNA damage, Rad53 is also phosphorylated and activated, and the dNTP levels in the cell are upregulated. Dun1 is an effector kinase downstream of Rad53,

whose activation leads to an up-regulation in the transcription of the ribonucleotide reductase (RNR) genes. The RNR complex catalyzes the rate-limiting step in the synthesis of dNTPs from NTPs, a process essential for both DNA repair and for normal replication. In addition, Sml1, an inhibitor of RNR, is degraded in response to DNA damage (254). Sml1 is the substrate for Dun1, making Dun1 directly responsible for Sml1 phosphorylation and its subsequent degradation (255). Analysis of genetic interactions revealed that the triple mutant with *dun1* resulted in a synthetic sick interaction (see Chapter 2; Table 1), yet no difference was observed in the CPT sensitivity of the triple mutant as compared to the *RNH* double mutant; the *sml1* triple was also as sensitive to CPT as the *RNH* double (results not shown). The observation that triple mutants are not more sensitive to CPT than the *RNH* double mutant could indicate an epistatic interaction between the RNaseH enzymes and control of cellular dNTP levels.

Detection of the "active" phosphorylated form of Rad53 by Western blot is widely used to follow S-phase checkpoint activation. Hyper-phosphorylated Rad53 can be detected as a shift in the mobility of the 92 kDa band corresponding to Rad53 on a protein gel. We examined whether Rad53 is activated in *RNH-* mutants by performing a Western blot against the phosphorylated form of Rad53 (Figure 30, upper panel). We observed that HU treatment of WT yeast cells caused a positive shift in Rad53 mobility related to phosphorylation and thus checkpoint activation. In contrast to cellular treatment with other DNA damaging agents, CPT-induced DNA lesions are not sensed by the *intra*-S-phase checkpoint protein Rad53 (256) and accordingly, we see no activation of Rad53 for the WT upon CPT treatment. However, we did note a minimal shift in the mobility of the Rad53 bands for the simple mutants *rnh1Δ* and *rnh2Δ* in response to CPT treatment, and a slight shift for the CPT treated *rnh1Δ rnh2Δ* double mutant.

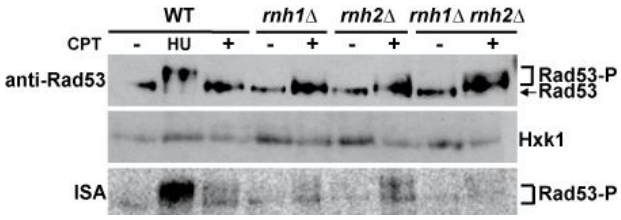

Figure 30. Western analysis against Rad53 (top) and Rad53 *in situ* kinase assay (ISA; below). HU treatment was used as positive and hexokinase (Hxk1) as loading control. Experiments performed by Nestor García Rodríguez.

To confirm whether CPT treatment of the *RNH-* mutants is able to activate the replication checkpoint we monitored Rad53 kinase activation directly using the Rad53 *in situ* kinase assay (ISA; (257)) (Figure 30, lower panel). We saw a weak Rad53 autophosphorylation in response to CPT-treated WT, *rnh1Δ, rnh2Δ* and *rnh1Δ rnh2Δ* yeast, albeit to lower levels than following HU treatment of the WT. These results support the previously described minor phosphorylation of Rad53 for the *rnh1Δ rnh2Δ* double mutant following HU or MMS treatment (99) and suggest that CPT leads to an increased replicative stress in the *RNH-* mutants. However, the threshold of hyper-phosphorylation of Rad53 necessary to trigger the S-phase DNA damage checkpoint is not reached, as the *RNH* double mutant, even following CPT treatment, shows no delay in S-phase progression.

The degradation of cyclin Clb2 is delayed in RNH- mutants

The protein levels of Sic1 following release from α-factor were monitored in yeast lacking RNaseH activity. Sic1 multiple phosphorylation and subsequent degradation is essential for the G1/S transition and the initiation of DNA replication. The timing of Sic1 degradation for the double mutant seemed similar to the WT (Figure 31A), and thus, would not account for the accelerated S-phase progression in our *RNH-* mutants. However, the *RNH* double mutant appeared to have lower levels of Sic1 throughout the cell cycle.

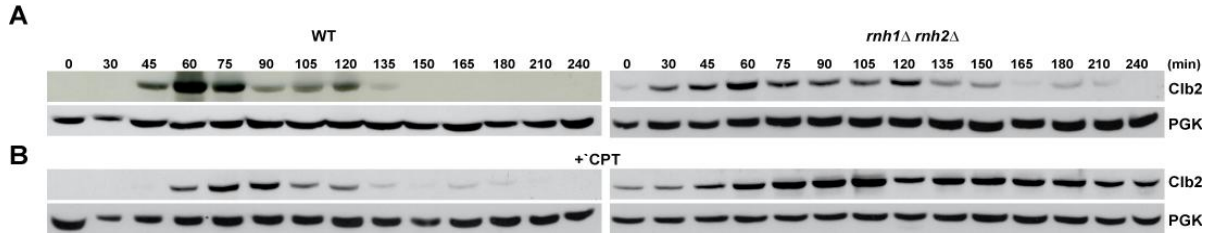

Figure 31. Western blot analysis of Sic1 and Clb2. **A.** Sic1 and Clb2 levels following release from α-factor. α-factor was re-added 60 minutes after release. **B.** Release of yeast cells in the presence of 10μg/ml CPT. Western analyses performed by Marta Muñoz Barrera.

The B-type cyclins Clb1-4 are required for mitotic events, such as spindle morphogenesis, but must be down-regulated for cytokinesis to take place (reviewed in (258)). Clb2 is proteolytically degraded in early anaphase, necessary for the exit from mitosis and re-entry into G1 of a new cell cycle (259). In response to microtubule destabilizing drugs, mitotic arrest of WT cells is maintained by high levels of Clb2 and Cdc28 kinase activities (260). We monitored the levels of Clb2 by Western blot during the cell cycle to investigate whether a disregulation of Clb2 levels could account for the prolongation of cells in late G2/M-phase in the *RNH-* mutant. Western blot analysis (Figure 31A) shows that Clb2 protein appears at 45 minutes post-release and is degraded from 135 minutes in the WT. However, in the double mutant, Clb2 protein was detectable even in the G1 synchronized sample and remains present until 210 minutes. The degradation of Clb2 is further delayed by treatment with CPT in both the WT and the *rnh1Δ rnh2Δ,* but in the case of the *RNH-* mutant, considerable levels of Clb2 protein can be observed throughout the complete time course (Figure 31B). These results may help explain why *rnh1Δ rnh2Δ* cells are held in G2/M-phase, since they cannot exit mitosis due to the high activity of Clb2. Additionally, this experiment reveals that RNaseH activity is required for the normal fluctuation of Clb2 protein since the cyclin is observed during G1 and S phases, when it is not normally active, and the levels of Clb2 remain elevated in the *RNH-* mutant. These results are very similar to those published for yeast mutants in *hct1* (*CDH1*), an activator of the APC (261).

The CDK Cdc28 is the key cell cycle regulator, whose activity declines as mitosis is completed due to the degradation of mitotic Clbs such as Clb2 and the accumulation of the G1-phase-specific Cdc28 inhibitor Sic1 (reviewed in (262)). Prevailing levels of Clb2 at G2/M and low levels of Sic1 throughout the cell cycle would explain why yeast cells lacking RNaseH activity manifest abnormal cell cycle transitions at G2/M and G1/S respectively, and may be the reason why *RNH-* mutants re-initiate DNA replication without having finished mitosis.

Nucleolar Cdc14 is constrained in RNH- mutants

The nucleolus is known to segregate after the nucleus, with the segregation of rDNA occurring in late anaphase (263). During anaphase, yeast cells must condense and compact the long rDNA array to ensure that segregation takes place before cytokinesis (264). We followed the progression of *RNH-* mutants though meta- and anaphase monitoring spindle morphology with tubulin staining. The percentage of cells in metaphase and anaphase was determined for the *RNH* double mutant and found to be similar to the WT (Figure 32A). However, the *rnh1Δ rnh2Δ* cells entered slightly earlier into metaphase, and metaphase itself seemed slightly longer (by 15 minutes approximately), consistent with earlier observations by flow cytometry of *RNH-* cells rushing through the S phase into G2/M.

The action of Cdc14 is required for rDNA segregation as it is necessary for the localization of the condensin complex to rDNA (265). Cdc14 is regulated by the inhibitory protein Net1, both being members of the RENT complex (for *re*gulator of *n*ucleolar silencing and *t*elophase), which also contains Sir2 with important roles in transcriptional silencing of the rDNA locus. Net1 binding of Cdc14 maintains Cdc14 inactive in the nucleolus during the cell cycle. Net1 only releases Cdc14 during anaphase, promoted by the FEAR (CDC *F*ourteen *E*arly *A*naphase *R*elease) and MEN (*M*itotic *E*xit *N*etwork). Net1 release allows active Cdc14 to dephosphorylate its downstream targets and stimulate the exit from mitosis and cytokinesis

(266). Of particular interest to this study, Cdc14 activity in anaphase also leads to the dephosphorylation and thus stabilization of Sic1 (267).

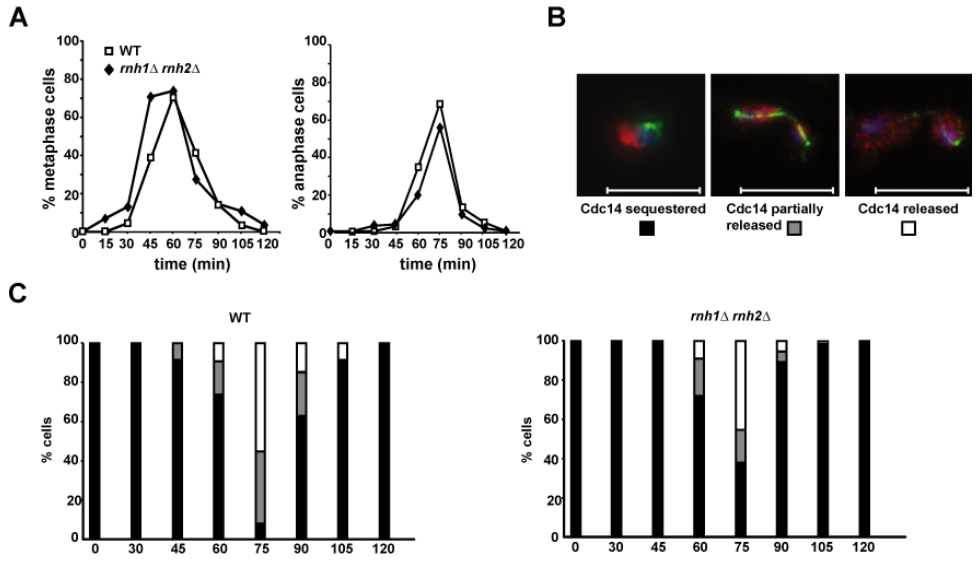

Figure 32. Reduced nucleolar Cdc14 is released in *RNH-* mutants. A. Percentages of metaphase and anaphase cells as determined by spindle (tubulin) morphology are shown for each timepoint. **B.** Representative images of 3HA-Cdc14 subcellular localization. Cdc14 is shown in red, microtubules (tubulin) are shown in green and DNA (DAPI) is shown in blue. **C.** Percentage of cells with 3HA-Cdc14 sequestered, partially released, or fully released for the WT and *rnh1Δ rnh2Δ* cells (left panel). At least 200 cells were counted at each timepoint. Size bar represents 10μm.

To address if the timing of Cdc14 release from the nucleolus was affected in *RNH-* mutants we investigated the localization of Cdc14 during the cell cycle following release from G1 synchronization. We first crossed *rnh1Δ rnh2Δ* yeast with a 3HA-tagged Cdc14 bearing strain and confirmed that the HA tag did not affect either CPT sensitivity or cell cycle progression of the *RNH* double mutant (data not shown). Next, cells were released from α-factor block in G1 and samples were fixed every 15 minutes (α-factor was re- added after 45 min to prevent re-entry into the next cell cycle) and the localization of Cdc14 was monitored by immunofluorescence in relation to spindle length. Cdc14 localization was recorded as sequestered in the nucleolus, partially released into the nucleus, or fully released and cytoplasmic (see Figure 32B for an example of each). Cdc14 was released from the nucleolus of *rnh1Δ rnh2Δ* cells with approximately the same kinetics as the WT (Figure 32C). However,

fewer cells were counted with partially- and fully-released Cdc14 in the *RNH-* mutant. This result could indicate that the FEAR (or MEN) pathway was not fully activated in the absence of RNaseH activity. Perhaps a critical level of Cdc14 release is necessary to trigger mitotic exit and this level is not reached in yeast lacking RNaseH activity.

RNH- mutants do not respond to the spindle assembly checkpoint (SAC)

The apparent delay in G2/M exit of the *RNH* double mutant could be a consequence of activation of the spindle assembly checkpoint (SAC) which, through Mad1 and Mad2 activity, delays the onset of anaphase in cells with defects in mitotic spindle assembly (for a recent review see (268)). To investigate whether activation of the SAC was responsible for holding of the *RNH-* mutants in late S/G2 we deleted the mitotic spindle checkpoint gene *MAD1* in *rnh1Δ rnh2Δ*. The triple mutant was viable, and CPT sensitivity at the level of viability and cell cycle progression (results not shown) were very similar to the double mutant. Spindle checkpoint mutants, such as *MAD* (*M*itotic *A*rrest *D*eficient) mutants, are sensitive to the microtubule destabilizing drug benomyl. Consequently, we decided to analyse the benomyl sensitivity of the *rnh1Δ rnh2Δ* double and *mad1Δ* triple mutant (Figure 33A). The *RNH* double and the *mad1* triple mutant were as sensitive to benomyl as *mad1Δ.* Such epistasis would imply that the RNaseH enzymes and Mad1 are found in the same pathway, implying that the SAC is defective in these mutants. Nevertheless, the benomyl sensitivity phenotype alone is not sufficient to classify a mutant as checkpoint defective.

Treatment with either benomyl or nocodazole (Noc), another microtubule destabilizing drug that activates the SAC, causes an interference of microtubule polymerization and attachment to kinetochores, such that cells are unable to progress into mitosis (269,270). Cells treated with Noc arrest with a 2N DNA content at the G2/M phase of the cell cycle, indicating that replication is complete but chromosome separation has not yet taken place. SAC mutants, such as the *mad* mutants, re-enter G1 of the next cell cycle with concomitant initiation of

replication. Given that the mutants are unable to complete mitosis correctly, further rounds of replication can lead to a higher than 2N DNA content that can be easily monitored by flow cytometry. In addition, the re-initiation of DNA replication without appropriate mitosis of the previously replicated genetic material can be observed by microscopy as the generation of new buds or "re-budding". To elucidate whether yeast lacking RNaseH activity bypass the SAC we analysed the *RNH* double mutant by FACS and microscopy following a prolonged incubation with Noc (Figure 33B). Cells were first synchronized with α-factor before release into Noc-containing medium and growth for 2 or 4 hours in continual presence of the drug (with re-addition of Noc every 90 minutes). WT cells treated with Noc exhibit a dumbbell phenotype of large budded cells, characteristic of G2/M arrest, and following 4h incubation just 10% of G2-arrested cells had more than one bud. In contrast 29% of large budded *rnh1Δ rnh2Δ* cells manifested the re-budded phenotype after 2h, and after 4h of continual Noc incubation 37% of *rnh1Δ rnh2Δ* cells were re-budded (Figure 33B), with more than half of these G2/M cells having more than one re-bud. The peak of cells corresponding to a 2N DNA content (Figure 33B, black arrow), was shifted slightly to the right for the *RNH-* mutant, which would infer that the majority of cells lacking RNaseH activity had a DNA content between 2- and 3N. Furthermore, a small group of cells with a cellular DNA content of 3-4N was observed in the *RNH* double mutant using flow cytometry (Figure 33B, blue arrow), further evidence of the re-initiation of DNA replication in these mutants. The percentage of re-budded cells was not as high for the *RNH* double mutant as for the *mad1* simple mutant, and the *mad1* triple mutant showed an additive effect in the proportion of re-budded cells and loss of viability.

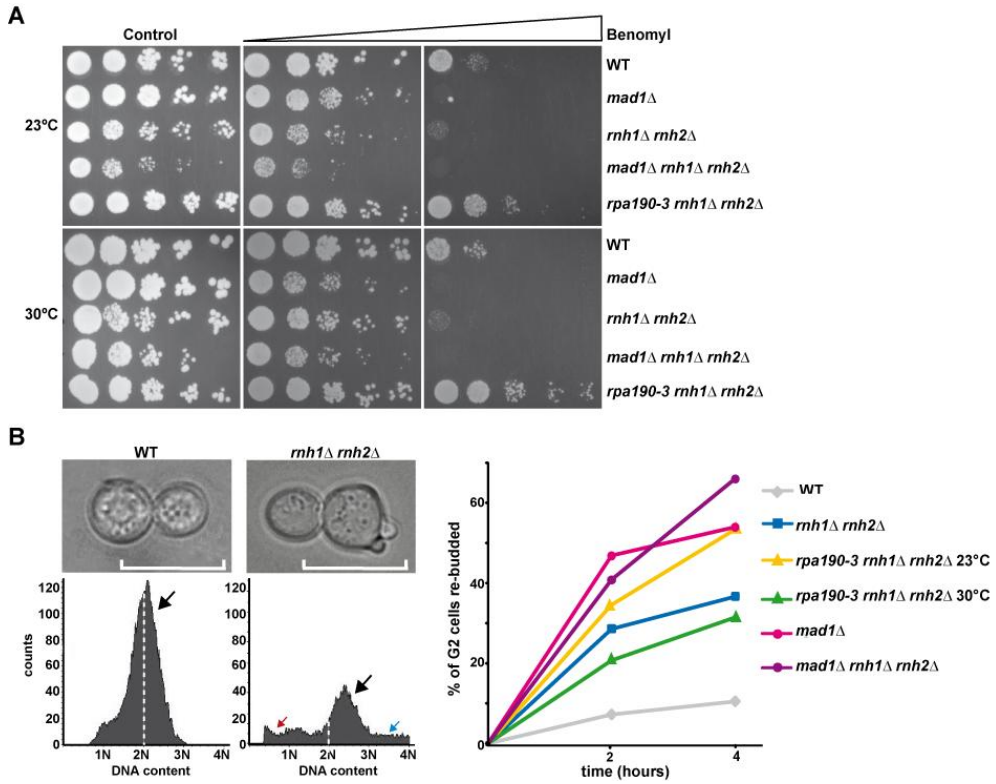

Figure 33. *RNH-* mutants do not respond to the spindle assembly checkpoint. A. Benomyl sensitivity drops at 5 and 10µg/ml. **B.** Representative microscope images of "re-budding observed in *rnh1Δ rnh2Δ* cells in G2/M following 4h Noc treatment (top). Size bar represents 10µm. Analysis of replication by flow cytometry following 4h Noc treatment (bottom). Black arrow showing population of cells with 2N DNA content; 2N content indicated by dotted line. Red arrow represents < 1N DNA content; blue arrow represents > 2N DNA content. Percentage of G2 cells re-budded (right).

To confirm whether the SAC was indeed activated in yeast lacking RNaseH activity we monitored the phosphorylation of Mad1, since Mad1 is hyperphosphorylated when the SAC is activated. Utilizing a GFP-tagged Mad1 strain we were unable to observe hyperphosphorylation of the Mad1 protein in the *RNH* double mutant by Western analysis (results not shown). Collectively, these results imply that yeast lacking RNaseH do not respond to the SAC and continue to replicate their DNA although chromosome separation has not yet been completed.

R-loops are responsible for chromosome segregation defects

To further monitor chromosome segregation in the *RNH-* mutants, we employed clamped homogeneous electrical field (CHEF) analysis, to separate replicating chromosomes. The yeast

genome contains 16 linear chromosomes, ranging from approximately 200kb to 2.2Mb. Chromosomes with branched DNA structures, such as replication forks and recombination intermediates, cannot migrate into the gel and remain trapped in the wells. Following alpha-factor synchronization, and release with or without CPT, we collected and embedded cells in low-melting agarose plugs at various timepoints. Replicating chromosomes were separated using CHEF analysis and then probes against two different chromosomes were applied (cV and cXII) to look at the replication and segregation of these chromosomes. We quantified linear molecules that are able to migrate into the gel (signal b, Figure 34A) and include fully replicated DNA, versus non-linear chromosomes that cannot migrate due to their branched structures and remain stuck in the well (signal a) and would include replication and recombination intermediates, (271,272). For the quantifications, the signal corresponding to time 0 (cells held in G1) was set as 100%, as one would expect no replication of DNA in G1 synchronized cells (nor recombination). A high bar in the quantifications corresponds to more signal in the gel and, therefore, more fully replicated molecules (Figure 34B).

Following release from G1, a signal can be detected in the well for WT at 30 minutes for chromosome V, as chromosomes are beginning replication; this signal would include replication bubbles, and replication forks. Through 60 to 90 minutes the signal in the gel is increasing, until the 120 minute timepoint where we observe the majority of the signal in the gel rather than the well, as chromosomes V and XII are fully replicated and resolved. At 150 minutes, for cV of the WT we can observe a second round of replication, with some signal once again in the well. The pattern for cXII of the WT is similar, although the appearance of the signal in the gel is slightly detailed. This result is compatible with the observation that the rDNA locus, located on cXII, is one of the last chromosome regions to be fully replicated and resolved (263). However in the presence of CPT, less signal is observed in the gel for cXII in the WT indicating that CPT leads to cXII-specific problems.

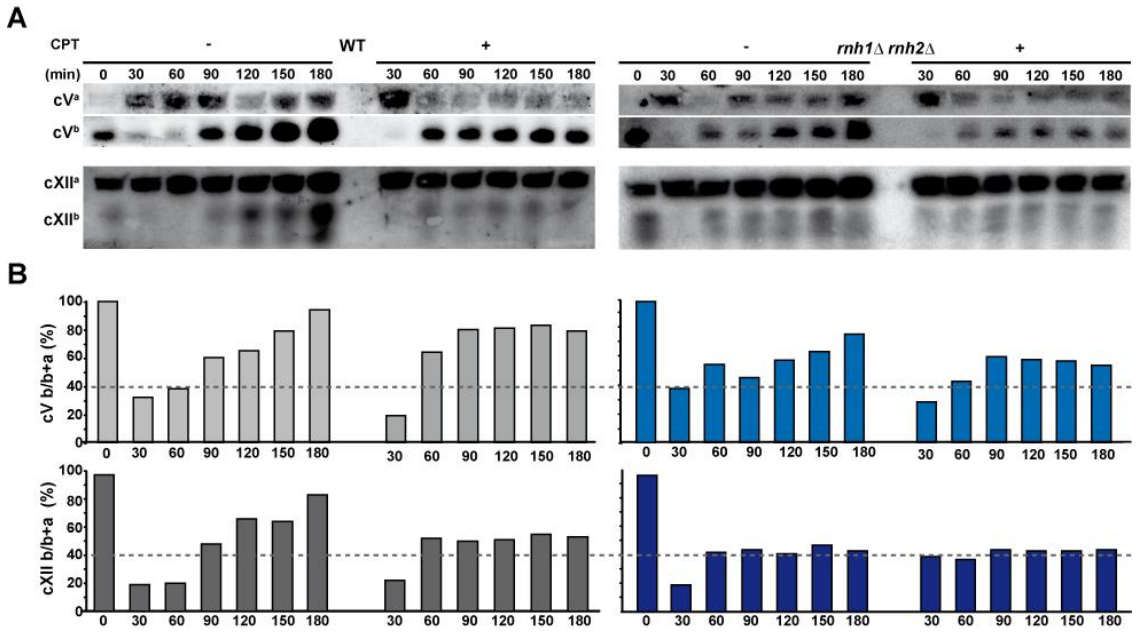

Figure 34. Yeast lacking RNase H activity show chromosome segregation defects. A. Analysis of replication status by CHEF of DNA from cells synchronized in G1 prior to release in the presence or absence of CPT 10µg/ml. Plugs were prepared with cells taken at the indicated time-points following release. Hybridization with cV-specific or cXII-specific probes. Nonlinear chromosomes (a), which include replication intermediates, correspond to the signal coming from the gel well. **B.** Quantification of the results (below). The intensity of chromosomal signal from the Southern blot that migrates into the gel (b) is plotted relative to total intensity of chromosome bands in the gel and well (b+a). 100% implies that 100% of DNA has replicated and entered the gel.

For cV of the *rnh1Δ rnh2Δ* mutant we can observe the signal in the gel appearing earlier than for the WT. This can be best seen by comparing the 60 minute timepoints for *rnh1Δ rnh2Δ* versus the WT. This result supports the earlier observation by flow cytometry analysis that double mutants show a faster S-phase transition than the WT. As for cV, we note that cXII molecules enter into the gel earlier for the double mutant. However, upon comparison of signals for cXII, we note a much lower signal corresponding to fully replicated cXII molecules for the *rnh1Δ rnh2Δ* mutant than for the WT and more perseverance of the well signal. Upon CPT treatment, we see the gel signal earlier for cV and cXII of the WT, with a higher signal at 60 minutes upon CPT treatment compared to non-treated cells. This difference is not observed in the CPT-treated *rnh1Δ rnh2Δ* cells, presumably because the S-phase transition is already quicker. CPT treatment may cause more nicking of the DNA, which could potentially lead to more strand breaks, and therefore lead to more linear molecules, explaining the apparent earlier entry of molecules into the gel. Chromosomes V and XII from CPT-treated *rnh1Δ rnh2Δ*

cells also seems to be more slightly more smeared than for the WT. Smearing observed in a CHEF analysis is analogous with more breakage of DNA, and would suggest more DSBs in genomic DNA from *rnh1Δ rnh2Δ* cells. It´s also interesting to note that a large fraction of the cXII-probed DNA remained trapped in the wells for the *RNH-* mutant with or without CPT treatment. This would suggest that cXII of the *RNH-* mutant contains structures blocking DNA migration, such as unresolved replication or recombination intermediates, and such structures could also impede the segregation of chromosomes. Furthermore, CPT treatment led to problems in the resolution of cV only for the *RNH-* mutant.

To verify these observations we performed a visual analysis of fixed cells to determine the percentage of large-budded cells, and we assessed the nuclear morphology of large budded cells using the DNA stain DAPI (Figure 35A, bottom left). Exponentially growing cells were classified according to the cell cycle stage by cellular morphology, and scored as: unbudded (G1), small budded (S), or large budded (G2/M), in the presence or absence of CPT (Figure 35A, top left). We considered nuclear material that remained solely with the mother, or was observed in the bud neck, as indications of problems in chromosomal segregation, in contrast to nuclear material observed in both sides of the large budded cell as would be expected for normal chromosome segregation. The WT showed a distribution of G1, S and G2/M phase cells typical of an exponentially growing culture (273). Significantly more large budded cells were observed for the *rnh1Δ rnh2Δ* double mutant, indicating the accumulation of cells that had replicated their DNA but had not yet undergone mitosis, and this difference was even more pronounced following a 3 hour CPT treatment. By this visual analysis, we noticed that CPT treatment caused an increase in the number of cells in G2 and in cell size (Figures 35A and 35B) for both the double mutant and the WT. Interestingly, *RNH-* yeast cells were already somewhat larger in size than the WT. Yeast cells typically measure 5-8 µm, however, a larger proportion of the cell population was observed to have a size above this threshold in the *rnh1Δ rnh2Δ* double mutant. CPT treatment caused an increase in cell size for the *rpa190-3* RNA PolI triple mutant at the permissive temperature of 23ºC, but this effect was suppressed at the

semi-permissive temperature of 30ºC. Therefore, we can conclude that CPT treatment leads to a RNA PolI transcription-mediated increase in cell size.

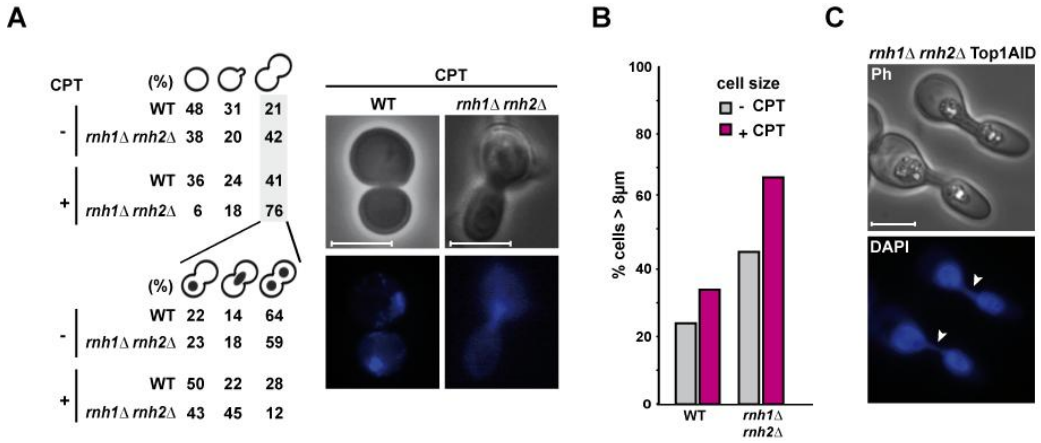

Figure 35. Yeast lacking RNase H activity show DNA segregation defects. **A.** Quantification of cell cycle stage by visual analysis of cell morphology (left, top). A detailed classification of the nuclear material segregation phenotype of large budded cells is depicted (left, bottom). Numbers were derived assessing the nuclear morphology of 600 DAPI stained cells. Representative image of DAPI-stained wild-type and *rnh1Δ rnh2Δ* cells after treatment with 10µg/ml CPT (middle panel). Ph, phase contrast. **B.** Size distribution of the cell population (right panel). Cells were counted as below or above the size threshold of 8 µm. **C.** Representative image of *rnh1Δ rnh2Δ* Top1AID cells after 165 minutes in the presence of IAA. DAPI-positive bridges indicated by white arrowhead. Ph, phase contrast. Size bars correspond to 10µm.

Importantly, fewer cells exhibited a normal segregation phenotype following CPT treatment. In the case of the nuclear signal at the bud neck, this increased for the WT upon CPT treatment from 14 to 22%, yet increased drastically more in the *RNH*$^{-}$ mutant, from 18 to 45%. Concomitantly the number of normally segregated cells in the CPT-treated *rnh1Δ rnh2Δ* mutant was very low, just 12%. It is worth mentioning that DAPI-stained nuclear material can be observed in the bud neck of cells that do not have segregation problems, as part of a normal replicative cycle; however, in a normally exponentially growing population we would not expect such a high proportion of cells with this phenotype. Moreover, the bud necks in the *rnh1Δ rnh2Δ* mutant in many cases were pronounced and appeared elongated (Figure 35A, right panel). These results indicate that the absence of RNaseH activity leads to the formation of replication or recombination intermediates, which cause the cells to be held in late S/G2 stages of the cell cycle and may impede chromosome segregation.

When Top1 protein was depleted from G1 synchronized *rnh1Δ rnh2Δ* yeast, cells were able to progress into the G2 stage but unable to complete mitosis and re-enter the next cell cycle (see Figure 20A), suggesting that the persistence of RNA:DNA hybrids was responsible for the holding of cells in the G2 phase. Furthermore, the majority of Top1 depleted *RNH-* cells were large budded and had extremely long necks when observed under the microscope (Figure 35C). Strikingly the DAPI stained nuclear material could be seen in the bud neck as a DAPI bridge (shown by arrowhead) connecting the mother and daughter nuclei. Such DAPI-positive bridges are representative of incompletely segregated chromosomal DNA, such as hemi-catenated sister chromatids (274) and such structures have been associated with increased to chromosome breakage or nondisjunction during mitosis. Taken together our results reveal that persistent RNA:DNA hybrids can lead to the accumulation of replication intermediates, culminating in difficulties in chromosome segregation and failure to complete mitosis.

RNH- mutants are prone to premature re-budding and apoptosis

Cells respond to impaired chromosome segregation by a delay in cytokinesis (reviewed in (275)). The fact that *RNH-* mutants don't show genetic interactions with mutants affected in NHEJ (e.g. *ku70Δ*; see Chapter 2, Table 1) indicates that RNaseH-dependent chromosome segregation defects do not lead to DNA breaks after sister chromatide disjunction. Indeed, cells lacking RNaseH activity rely on HR, but NHEJ would be required to process such DNA breaks. In contrast to WT cells, where nocodazole treatment arrests cells at the G2/M phase of the cell cycle, *rnh1Δ rnh2Δ* cells re-initiated DNA replication without having undergone mitosis. We therefore asked whether the premature DNA replication could induce apoptosis in *RNH-* mutant cells.

Indeed, we observed a substantial loss of viability of Noc treated *rnh1Δ rnh2Δ* cells (Figure 33B), which was exaggerated by prolonged treatment of cells with nocodazole (results not shown). In addition measurement of cellular DNA content by flow cytometry revealed a sub-population of *rnh1Δ rnh2Δ* cells with a less than 1N cellular DNA content (Figure 33B, red

arrow), which may be due to cells undergoing apoptotic DNA degradation (276). We determined the percentage of apoptosing cells by microscopic analysis of cells using methylene blue staining, which stains dying or dead cells with defective cell wall integrity (Figure 36A). A considerable increase in positively stained cells was observed in the *RNH* double mutant after 2 hours of Noc treatment; this difference was even greater after 4 hour treatment, reaching 56% of *rnh1Δ rnh2Δ* cells compared to less than 5% for the WT. In parallel we monitored DNA fragmentation, a typical marker of apoptosis, using DAPI staining of nuclear DNA (Figure 36B). The RNaseH lacking yeast had almost twice as many cells with the DAPI nuclear material stain disrupted into several signals as the WT, with the number of cells containing fragmented nuclear material increasing with the length of nocodazole treatment.

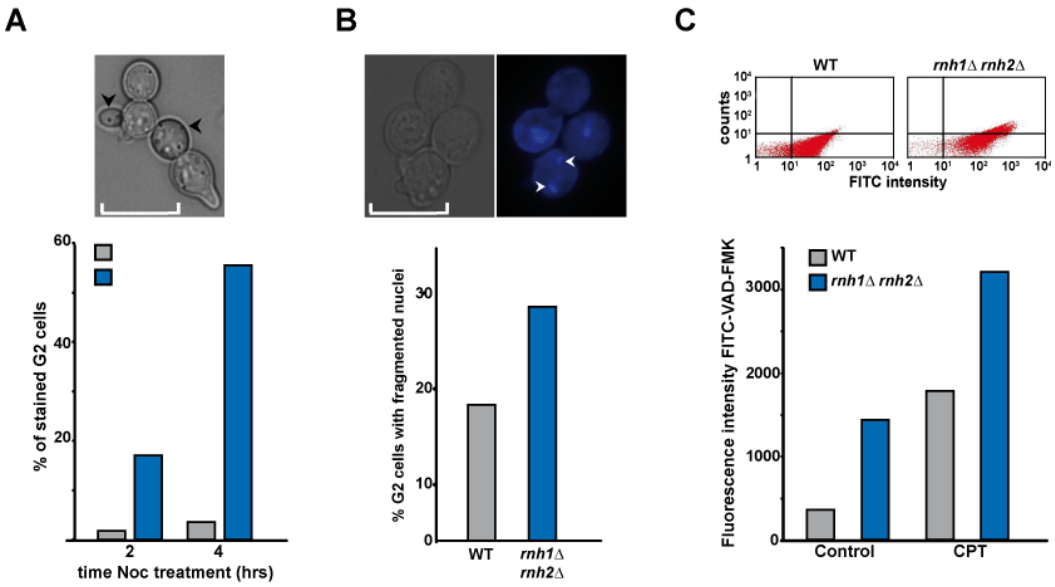

Figure 36. Nocodazole treatment of *RNH*⁻ mutants causes re-budding and apoptosis. A. Methylene blue stained cells (indicated by black arrowheads) in the representative image of the *RNH* double mutant after 2h Noc treatment (top). Size bar represents 10µm. Percentage of methylene blue stained G2 cells (bottom). **B.** Representative microscope image of *rnh1Δ rnh2Δ* cells with fragmented nuclei (indicated by white arrowheads). Percentage of cells with fragmented nuclei, as determined by visual inspection of DAPI stained cells after 2h NOC treatment. **C.** Detection of FITC-VAD-FMK positive cells by flow cytometry for the analysis of metacaspase activation. Representative flow cytometry profiles (top) and quantification of fluorescent intensity (bottom).

Consequently, we analysed other features of apoptosis in *S. cerevisiae*. To do so, we detected the amount of activated metacaspase by flow cytometry with the caspase activity indicator

FITC-VAD-FMK (277). Significantly more cells with activated metacaspase were detected in the *RNH* double mutant than in WT cells (Figure 36C). Furthermore, the production of reactive oxygen species (ROS), monitored by flow cytometry with the detection of H_2DCFA-FITC, was increased 5.7 fold in *rnh1Δ rnh2Δ* yeast with respect to the WT (results not shown), and apoptosis has been reported to be preceded by an increased generation of ROS (reviewed in (278). CPT treatment itself led to an increase in both the production of ROS and the activation of metacaspases, consistent with the reported effects of CPT in inducing apoptosis in other organisms (279-281). Noc treatment held WT cells at the G2/M phase of the cell cycle, however, *rnh1Δ rnh2Δ* cells re-initiated DNA replication without having undergone mitosis, with an associated loss of viability caused by the activation of apoptosis.

DISCUSSION for CHAPTER 3

Lack of RNaseH Activity Leads to Abnormal Cell Cycle Transitions at G2/M and G1/S

Given the connection between RNaseH activity and the rDNA described in the first two chapters and based on the observation that S-phase transition is altered in cells lacking RNaseH activity, we strove to dissect how R-loops may interfere with cell cycle regulation. We first observed that Sic1, a stoichiometric inhibitor of Cdk1-Clb (B-type cyclins) (282), became essential for viability in these mutants (see Figure 27). Sic1 prevents cells from a premature entry into S-phase and its phosphorylation-induced degradation allows cells to initiate DNA replication (236). Sic1 levels accumulate during mitosis and are controlled by the activity of the phosphatase Cdc14. Cdc14 is constrained in the nucleolus during the cell cycle and only becomes activated upon nucleolar liberation in anaphase. Cdc14 phosphatase activity causes the accumulation of Sic1, by dephosphorylating and activating the *SIC1* transcription factor Swi5 (283), and by dephosphorylation of Sic1 itself, thereby stabilizing the protein (267). Furthermore, Cdc14 activity triggers mitotic exit inducing the degradation of mitotic cyclins (266,284). Yeast lacking RNaseH activity had lower levels of Sic1 protein throughout the cell cycle, and the degradation of cyclin Clb2 was significantly delayed (Figure 31), indications that Cdc14 may not have been fully active in *RNH-* mutants.

RNH- Mutants are partially defective in nucleolar Cdc14 release

Yeast uses an elaborate mechanism to control Cdc14 activity. At S phase entry, Cdc14 is 'caged' in the nucleolus by its competitive inhibitor Net1 (285). Net1, a core subunit of the RENT complex, is a Sir2-associated nucleolar protein that stimulates transcription by RNA PolI and regulates nucleolar structure (286). Indeed, the timing of Cdc14 release from the nucleolus occurred normally in the *RNH-* mutants, but fewer cells released Cdc14 (see Figure 32). This finding points to the possibility that the lack of RNaseH enhances nucleolar Cdc14 retention. The role of Net1 in RNA PolI transcription may link R-loop formation and Cdc14 retention,

although such a connection still needs to be explored. Interestingly, Net1 has been shown to stimulate RNA PolI transcription and to regulate nucleolar structure independently of controlling mitotic exit (287). It should be noted that deletion of the *NET1* paralogue *TOF2* has been shown to have synthetic genetic interactions with *TOP1* and *HPR1* (288,289). Interestingly, R-loop formation is stimulated in cells lacking Top1 or Hpr1 (19,60) but we could not detect a genetic interactions between *RNH* and *TOF2* suggesting that Tof2 may not be involved in rDNA-dependent R-loop processing.

Apart from its role in the cyclin B proteolysis, Cdc14 is required for the localization of the condensin complex to rDNA to resolve the sister chromatids held together at the rDNA loci (265). When released by the FEAR pathway, active Cdc14 was required for the proper targeting of condensin to rDNA during anaphase (290). Perhaps, a critical level of active Cdc14 is required to complete sister chromatid separation. It would be very interesting to address whether the localization of the condensin complex to rDNA is affected in the *RNH-* cells, and if mis-localized condensin could be related to a defect in sister chromatid decatenation. Also of interest to this study are reports that the polo-like kinase Cdc5 promotes the nucleolar release of Cdc14 by stimulating the degradation of Swe1, and high levels of Swe1 were shown to impair FEAR activation (291). In Chapter 2 of this thesis, we found the triple mutant with *swe1* to be viable and have large sized spores; furthermore, the triple mutant suppressed the CPT sensitivity of the *RNH-* cells (see Table 1). Therefore, it might be worthwhile monitoring the timing of Cdc14 nucleolar release in the *swe1* triple mutant, to see whether Cdc14 release is normalized in the absence of Swe1 activity.

A further role of Cdc5 in yeast is to regulate sister chromatid separation by phosphorylation of the cohesin subunit Scc1 (292). For successful chromosome segregation, cohesion complexes must be removed by separase (293), and as sister chromatids are frequently catenated or connected by hemicatenates (274), these structures must also be resolved before migration of duplicated genetic material into the daughter cell. The *S*tructural *M*aintenance of

*C*hromosomes complex Smc5-Smc6 plays a key role in cohesin functions (294), and the rDNA has been shown as a major binding site for the Smc5-Smc6 complex (295). Furthermore, Smc5-Smc6 may contribute to the accurate restart of RFs after pausing (296) and we observe frequent RF pausing across the rDNA locus in yeast cells lacking RNaseH activity. Therefore, it would be interesting to investigate whether there is a defect in cohesin binding at the rDNA locus and to elucidate the impact of deletion of Smc complex members on the segregation of chromosomes in *RNH-* yeast. Moreover, as *smc5-smc6* mutants could enter anaphase before a complete DNA replication of the rDNA array (296), it would be particularly interesting to see how deletion of Smc complex members would affect the cell cycle progression of yeast lacking RNaseH activity.

Separase is activated when securin is targeted for degradation by a ubiquitin ligase, the anaphase promoting complex/cyclosome (APC/C) (for a review see (297)). Notably, Cdc14 is required to dephosphorylate Cdh1, and this event is needed to trigger APC activation. An alternative possibility for the defective chromosome segregation observed in yeast lacking RNaseH activity, may be that the lower levels of nucleolar released Cdc14 are not sufficient to activate the APC/C. A read-out to test for this possibility would be to look at Cdc20, an activator of the APC (117) and see whether the APC is effectively activated in yeast lacking RNaseH activity.

Persistent R-loops Impede Chromosome Segregation

Christman *et al.* found that cXII, and specifically the presence of the rDNA locus impeded the complete segregation of replicating chromosomes of *top1Δ* yeast (298). Moreover, it had been found that rDNA segregation in the absence of Cdc14 takes place if rRNA genes were not transcribed (299) and high rates of RNA PolI transcription have been reported to impede rDNA segregation by promoting the establishment of rDNA linkages (300). In this chapter we describe that persistent RNA:DNA hybrids can lead to unresolved replication or recombination intermediates, which prevent cells from exiting mitosis. Intrinsic segregation problems were

specifically observed for the rDNA-harbouring chromosome XII of yeast lacking RNaseH activity (Figure 34). Furthermore, the incompletely segregated chromosomal DNA of the *RNH-* mutant cells was evident as DAPI-positive bridges in pronounced and elongated bud necks connecting the mother and daughter nuclei (see Figure 35). A consequence of such events may be increased chromosome breakage or non-disjunction (the failure of the normal separation of chromosomes to opposite poles during nuclear division), and indeed *RNH-* mutants suffer from an elevated loss of heterozygosity (LOH), and a significant increase in spontaneous DNA damage (see Figure 12). It remains to be determined whether the DNA in these bridges is in fact rDNA. However, the LOH observed in yeast lacking RNaseH activity corresponded to chromosome III, at a non-rDNA locus, and such LOH could be attributed to the loss of chromosome III due to defective chromosome segregation. Likewise, we show that CPT hinders the segregation of chromosome V (see Figure 34), further evidence that persistent R-loops impede chromosome segregation. Similar anaphase chromosome bridges have been observed in yeast mutants lacking condensin or Topoisomerase II (Top2) (301), and are also a feature of solid tumours in humans (302,303). The yeast Rnh203 accessory subunit physically interacts with Top2 (304), raising the possibility that the Rnh2 complex might direct Top2 to R-loop associated anaphase chromosome bridges. The 'so-called' NoCut checkpoint has been suggested to delay cytokinesis in response to impaired chromosome segregation (305). NoCut inhibits completion of cytokinesis in the budding yeast *top2* mutant (reviewed in (306)). Thus, if the correct targeting of Top2 activity is constrained in *RNH-* mutants it is conceivable that the NoCut checkpoint is activated in order to delay cytokinesis.

<u>*RNH-* mutants are prone to premature re-budding and apoptosis</u>

We noted that *RNH-* cells re-bud and initiated DNA replication without having completed chromosome separation (Figure 33). These events were associated with a loss of viability caused by the activation of apoptosis. Interestingly, fewer cells exhibited rebudding when RNA PolI transcription was down-regulated (Figure 27), suggesting that a high rate of transcription

at the rDNA locus leads to segregation defects in the *RNH-* mutant, that cause mitotic arrest. CPT-mediated DNA damage has been reported to lead to an increased ROS production and increased apoptosis (280,281,307), however, there are no reports to our knowledge that such increases are related to R-loops. The uncoupling of DNA replication from the cell cycle, such as an inappropriate activation of S phase, can contribute to apoptosis (277). On the other hand, R-loops could induce apoptosis by causing chromosome segregation constrains, and at the same time by interfering with checkpoints that would normally restrain subsequent cell cycle events such as M/G1 or G1/S phase transition. It is worth noting that the Polα-primase itself undergoes cell cycle-dependent phosphorylation and dephosphorylation, becoming phosphorylated and activated early in S phase and dephosphorylated while cells exit from mitosis (308). As such events depend upon a functional Cdc28 complex (309), the mis-regulation of cyclins observed in yeast lacking RNaseH activity could allow the primase complex to still be active during G2/M stages of the cell cycle, thus permitting TIR and/or re-replication events.

R-loop-Mediated Replication Cannot By-Pass the Need for Canonical Origin Firing

Low Sic1 levels are associated with premature S phase entry and problems in M/G1 transition, both phenotypes that we identified in yeast lacking RNaseH activity. Premature S-phase entry could also be attributed to genomic, R-loop dependent DNA replication initiation. To gain more insight into this possibility, we tested if the need for Cdc6 and Cdc7 is bypassed in *RNH-* cells. *CDC6* codes for an essential component of the pre-replicative complex (pre-RC) needed to load Mcm2-7 at origins of replication (239), while *CDC7* codes for the kinase, whose phosphorylation of Mcm2-7 is required for origin firing (4). Both genes are essential for replication initiation and cell viability, and their absence caused lethality in a *RNH-* strain background. Surprisingly, temperature sensitivity at 30°C of the *cdc7-4* allele was alleviated in cells lacking RNaseH activity (Figure 28). In contrast to the CPT-resistant *cdc7-4* allele, *cdc7Δ*

cells carrying a *mcm5-bob1* mutation were CPT-sensitive, which may be related to the dual function of Cdc7 in replication initiation and post-replicative repair (243).

Critical Role of the *MRC1*-Complex in Yeast Lacking RNaseH Activity

A key finding from this study was the observation that the *MRC1*-complex is required for viability and CPT-resistance in yeast lacking RNaseH activity (see Figure 29). We find that *RNH-* mutants were sensitive to the microtubule destabilizing drug benomyl; however the spindle assembly checkpoint was not activated. Interestingly, mutants in *mrc1, csm3* or *tof1* are described as benomyl sensitive (256) and it was shown that cells with chromatid cohesion defects, such as Ctf8-RFC complex mutants are also sensitive to benomyl (310). The *mrc1* simple mutant was not CPT sensitive, suggesting that CPT itself does not affect cohesion, however in combination with the lack of RNaseH activity, the triple mutant was in many cases synthetic lethal, and extremely sensitive to CPT. Although Mrc1 function is mainly related to replication fork stabilization in response to replicative constrains (224,247), these observations suggest that the critical role of the *MRC1*-complex in yeast lacking RNaseH activity may be related to cohesion functions. Indeed, the human Timeless-Tipin (Tof1-Csm3) were shown to co-purify with cohesion subunits (311), and the Tof1 orthologue in *C. elegans,* Tim1, is required for proper chromosome cohesion and segregation (312). Consequently, it will be interesting to examine the contributions of the cohesin subunits to the viability and chromosome segregation phenotypes of yeast lacking RNaseH function.

The *MRC1*-complex may also contribute to stabilize rDNA replication (313). Mrc1 itself can be phosphorylated by Hog1 in response to osmotic stress (250). This osmotic stress induced S-phase checkpoint acts to prevent conflicts between DNA replication and transcription (250). In a similar fashion, Mrc1 could be required to co-ordinate replication through the rDNA in *RNH-* mutants. Mrc1 has been shown to induce a replicative checkpoint, leading to phosphorylation by Rad53 in response to replicative stress (109). However, we find that neither the loss of RNaseH activity, nor CPT treatment is sufficient to activate Rad53

phosphorylation. CPT does not affect S phase progression in WT or *RNH-* cells, although, it does provoke a delay in G2/M phases of the cell cycle, suggesting that CPT lesions are not sensed as DNA lesions during S-phase progression. Mec1 is a master protein in the checkpoint, acting upstream of Mrc1. It was therefore interesting, given the important genetic interaction of the RNaseH enzymes with Mrc1, to observe in Chapter 2 that the *mec1sml1* quadruple mutant was viable, although spores were smaller in size and more sensitive to CPT than the *RNH* double mutant (see Table 1). This result supports that the important role of Mrc1 in maintaining the viability of yeast cells lacking RNaseH activity is not related to the Rad53-dependent replicative checkpoint.

Loss of RNaseH Activity Does Not Activate the Rad53-Dependent S-phase Checkpoint

Finally, it is interesting to note that yeast lacking RNaseH activity suffer from increased DNA damage (see Chapters 1 and 2), yet *RNH-* cells did not activate the Rad53-dependent S phase checkpoint. This finding is in contrast to yeast *hpr1* mutants, which also have been shown to accumulate R-loops, leading to a constitutive activation of the Rad53-signalling pathway (314). On the other hand, *hpr1* mutants required a functional S-phase checkpoint but not DSB repair for survival (314), while DSB repair is critical for the viability of *RNH-* mutants even in the absence of exogenous stress. Both, *hpr1Δ* and *rnh1Δ rnh2Δ* show a genetic growth defect with *top1Δ* (60,288,289). However, Hpr1 and RNaseH may have a more specialized role in the avoidance of R-loop formation in genomic or rDNA, respectively.

RNaseH Enzymes Play A Critical Role in Preventing Aneuploidy

As detailed in Chapter 1, the RNaseH and Top1 enzymes play key roles in protecting the eukaryotic genome by preventing unscheduled TIR events mediated by R-loops, with particularly important repercussions on genome instability and cancer. We also highlight the criticality of RNaseH activity in preventing non-disjunction, a major causative factor for aneuploidy, one of the most common characteristics of human tumours (315). It remains to be

determined whether the aberrant segregation of chromosomes in the *RNH-* mutants observed in this study are the cause of defects in chromosome cohesion or condensin activities.

6. CONCLUSIONS

Chapter 1

1. Chemical (CPT) or degron-mediated depletion of Top1 activity promotes R-loop formation and induces cell death in RNaseH lacking yeast.

2. R-loops promote the formation of unscheduled origin-independent replication intermediates indicative of transcription-induced replication (TIR) in ribosomal DNA at late S/G2 of the cell cycle.

3. Replication by TIR paused at sites of protein-DNA interaction, which points to the possibility that TIR is driven by non-canonical replication machinery.

4. TIR is RNA PolI transcription-dependent.

Chapter 2

5. The homologous recombination (HR), post-replicative repair (PRR), break-induced repair (BIR) and nucleotide excision repair (NER) pathways are required for viability or are essential to combat the genotoxic constrains in CPT-treated RNaseH lacking cells.

6. Transcription-coupled repair (TCR), a NER sub-pathway may play a prominent role in the repair of CPT damage in RNaseH mutants.

7. The genotoxic effects of CPT-treatment can be enhanced or alleviated by alterations in the structural integrity of rDNA or by down-regulation of RNA PolI transcription, respectively.

8. TIR is not dependent on Rad18, Rad51 or Srs2 activities.

Chapter 3

9. RNaseH H$^-$ cells enter prematurely into S-phase, making Sic1 essential to maintain viability in the absence of RNaseH activity.

10. R-loops cannot bypass the need for Cdc6 and Cdc7 in genome replication but partially alleviate the temperature sensitive phenotype of the *cdc7-4* mutation.

11. The *MRC1*-complex is required to combat the R-loop induced constrains in a Rad53-independent manner.

12. R-loop dependent alterations in nucleolar organisation constrain nucleolar Cdc14 release.

13. Constrained Cdc14 activity precedes the mis-regulation of Clb2 (up) and Sic1 (down) protein levels.

14. R-loops constrain chromosome segregation and lead to the formation of 'chromosome bridges'.

15. R-loop-mediated chromosome segregation defects are not monitored by the spindle assembly checkpoint (SAC).

16. R-loop dependent replication and chromosome segregation constrains induce apoptotic events.

7. MATERIALS & METHODS

1. MEDIA

1.1 Bacterial media

LB: (Lysogeny broth)**:** 0.5% yeast extract, 1% tryptone and 1% NaCl, adjusted to pH 7.0.

LB+Amp: LB media supplemented with 80μg/ml of ampicillin (Sigma).

For solid media 2% agar is added.

1.2 Yeast media

YPAD: 1% yeast extract, 2% peptone, 2% glucose supplemented with 20mg/l of adenine.

YPAG: 1% yeast extract, 2% peptone, 3% glycerol supplemented with 20mg/l of adenine.

S: synthetic minimal medium, 0.17% YNB, 0.5% ammonium sulphate, that can be supplemented with different carbon sources, and with amino acids (leucine, tryptophan, histidine, methionine, lysine, aspartate, threonine, adenine and uracil) added to the final concentration as described by (316).

SC: S media supplemented with 2% glucose and amino acids.

SD: S media supplemented with 2% glucose (no amino acids).

SGL: S media supplemented with 3% glycerol, 2% lactate and amino acids.

SGAL: S media supplemented with 2% galactose and amino acids.

SC+FOA: S media supplemented with 500mg/ml of 5-Fluorotic acid (5-FOA) and amino acids. Uracil was added at half the usual concentration.

Sporulation media (SPO): 1% potassium acetate, 0.1% yeast extract, 0.005% glucose, supplemented with half the usual amount of each amino acid as used for SC media.

2. STRAINS AND GROWTH CONDITIONS

2.1 Escherichia coli strains

DH5α: F´ *ΔlacU169 Φ80 lacZΔM15 supE44 gyrA96 recA1 relA1 endA1 thi-1 hsdR17* (317).

2.2 Saccharomyces cerevisiae strains

The genotypes of all yeast strains used in this thesis are indicated in Table 2. Yeast strains used in this study were derived from the YKL83 strain (124), based on W303-1a, unless otherwise stated. If not generated by a direct knock-out in the YKL background, mutant strains were backcrossed at least twice to the YKL83 strain background. Gene deletions were constructed by PCR-based methods using various template plasmids: pFA6a-*kanMX6* (318), pAG32-*hphMX4* (Euroscarf), pAG25-*natMX4* (Euroscarf) and pFA6a-*klLEU2MX6* (kindly provided by B. Pardo). Deletion mutants were verified by Southern blot, or by PCR analysis from genomic DNA preparations with primers complementary to sequences within the gene cassette and upstream of the disrupted gene locus. All experiments were performed with several meiotic segregants of the same genotype to ensure they behaved similarly.

Meiotic segregants from crosses with the *pif1-m2* strain were confirmed by PCR from genomic DNA using the forward primer with sequence: TGTAATATTATCCATTGAGC, and reverse primer: TATCATTTCCAAACTTCTCT. The resulting 620bp band was digested with *Xho*I as the mutation creates a novel *Xho*I site. To detect whether crossed strains were wild-type *RAD5* or *rad5-535,* PCR was performed from genomic DNA with the forward primer: GCAGCAGGACCATGTAAACG, and reverse primer: AAACTCGTTACTCCACTGCG. The resulting PCR fragment was digested with MnlI, as the mutation creates an additional MnlI site. Digestion of WT *RAD5* PCR products leads to two fragments of 155 and 182bp, or three fragments of 155, 120, and 62 bp for digested *rad5-535* PCR products, separated on a 3% agarose gel, respectively.

2.3 Genetic analyses

Some strains were generated by genetic crosses, using standard methods. Parental strains were crossed on solid YPAD, diploids were selected and sporulated on SPO media for 4-5 days. Tetrads were dissected in a Singer MK1 micromanipulator (Singer LTD) after treatment with 2mg/ml zymolyase 20T (USBiological) for 3 min. The genotype was determined by replica plating on different selective media and the sex was determined by the ability to mate with the reporter strains F4 (**a**) and F15 (α).

2.4 Growth conditions

The *rpa190-3* and *rrn3-8* RNA PolI temperature-sensitive mutants, used in Chapter 1, are unable to grow at 37ºC. Experiments were performed at the permissive or semi-permissive temperatures of 23ºC and 30ºC, respectively. Growth of the *cdc7-4* strain is blocked in G1 phase at 37ºC. Experiments were performed at the permissive or semi-permissive temperatures of 23ºC and 30ºC, respectively. All other experiments were performed at 30ºC unless otherwise stated.

2.5 Degron strains

An auxin-inducible degron (AID) strain was created to control the protein levels of Top1, in order to produce a conditional triple mutant with *rnh1Δ rnh2Δ.* The AID system, developed by Kohei Nishimura *et al.*, involves a plant-specific mechanism that responds to the plant hormone auxin (155) (Figure 37). Auxin binds to the transport inhibitor response 1 (TIR1) protein and promotes the binding of the SCF (Skp1, Cullin and F-box protein) complex. The SCF in turn recruits the E3 ubiquitin ligase and polyubiquitinates the SCF^{TIR1}, targeting it for degradation by the 26S proteasome. Expressing the TIR1 protein in yeast cells, which can assemble a functional SCF^{TIR1} complex due to the conserved nature of the Skp1 protein (319), permits the degradation of the protein of interest tagged with the auxin-binding domain, upon the addition of auxin.

The AID degron system was crossed into the *rnh1Δ rnh2Δ* strain, to create strain RS315 expressing *TIR1* under control of the constitutive ADH promoter. The Top1 protein was tagged at the C-terminus with the IAA17 auxin-binding domain, which was amplified by PCR from the plasmid pKan–AID*–9myc (320) (see Table 3 for a list of plasmids used in this thesis) using primers specific for the protein of interest, and included the gene for GEN resistance. Subsequently, the *rnh1Δ rnh2Δ* degron-containing strain RS315 was transformed with the respective PCR products, and positive candidates were selected by growth on plates containing HYG, NAT and GEN. The functionality of the aid strain was confirmed by halo assays, drop tests and Western blot analysis against the 9Myc tag.

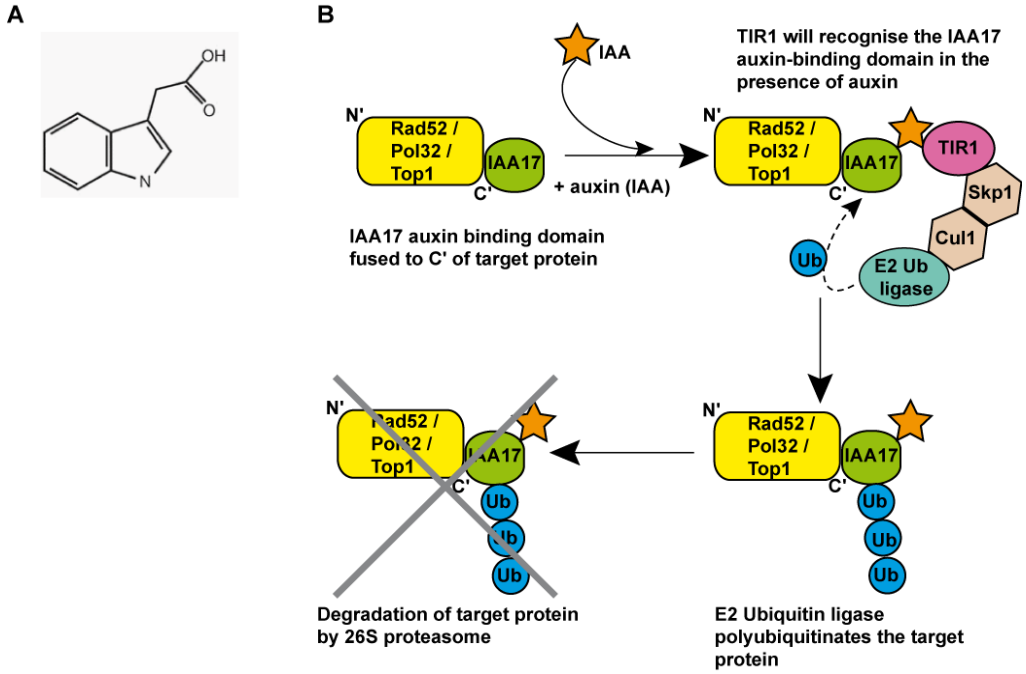

Figure 37. Schematic illustration of the auxin inducible degron (AID) system. Adapted from (155).

3. TRANSFORMATIONS

3.1 Transformation of bacteria

Competent bacterial cells were prepared using the method of Hanahan *et al.* (317), modified by Inoue *et al.* (321). 100µl of competent cells were mixed with 50-100ng of DNA and incubated on ice for 30 min, then cells were subjected to heat-shock at 42ºC for 1 min followed by 1 min

on ice. 600µl of LB media was added and cells were incubated at 37ºC for 45 min. Finally, cells were collected and plated on LB+Amp.

3.2 Transformation of yeast

Yeast cells were transformed according to the method described by Ito *et al*. (322) and modified by Gietz *et al.* (323). 30ml of cells growing in YPAD to an OD_{600} 0.4-0.6 were collected and washed with sterile water. Cells were then washed with 100mM LiAc and a "transformation mix" added, consisting of 240µl 50% PEG_{3350}, 36µl LiAc 10M, 5µl SS-DNA (10mg/ml) and 0.1-10µg DNA. Cells were vortexed vigorously to mix and incubated at 30ºC for 30 min, followed by a heat-shock at 42ºC for 20 min. Finally, cells were washed with sterile water and plated on selective medium.

3.3 Plasmid isolation from E.coli cells

Plasmid DNA was extracted from 1.5 ml of an overnight culture growing in LB+Amp at 37ºC. The isolation was performed with the boiling method described by Holmes and Quigley (324).

3.4 Yeast DNA extraction

Yeast genomic DNA was extracted according to the yeast DNA miniprep protocol described by Amberg *et al.* (325).

4. VIABILITY ASSAYS

4.1 Growth rate determination

The optical density is proportional to the number of cells, and therefore the growth rate of yeast strains (represented as the doubling time) can be quantified by monitoring the change in optical density at 600nm. Yeast strains were grown overnight to stationary phase. Cells were diluted in fresh YPAD to an OD_{600} of 0.1, and the OD was taken every hour. Optical density was plotted as a function of time on a semi-log scale.

4.2 Viability assays

Viability and sensitivity to genotoxic agents were determined by drop test assays. Yeast cells were adjusted to an initial OD_{600} of 0.4, then serially diluted 1:10 and spotted onto plates with or without different genotoxic agents at the indicated concentrations. Plates were incubated at 30ºC for 3 days, except for temperature-sensitive mutants that were incubated at the corresponding permissive or semi-permissive temperatures.

For UV irradiation, cells were serially diluted and spotted onto YPAD plates, irradiated with 50 or 100 J/m^2 UVC light in a UV-Mat (Dr. Gröbel UV-Elektronik GmbH) irradiation chamber, and incubated in the dark at 30°C for 3 days.

4.3 Survival assays

A sample of exponentially growing cells was taken from a liquid YPAD culture and plated on a YPAD plate – this point was considered as time 0. At time point 0, 10µg/ml CPT was added to the medium and cells were incubated for 24 hours, with appropriate dilutions to maintain cells in the exponential phase of growth. At determined time points, cells were taken from the population and plated onto YPAD plates. Cells were counted after 3 days growth, and presented as the percentage of surviving cells, with respect to time 0, set as 100% survival.

4.4 Halo assays

To confirm whether a yeast strain is *bar1Δ*, or to confirm the functionality of an aid degron strain, 100µl of cells at OD_{600} 0.2 were streaked over the surface of a YPAD plate to create a lawn. Once dry, a sterile filter paper disc was laid onto the plate surface, and 2 µl of either α-factor or IAA was dropped onto it. A halo, or clearing in the lawn of cells around the paper circle containing α-factor or IAA was observed if cells were *bar1Δ* or if cells contained the functional aid degron system, respectively (Figure 38).

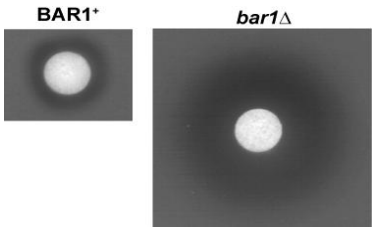

Figure 38. An α-factor halo assay to test for *bar1Δ* phenotype of a yeast strain.

4.5 Cell size distribution

The size distributions of various yeast strains were analyzed using the COULTER COUNTER® Cell and Particle Counter (Beckman Coulter). The proportion of cells above or below the size threshold of 8 μm was determined.

5. RECOMBINATION AND MUTATION ASSAYS

5.1 A-like faker assay (ALF)

The formation of **a**-mating cells from MATα strains was scored as described (132) with some modifications. Briefly, MATα strains were grown on YPAD plates for three days to obtain single colonies. A-like faker cells were selected by growing on YPAD plates overnight at 30ºC. Cells were then transferred onto a mating tester lawn of MATα (F15 strain) by replica plating followed by incubation at 30º overnight. The mated lawn was then replica plated to SD medium and mated products were counted. Total cells were grown on YPAD plates. ALF frequency was calculated as mated products/total cells. Each ALF frequency value was obtained by the mean of at least two different fluctuation tests of four independent colonies each. Data are shown as the mean ± standard deviation. Differences between groups were examined by Student's *t*-test.

5.2 *Interrupted LEU2 recombination assay*

Cells were transformed with the pRS314LB direct repeat recombination system (326) (Figure 39). This plasmid carries the *TRP1* selectable marker, and an interrupted *LEU2* coding sequence (interrupted by 31bp of sequence). Yeast strains were grown on solid SC media containing all amino acids for 3 days at 26ºC. Single colonies were re-suspended in water and serial dilutions plated onto SC lacking tryptophan and leucine as fluctuation assays. Recombination frequencies were obtained by comparison to the total number of colonies obtained on SC lacking tryptophan plates. Each recombination or mutation value was obtained as the mean value of three different fluctuation tests and each fluctuation test represents the median value of 6 independent colonies. The fold change numbers represent the rate relative to WT, which was expressed as 1. Values are expressed as the mean ± standard deviation (SD). Significance values (p) were obtained following Student´s *t* test for pairwise comparisons of data.

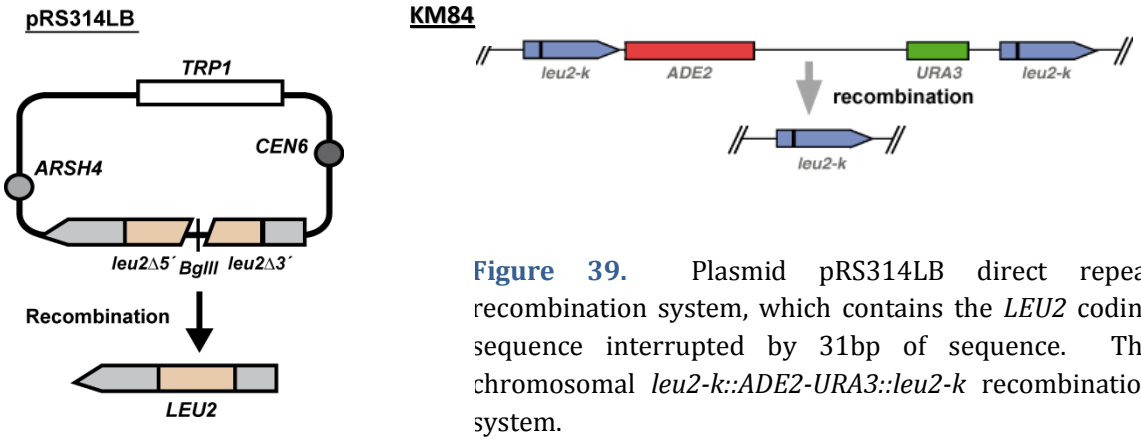

Figure 39. Plasmid pRS314LB direct repeat recombination system, which contains the *LEU2* coding sequence interrupted by 31bp of sequence. The chromosomal *leu2-k::ADE2-URA3::leu2-k* recombination system.

5.3 *Ribosomal DNA recombination assay*

Strains were crossed with *leu2-k::ADE2-URA3::leu2-k* harbouring strains (146) in order to express the intra-chromosomal recombination system (Figure 39). Prior to recombination in the rDNA, cells are *URA3+* and therefore are sensitive to 5-FOA. *URA3* and *ADE2* markers are lost when recombination occurs between the two flanking mutated *LEU* genes, and cells are

now resistant to 5-FOA. Strains containing the chromosomal system were first streaked onto SC plates lacking adenine and uracil for 2 days, and then streaked onto SC plates supplemented with all amino acids for a further 2 days. Fluctuation tests were performed as previously described, with serial dilutions plated onto SC lacking uracil to score totals, and onto SC+FOA plates to score recombinants.

5.4 Lau^r mutation assay

Mutation frequencies were determined from cells transformed with the pCM184-LAUR plasmid (134). Fluctuation tests were performed as previously described, with serial dilutions plated onto SC lacking uracil to score totals, and onto SC+FOA plates to score mutators.

5.5 Canavanine mutation assay

Forward mutation frequencies of nuclear DNA were obtained by fluctuation test as previously described, comparing the number of colonies growing on SC-Arg plates (SC media lacking arginine) containing 60mg/ml canavanine to the total number of colonies obtained on SC.

6. CELL CYCLE SYNCHRONIZATION AND PROGRESSION ANALYSIS

6.1 Alpha factor synchronization

Cell cycle progression was determined by measuring DNA content using flow cytometry. *MAT***a** yeast recognize the presence of alpha factor (α-factor), and respond by growing protrusions known as schmoos, and halt cell growth in the G1 phase of the cell cycle. Following release from α-factor, the synchronized population of cells continues to grow.

For G1 synchronization, cells were grown to OD_{600} 0.4 in YPAD medium and synchronized by incubation with 1μg/ml α-factor (Biomedal) for 90 minutes. An additional 1μg/ml α-factor was added for a further 90 minutes. Cells were released from α-factor treatment by washing three times in pre-warmed, fresh YPAD medium. For the G1 synchronization of *bar1Δ* cells, which are more sensitive to α-factor than *BAR1* strains, a lower concentration of 0.3μg/ml was used.

Since *bar1Δ* yeast lack expression of the aspartyl protease that cleaves and inactivates α-factor, cells were released by washing three times in pre-warmed, fresh YPAD medium containing 0.1mg/ml Pronase E (Sigma).

6.2 Flow cytometry analysis of cell cycle progression

Following α-factor synchronization and release, samples of 1ml were taken at indicated times, fixed in 70% ethanol and stored at -20ºC for analysis by flow cytometry. Samples were washed in 1x PBS (see Appendices for buffer compositions) and then resuspended in 1x PBS containing 5μg/ml propidium iodide, following RNase A (1mg/ml) overnight treatment. Cell doublets were separated by brief sonication and cell cycle progression was analyzed by flow cytometry using a FACSCalibur (Becton Dickinson) with CellQuest software.

6.3 Nocodazole synchronization

For flow cytometry analysis of the release from nocodazole synchronization, cells were grown to OD_{600} 0.4 in YPAD medium, and synchronized in G2 phase of the cell cycle by incubation with 15μg/ml nocodazole for 90 minutes, with 1% DMSO added to aid dissolution. Cells were washed and released in pre-warmed, fresh YPAD medium. 1ml samples were taken at specified time points following release and fixed in 70% ethanol at -20ºC for later analysis by flow cytometry.

For analysis of rebudded cells, yeast strains were grown to OD_{600} 0.4 in YPAD medium and synchronized, as previously described, with α-factor. Cells were released in pre-warmed, fresh YPAD medium in the presence of 15μg/ml nocodazole and 1% DMSO. 1ml samples were taken at specified time points and fixed for flow cytometry analysis as previously described. Nocodazole was added every 60 minutes during the incubation.

6.4 Induction of AID degron strains

Cells were grown to OD_{600} 0.4 in YPAD medium and synchronized in G1 as before. In the last 30 minutes of α-factor incubation, 5μM IAA was added to the medium to induce degradation of the aid-tagged protein. Cells were released into fresh YPAD medium and samples were collected for FACS cell cycle progression analysis, protein extraction for Western analysis, and genomic DNA extraction for 2D-gel.

7. SOUTHERN BLOT ANALYSIS OF DNA FRAGMENTS

7.1 Genomic DNA extraction

10ml of cells growing in YPAD to OD_{600} 1 were collected and washed. Cells were spheroplasted by incubation in 320μl spheroplasting buffer (see Appendices for buffer compositions) containing 150μg/ml zymolyase and 1% (v/v) β-mercaptoethanol at 37°C with occasional mixing for 60 min. Following centrifugation at 13,000rpm for 30 seconds, the pellet was resuspended in 370μl cocktail gently buffer. A volume of 16μl 10% SDS was added, the mix gently agitated and incubated at 65°C for 30 min, followed by the addition of 85μl 5M potassium acetate with incubation with on ice for 1h. After centrifugation for 15 min at 13,000 rpm, the supernatant was transferred to a new tube and DNA was precipitated with 1.2ml 96% ethanol for 30 minutes at -20ºC. The pellet, following 10 min centrifugation at 13,000rpm, was resuspended in 300μl TE containing 0.1mg/ml RNase A and incubated at 37°C for 30 min. 200μl of phenol and chloroform were added and well mixed, and the upper phase was carefully transferred into a new Eppendorf tube following 5 min centrifugation at 13,000rpm. DNA was precipitated with 1ml 96% ethanol and 120μl NaCl 2.5M followed by centrifugation at 13,000rpm for 10 minutes, and a 500μl 70% ethanol wash of the pellet. The dried pellet was finally resuspended in 30μl TE. The purified DNA was digested for 5 hours with the determined restriction enzyme and loaded onto a 0.8% TAE-buffered agarose gel. Electrophoresis was carried out without ethidium bromide at 2 V/cm for 30h. .

7.2 Alkaline DNA transfer

Following separation of DNA fragments by electrophoresis, gels were treated with 0.25M HCl for 10 min, washed with water and then incubated with denaturation buffer for 30 min. DNA was transferred to nylon membrane Hybond XL (Amersham) by capillary action in denaturation buffer for 12-16 h. After UV-crosslinking (70 mJ/cm^2), membranes were washed briefly with 2X SSC buffer and allowed to air-dry.

7.3 DNA hybridization

Membranes were hybridized with various radioactive DNA probes. For α^{32}P-dCTP labelling, 100ng of denatured DNA was mixed with 1mM random hexanucleotides, 0.5mM dATP, dGTP and dTTP, 25µCi α^{32}P-dCTP and 2U of Klenow DNA polymerase. The mix was incubated at 37ºC for 1h and non-incorporated radioactive nucleotides were then removed by using a G50-Sephadex column. Membranes were pre-incubated at 65ºC for 30 min in hybridization solution with constant rotation. Hybridization was performed at 65ºC for 12-16 h in 10-15ml hybridization solution containing the radioactive probe, previously denatured at 100ºC for 5 min. Following hybridization, unbound probe was washed off the membrane during two washes of 30 min at 65ºC using 50ml wash solution. For re-hybridization, probes were stripped off the membranes by washing three times with 500ml boiled stripping solution for 15 min.

7.4 Signal quantification

Radioactive signals were detected by exposure of the membranes on PhosphorImager screens (Fuji) that were scanned by a PhosphorImager FujiFilm FLA 5100. Quantification of the signal was performed with the Image Gauge software (Fuji).

7.5 Analysis of extrachromosomal rDNA circles

For separation of ERCs, about 1µg CTAB-extracted genomic DNA from exponentially growing cells was digested with 15U *Bam*HI in 20 µl of 1x buffer for 6hrs at 37°C and separated by gel

electrophoresis in 0.6% TBE-buffered agarose gel at 2 V/cm for 30hrs. ERCs were detected by hybridization with ribosomal probe A, following alkaline transfer to Hybond XL (Amersham) membrane. ERC levels were normalized against the rDNA repeat and expressed as fold change relative to the amount of ERCs in WT cells.

8. *BI-DIMENSIONAL AGAROSE GEL ELECTROPHORESIS (2D-GEL)*

2D-gel first separates restriction-digested RIs by mass (1st dimension), and the 2nd dimension, performed in the presence of ethidium bromide (EtBr), separates molecules by their three-dimensional shape. When a linear DNA molecule (n) is replicated, it progressively doubles in mass until reaching a fully replicated linear molecule (2n), and will adopt various bubbled or branched structures in the process, depending on where the closest site of replication initiation is located (Figure 40). Following transfer onto a membrane, replication across the DNA fragment of interest can be detected using specific probes.

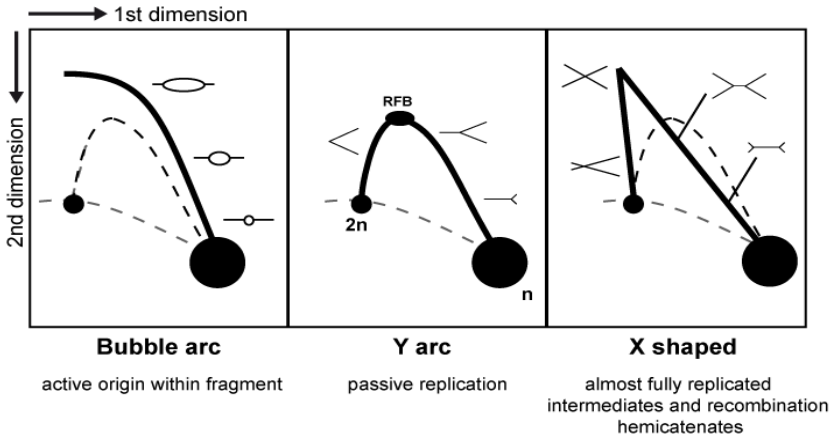

Figure 40. Schematic representation of two-dimensional gel analysis (2D-gel). The types of replication intermediates (RIs) that can be detected, include: bubble arcs, corresponding to an active origin within the fragment; simple Y arcs, which represent passive replication from an outside origin by a single replication fork entering from one end of a restriction fragment; and spikes above the 2n spot, which correspond to X-shaped molecules such as almost fully replicated molecules, converged forks and recombination hemicatenates. The n spot represents non-replicating linear molecules. Information adapted from (327).

In order to monitor RI formation by 2D-gel, cells were released from α-factor synchronization into minimal medium lacking adenine. Work by Aiko Matsui *et al.* demonstrated that removal

of essential nutrients can slow progression through the yeast cell cycle (328). We observed that entry into S-phase was specifically delayed in the *RNH* double mutant when released into minimal medium lacking adenine, but not into medium lacking other amino acids, such as leucine or tryptophan (Figure 41). This delay helped to ensure that CPT was efficiently taken up by the cells upon α-factor release. It is interesting to note that only *rnh1Δ rnh2Δ* mutants cannot proceed through S-phase in the absence of Trp, because Trp has been shown to act as a Top1-DNA anchor (329).

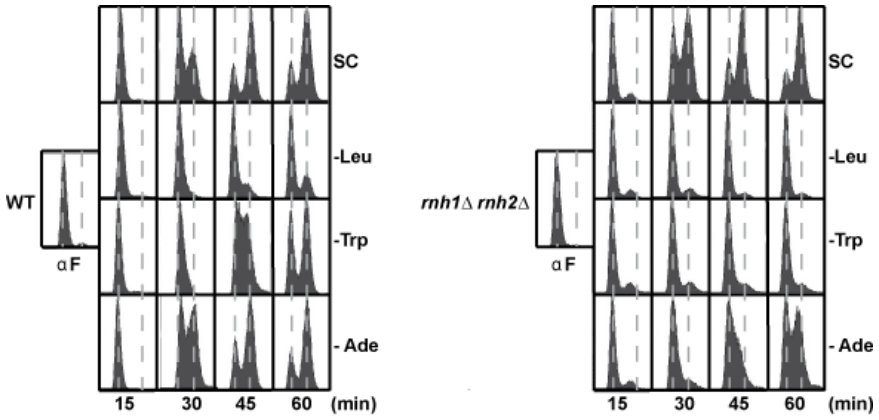

Figure 41. FACS showing synchronization in SC and release into SC, SD-Leu, SD-Trp or SD-Ade.

Cells were synchronized in G1 with α-factor and released into minimal medium lacking adenine and containing 10μg/ml CPT. 100ml samples were retrieved at the specified time points following release (in minutes) and cooled down on ice. To each sample, 0.1% sodium azide (final concentration) was added, since sodium azide immediately stops DNA replication (327).

Following centrifugation, cells were washed with cold water and resuspended in 2.4ml spheroplasting buffer and incubated for 20 min at 30ºC, followed by a 30 min incubation at 37ºC. Spheroplasts were collected by centrifugation and the cell pellets were carefully resuspended in 1.125 ml of G2 solution. After solubilization, 25μl of RNase A (10mg/ml) and 75μl of freshly prepared proteinase K (20mg/ml) were added and the sample was incubated at

50ºC for 45-60 min. The solution was centrifuged at 8500 rpm for 10 min and the supernatant was transferred to a new tube. Then, 750µl of chloroform/isoamyl alcohol 24:1 at RT was added and the solution was mixed repeatedly. After 10 min centrifugation at 8500 rpm, the upper aqueous phase was recovered and DNA was precipitated by adding 2 volumes of CTAB Solution II. The sample was centrifuged for 10 min at 8500 rpm and the pellet was resuspended in 0.8ml of CTAB Solution III and 0.2ml of 2.5M NaCl. DNA was precipitated with 1 volume of isopropanol and centrifuged at full speed for 10 min. The pellet was briefly rinsed with 96% ethanol, air-dried and resuspended in 250µl of 2mM Tris-HCl pH 8.

In a total volume of 100µl, about 5µg of CTAB-extracted genomic DNA was digested with 40 units *Bgl*II for 6 hrs. DNA was precipitated with 1 volume of isopropanol and 20µl 2.5M NaCl, followed by centrifugation at full speed for 15 min. The pellet was washed in 96% ethanol, air-dried and resuspended in 20µl of 2mM Tris-HCl pH8 with loading buffer.

Replication intermediates were resolved by 2D gel electrophoresis using a 20 cm x 25 cm gel tray. The first dimension was carried out at room temperature in 0.4% agarose gels in TBE 1X at 45 V (28 mA) for 18 hours. Gels were stained with 0.33µg/ml EtBr in water for 30 min and DNA fragments between 3-12 kb were cut off and rotated 90º for the second dimension electrophoresis in a 20 cm x 25 cm gel tray. These fragments were resolved in the second dimension in 1% agarose gels in TBE 1X containing 0.33µg/ml ethidium bromide at 140 V (75 mA) for 16 hours. This electrophoresis was performed at 4ºC and with buffer re-circularization. After electrophoresis, gels were treated and transferred to a Hybond XL (Amersham) membrane by alkaline transfer. Replication intermediates were detected by hybridization with specific ^{32}P-labeled DNA probes: probe A of 4.6kb that hybridizes within the non-transcribed intergenic region (NTS1) and probe B of 4.5kb that hybridizes within the 35S gene. Probe A was generated from the PCR product obtained using the primers: forward: GTGGTATTTCACTGGCGCCGA, and reverse: ATAACCGCAGCAGGTCTCA. Probe B was generated

from the PCR product obtained using the primers: forward: CAACCCTGACGGTAGAGTAT, and reverse: ATTTCACTGGGCCAGCATCA.

Signals were quantified using a PhosphorImager with ImageGauge software (FUJI). The relative intensity of replication intermediates was normalized to the signal intensity obtained in the 1n-spot (non-saturating exposure). Gel images represented in the figures are optimal exposures to show the replication intermediates. Scanned images were optimized, in some cases, for brightness and contrast, but no gamma corrections or any other manipulations were carried out.

8.1 Characterization of replication intermediates

Following *Bgl*II digestion and isopropanol precipitation, DNA was resuspended in 2mM Tris-HCl pH8.0 and subjected to heat or enzymatic treatments as previously described (154). In brief, to induce branch migration, DNA was incubated at 56°C for 1h in the presence of 10mM EDTA pH8. For the strand displacement reaction, Klenow polymerase was used. Stepwise, 1 µl of nucleotide mix (5mM each of dATP, dCTP, dGTP, dTTP; Pharmacia), 1µl of gp32 protein (Biolabs, 4µg/µl), a single-stranded DNA binding protein that binds at 3´ hydroxyl group, and 1µl of Klenow (Takara; 5U/µl) were added to 17 µl of restriction enzyme-digested DNA in 1× restriction buffer and were incubated for 1h at 37° C. For R-loop removal, 1µl RNase H (Biolabs; 5U/µl) was added to 19 µl of restriction enzyme-digested DNA in 1× restriction buffer and incubated for 1h at 37°C.

8.2 Characterization of RF pausing sites

For characterization of RF pausing sites, replication intermediates from *rnh1Δ rnh2Δ* cells were compared to *fob1Δrrm3Δ* after growth with 10µg/ml CPT for 105 minutes or 60 minutes, respectively, following release from α-factor synchronization.

9. CLAMPED HOMOGENEOUS ELECTRIC FIELD (CHEF) GEL ELECTROPHORESIS

9.1 Agarose plug preparation

DNA was extracted from approximately 10^8 cells per low melting agarose (Pronadisa) plug as previously described (330). Briefly, yeast cells were washed in 50mM EDTA pH8 and then resuspended in 600µl CPES with 1.2M D-sorbitol and freshly added zymolyase 20T at 1mg/ml to hydrolyze the cell walls. The spheroplasts formed are embedded in 1ml 2% low-melting-point agarose prepared in CPE. This mixture was pipetted into moulds and allowed to cool and solidify during 10 minutes at 4ºC. Plugs were subsequently transferred to 10ml tubes and incubated for 4 hours at 30ºC with 5ml CPE. The solution was poured off and the plugs were incubated overnight at 50ºC in 5ml TESP. Plugs were washed three times at 50 ºC for 30 min, then twice at room temperature with TE. Finally the plugs were covered with 5ml 50mM EDTA pH8 and stored at 4ºC.

9.2 Analysis of replicating chromosomes

To analyze the replication status of chromosome cXII in exponentially growing cells, samples were retrieved at the specified time points following release (in minutes) from α-factor synchronization in the presence or absence of 10µg/ml CPT. Genomic DNA was extracted in low-melting agarose plugs as described previously. Replication intermediates were separated using a CHEF Mapper (Bio-Rad), with a linear voltage gradient of 6.0V/cm, pulse time of 0.22 s to 266 s, switch angle of 120º, in 0.5x TBE buffered-1% agarose gel for 15.2 hrs at 14°C, as previously described (327). For hybridization, ^{32}P-labelled probes for cV or cXII were used. cV probe was generated from PCR with forward primer: GTACGGTGGCCATTCTATGT, and reverse primer: AGATCCAGTAATGTGTTGGA. The previously described ribosomal probe A was used to probe cXII.

9.3 rDNA array repeat length determination

rDNA repeat length was determined by CHEF analysis of approximately 10^8 cells per LM-agarose plug. Cell lysis and chromosome separation conditions were carried out as previously described (75). In brief, electrophoresis was performed in a Bio-Rad CHEF Mapper, using a voltage gradient of 3.4V/cm, pulse time of 300-900s, switch angle of 120º, in 0.8% agarose gel in 0.5x TBE for 68 hrs at 14ºC. Chr. XII was detected by hybridization with ribosomal probe A.

10. MICROSCOPY

For wide-field fluorescence microscopy, a Leica DM-6000B equipped with a 100×/1.40 NA oil immersion objective lens was used, with the appropriate light excitation and emission conditions (Table 4). Images were taken using a digital charge-coupled device camera (DFC350; Leica) and LAS AF software (Leica).

	Leica filter	λ excitation	λ emission
DAPI	A4	360nm	470nm
Mitotracker orange	N3	546nm	600nm
GFP	L5	395nm	509nm
YFP	L5	514nm	527nm
mRFP	N3	584nm	607nm

Table 4. Light excitation and emission conditions for fluorescence microscopy.

10.1 Fixation of cells

Cells were fixed in 2.5% formaldehyde and 0.1M potassium phosphate buffer pH6.4 for 10 min. Cells were then washed twice with 0.1M potassium phosphate buffer pH6.6 and resuspended in 0.1M potassium phosphate buffer pH7.4. Fixed cells were stored at 4ºC. For DAPI staining, cells were fixed in 3.7% formaldehyde and 0.1M potassium phosphate buffer pH6.4 for 10 min. Cells were then washed twice with 0.1M potassium phosphate buffer pH6.4 and resuspended in 0.1M potassium phosphate buffer pH6.4. Cells were permeabilized using 1ml 80% ethanol

for 10 min, washed in 0.1M potassium phosphate buffer pH6.4 and incubated in 1µg/ml DAPI for 5 min in the dark.

10.2 Classification of nuclear phenotypes

For each sample, 600 previously fixed cells were counted from three independent experiments using Phase contrast (Ph) and the fraction of cells with no bud (G1), a small bud (smaller than one half of the yeast cell; S phase) or a large bud (equal or larger than one half of the yeast cell; G2) was noted. Nuclear segregation phenotypes for G2 cells were determined using DAPI fluorescent nuclear DNA stain.

10.3 Quantification of Rad52-YFP foci

Rad52-YFP foci formation was analysed by transforming cells with the plasmid pWJ1213 (*LEU2*, Rodney Rothstein) or p316-*RAD52*-YFP (URA3, Marina Murillo/Félix Prado). Transformants were grown to exponential phase in SC-Leucine or SC-Uracil liquid cultures and foci formation was detected by fluorescence microscopy using a L5 filter. Approximately 600 cells derived from three independent transformation experiments were analysed for each strain.

For time-course analysis of Rad52-YFP foci, cells expressing *RAD52*-YFP were synchronized with α-factor and released in the presence or absence of 10µg/ml CPT. Samples were retrieved at the specified time points following release (in minutes) and fixed with 2.5% formaldehyde. Approximately 600 cells derived from three independent colonies were analyzed for each condition. Data are shown as the mean ± standard deviation. Differences between groups were examined by Student's *t*-test.

10.4 Determination of nucleolar Rad52-YFP foci co-localization

For co-localization of Rad52-YFP foci with the nucleolar marker Nop1, cells were co-transformed with the Rad52-YFP expressing plasmid and a plasmid expressing Nop1-mRFP

(331). Transformants were grown to exponential phase in selective SC medium to maintain the plasmids, in the presence or absence of 10μg/ml CPT for 3 hrs, and fixed using 2.5% formaldehyde. YFP and RFP fluorescence were detected by wide-field fluorescence microscopy using L5 and N3 filters. The number of Rad52-YFP foci were counted and noted as co-localizing or not with the Nop1-mRFP signal. Approximately 600 cells derived from three independent transformants were analyzed for each strain. Data are shown as the mean ± standard deviation. Differences between groups were examined by Student's *t*-test and were considered statistically significant for p-values<0.05. Images were assembled in Photoshop (Adobe) with only linear adjustments.

10.5 Analysis of Rebudding

Cells were synchronized with α-factor and then released in the presence of 15μg/ml nocodazole with 1% DMSO. Nocodazole was repeatedly added every 60 min. 1ml samples of cells were retrieved at the indicated time points and fixed with formaldehyde. The percentage of G2 cells showing more than one bud was scored. Images were assembled in Photoshop (Adobe) with only linear adjustments.

10.6 Methylene blue staining of dead cells

1ul of 10mM methylene blue was added per 500μl of fixed cells and incubated for 5 min. Cells were analysed using bright field microscopy and the number of blue-stained cells was scored.

11. IMMUNOFLUORESCENCE

11.1 Cdc14 and α-tubulin staining

Immunofluorescence analysis of 3HA-Cdc14 and tubulin was performed as described in (266). Briefly, cells were fixed overnight in 3.7% formaldehyde and 0.1 M potassium phosphate buffer, pH 6.4. Cells were then washed twice with 0.1 M potassium phosphate buffer, pH 6.4 and resuspended in sorbitol citrate (see Appendices for buffer compositions). Fixed cells were

digested with 0.1 mg/ml zymolyase-100T (US Biological) and 1/10 volume of glusulase (PerkinElmer) at 30°C for 10 min. Cells were washed then resuspended in sorbitol citrate. 3HA-Cdc14 was detected using anti-HA antibody (HA.11; Covance) at 1:150 and anti–mouse Cy3 antibody (Jackson ImmunoResearch Laboratories, Inc.) at 1:1000. Anti-tubulin (Abcam) and anti–rat FITC (Jackson ImmunoResearch Laboratories, Inc.) antibodies were used at 1:200. All antibodies were diluted in PBS with 1% BSA. Microscope preparations were analyzed at 25°C using a Leica DM-6000B equipped with a 100×/1.40 NA oil immersion objective lens. Images were taken with a digital charge-coupled device camera (DFC350; Leica) and LAS AF (Leica) software.

11.2 RNA:DNA hybrid detection

In order to analyse the formation of RNA:DNA hybrids, strains were first synchronized with α-factor, before incubation with 1mM IAA for 30 minutes and release into fresh medium containing IAA. Cells were fixed and immunofluorescence was performed as for *12.1* using the S9.6 antibody (ATCC) at 1:200 diluted in PBS with 1% BSA, and anti-mouse Alexa 546 (Invitrogen) antibody at 1:500.

12. *ANALYSIS OF ROS AND APOPTOSIS*

Intracellular *r*eactive *o*xygen *s*pecies (ROS) were detected and measured by flow cytometry using the ROS indicator H_2DCF-DA (Life Technologies). Upon cleavage of the acetate groups by oxidation, the non-fluorescent H_2DCFCA is converted to the highly fluorescent 2´-7´-DCF. Cells were grown to exponential phase in YPAD. 1ml of cells were resuspended in 1 x PBS containing 5μM H_2DCF-DA (prepared directly before use) and incubated in the dark for 30 minutes before sonication. Fluorescence intensity was measured in the fluorescein range (FL1 channel, 525-550nm), and adjusted for autofluorescence from non-stained cells.

Caspase activity was detected using FITC-VAD-FMK (Promega), which irreversibly binds to activated metacaspases. 1ml of exponentially growing cells were resuspended in 1 x PBS

containing 1μM FITC-VAD-FMK. Samples were incubated in the dark for 10 minutes before sonication. Emission signals were detected in the fluorescein range (FL1 channel, 525-550nm), and fluorescent intensity was measured, with adjustment for autofluorescence from unstained cells.

13. PROTEIN ANALYSIS

13.1 Protein extraction

Yeast protein extracts were prepared from approximately 10^8 cells by trichloroacetic acid precipitation as described (332) with some modifications. Cells were washed with water and resuspended in 200μl of 20% trichloroacetic acid at room temperature. After addition of the same volume of glass beads (Sigma), cells were disrupted by vortexing 7-10 times for 30 seconds at 4ºC with intervals of 1 min on ice. After recovering the supernatant in a new tube, glass beads were washed with 600μl of 5% trichloroacetic acid, and the resulting extract was spun for 5 min at 13000 rpm. The pellet was resuspended in 100μl of Laemmli buffer, neutralized by adding 50μl of 1M Tris base, boiled for 5 min, and finally clarified by centrifugation.

13.2 Western blot analysis

Protein extracts were separated by sodium dodecyl sulphate-polyacrylamide gel electrophoresis (SDS-PAGE) at 200V for 1-3 h in running buffer using 8% polyacrylamide (37.5:1) gel, unless otherwise specified. ColorBurst™ Electrophoresis Marker (Sigma) was used as protein molecular weight marker. Gels were transferred to a previously methanol-activated PVDF membrane (Immobilon-P, Millipore) applying 30V for 12-16 hours at 4ºC and submerged in transfer buffer using the Mini Trans-Blot (BioRad). After the transfer, membranes were washed with methanol and air-dried. Transfer efficiency was checked by staining with Ponceau S.

Membranes were blocked at room temperature during 1h with gentle shaking in 5ml of TBS-Tween-Milk (1% Tween-20, 5% milk powder), unless otherwise stated. Membranes were then incubated with the corresponding primary and secondary antibodies as indicated. Finally, membranes were washed three times with TBS-Tween and chemiluminescence was detected using the HRP substrate (Millipore) and exposition to photographic films (Kodak X-Omat LS film).

13.3 Analysis of Clb2 levels

The levels of Clb2 protein were followed during one cell cycle following release from a G1 block with α-factor. Cells were released into pheromone-free medium with or without CPT for 60 minutes, when small buds were observed, at which point α-factor was re-added. TCA-extracted protein was separated on a 10% polyacrylamide (37.5:1) gel. PVDF membrane was blocked with TBS-milk (5%) The rabbit α-Clb2 primary antibody (Santa Cruz Biotechnology) was incubated at 4ºC overnight at 1:2000 dilution, and the secondary donkey anti-rabbit ECL HRP-labelled antibody (Amersham) was incubated at 4ºC overnight at 1:10,000 dilution, both in TBS-Tween-Milk (0.03% Tween, 5% milk).

Mouse α-PGK1 was used as loading control (Invitrogen), following block with PBS-Tween-Milk (0.1% Tween, 5% milk). The primary antibody at 1:20,000 dilution and the secondary (α-HRP ECL anti-mouse (GE Healthcare) at 1:10,000 dilution, were both incubated at 4ºC overnight in PBS-Milk-BSA (1% milk, 1% BSA).

13.4 Analysis of Sic1 levels

The levels of Sic1 protein were followed during one cell cycle, with synchronization as described in *14.3*. TCA-extracted protein was separated on a 12% polyacrylamide (37.5:1) gel. PVDF membrane was blocked with TBS-Milk (5% milk). The rabbit α-Sic1 primary antibody (Santa Cruz Biotechnology) was incubated at 4ºC overnight at 1:500 dilution, and the secondary donkey anti-rabbit ECL HRP-labelled antibody (Amersham) was incubated at 4ºC

overnight at 1:10,000 dilution, both in TBS-Tween-Milk (0.05% Tween, 5% milk). Mouse α-PGK1 was used as loading control as for *13.3*.

13.5 Analysis of Rad53 phosphorylation

Phosphorylation of Rad53 protein was used as an indicator of checkpoint activation. Yeast cells were grown in the presence or absence of 10ug/ml CPT. WT cells were grown in the presence of 200mM hydroxyurea (HU) as a positive control for Rad53 hyper-phosphorylation. Phosphorylated forms of Rad53 were detected by incubation with anti-Rad53 (λC-19) primary antibody (Santa Cruz Biotechnology) at 1:500 dilution for 1-2 hrs.

Protein extracts were run for the Rad53 *in situ* kinase assay and the auto-phosphorylation reaction was performed as described (257).

13.6 Confirmation of AID-tagged protein depletion

Yeast cells were grown in YPAD at 30ºC to exponential phase. Protein degradation was induced by the addition of 1.5mM IAA to the media, with incubation for 30 or 60 minutes. Top1-9Myc protein levels were detected by incubation with the mouse anti-c-Myc primary antibody (Abcam) at 1:1000 dilution at 4ºC overnight, and goat anti-mouse IgG-HRP (Sigma) at 1:10,000. The truncated IAA17 peptide (AID*) (320) adds an extra 4.7kDa, approximately, to the size of the protein. Mouse α-PGK1 was used as loading control as for *13.3*.

Table 2. Yeast strains used in this study.

Strain	Genotype	Source
YKL83	*MAT***a** *ubr1Δ::GAL-UBR1::HIS3 ade2-1 trp1-1 ura3-1 his3-11,15 leu2-3,112 can1-100*	(124)
RS310	YKL83; *rnh1Δ::hphMX4*	This study
RW027.17	YKL83; *rnh201Δ::natMX4*	This study
RW025.C	YKL83; *rnh1Δ:: hphMX4 rnh201Δ::natMX4*	This study
RS072	*MAT***α** YKL83	This study
RS075	*MAT***α** YKL83; *rnh1Δ::HYG rnh201Δ::NAT*	This study
RS153	YKL83; *rad1Δ::HIS*	This study
RS154	YKL83; *tdp1Δ::KAN*	This study
RS287	YKL83; *rad1Δ::HIS tdp1Δ::KAN*	This study
RS130	YKL83; *rad1Δ::HIS rnh1Δ::hphMX rnh201Δ::natMX4*	This study
RS129	YKL83; *tdp1Δ::KAN rnh1Δ::hphMX rnh201Δ::natMX4*	This study
RS128	YKL83; *rad1Δ::HIS tdp1Δ::KAN rnh1Δ::hphMX rnh201Δ::natMX4*	This study
BY4741	MAT**a** *trp1-1 ura3 Δ0 leu2Δ0 his3Δ0 met15Δ0*	Euroscarf
YMR234W	BY; *rnh1Δ:: KAN*	Euroscarf
YNL072W	BY; *rnh201Δ:: KAN*	Euroscarf
RS171	BY; *rnh1Δ:: KAN rnh201Δ::natMX4*	This study
RS103	YKL83; *leu2-k::URA3-ADE2::leu2-k*	This study
RS105	*rnh1Δ::hphMX4 leu2-k::URA3-ADE2::leu2-k*	This study
RS108	*rnh201Δ::natMX4 leu2-k::URA3-ADE2::leu2-k*	This study
RS111	*rnh1Δ:: hphMX4 rnh201Δ::natMX4 leu2-k::URA3-ADE2::leu2-k*	This study
NGY203	YKL83; *fob1Δ::kanMX4*	This study
RS179	YKL83; *rrm3Δ::kanMX4*	This study
RS165	YKL83; *fob1Δ::kanMX4 rnh1Δ::hphMX rnh201Δ::natMX4*	This study
RS204	YKL83; *rrm3Δ::kanMX4 rnh1Δ::hphMX rnh201Δ::natMX4*	This study
RS182	YKL83; *fob1Δ::kanMX4 rrm3Δ::kanMX4*	This study
RS031	W303; *bar1Δ RAD5*	This study
RS149	YKL83; *rnh1Δ::hphMX rnh201Δ::natMX4 bar1Δ*	This study
RS364	*TOP1*$^{AID*\text{-}9myc}$*::KanMX rnh1Δ::hphMX rnh201Δ::natMX4 bar1Δ URA3:: ADH1-AtTIR1*^{9myc}	This study
RS284	YKL83; *rpa190-3*	This study
RS230	YKL83; *rpa190-3 rnh1Δ::hphMX rnh201Δ::natMX4*	This study
RS266	YKL83; *rrn3-8*	This study
RS267	YKL83; *rrn3-8 rnh1Δ::hphMX rnh201Δ::natMX4*	This study

RWY020.2	YKL83; *rad27Δ::natMX4*	This study
TOI-1Bu	W303; *top1Δ::hisG*	A.Aguilera
RS375	YKL83; *hmo1Δ:: KAN*	This study
RS376	YKL83; *hmo1Δ:: KAN rnh1Δ::hphMX rnh201Δ::natMX4*	This study
RS377	YKL83; *tof2Δ:: KAN*	This study
RS378	YKL83; *tof2Δ:: KAN rnh1Δ::hphMX rnh201Δ::natMX4*	This study
RS392	W303; *nsr1Δ:: HIS*	This study
RS221	YKL83; *nsr1Δ:: HIS rnh1Δ::hphMX rnh201Δ::natMX4*	This study
RS393	YKL83; *rpa12Δ::LEU*	This study
RS215	YKL83; *rpa12Δ::LEU rnh1Δ::hphMX rnh201Δ::natMX4*	This study
RS394	YKL83; r*pa49Δ::KAN*	This study
RS216	YKL83; *rpa49Δ::KAN rnh1Δ::hphMX rnh201Δ::natMX4*	This study
RS307	YKL83; *uaf30Δ:: KAN*	This study
RS308	YKL83; *uaf30Δ:: KAN rnh1Δ::hphMX rnh201Δ::natMX4*	This study
RS379	YKL83; *rif2Δ:: KAN*	This study
RS380	YKL83; *rif2Δ:: KAN rnh1Δ::hphMX rnh201Δ::natMX4*	This study
Pif1-m2	W303; *pif1-m2*	(6)
RS395	*pif1-m2 rnh1Δ::hphMX rnh201Δ::natMX4*	This study
RS381	YKL83; *rad16Δ:: KAN*	This study
RS382	YKL83; *rad16Δ:: KAN rnh1Δ::hphMX rnh201Δ::natMX4*	This study
RM132-BBL	*rad3-2 ade2-1 Can^r his7 lys2-2 tyr1 leu1 trp5 met13-c cyh2r ura3*	R.Malone
RS383	YKL83; *rad3-2 rnh1Δ::hphMX rnh201Δ::natMX4*	This study
RS018	W303; *rad9Δ::hphMX*	This study
RS214	YKL83; *rad9Δ::hphMX rnh1Δ::hphMX rnh201Δ::natMX4*	This study
RS396	YKL83; *chk1Δ:: KAN*	This study
RS213	YKL83; *chk1Δ:: KAN rnh1Δ::hphMX rnh201Δ::natMX4*	This study
RS397	YKL83; *tel1Δ:: KAN*	This study
RS398	YKL83; *tel1Δ:: KAN rnh1Δ::hphMX rnh201Δ::natMX4*	This study
DD379	W303; *rad24Δ::TRP1*	(333)
RS166	YKL83; *rad24Δ::TRP1 rnh1Δ::hphMX rnh201Δ::natMX4*	This study
RS384	YKL83; *dunl1Δ::KAN*	This study
RS385	YKL83; *dun1Δ:: KAN rnh1Δ::hphMX rnh201Δ::natMX4*	This study
YJT74	W303; *mec1Δ::LEU2 sml1Δ::URA3*	This study
RS399	YKL83; *mec1Δ::LEU2 sml1Δ::URA3 rnh1Δ::hphMX rnh201Δ::natMX4*	This study
MCY012	YKL83; *sml1Δ::URA3*	This study

RS400	YKL83; *sml1Δ::URA3 rnh1Δ::hphMX rnh201Δ::natMX4*	This study
RS286	YKL83; *pol32Δ::hphMX*	This study
YH6120-8B	W303; *rad18Δ::KAN TRP1*	A. Aguilera
RS236	YKL83; *rad18Δ::KAN rnh1Δ::hphMX rnh201Δ::natMX4*	This study
RS386	YKL83; *shu1Δ:: KAN*	This study
RS387	YKL83; *shu1Δ:: KAN rnh1Δ::hphMX rnh201Δ::natMX4*	This study
WKU70-1B	YKL83; *yku70Δ::hphMX*	A. Aguilera
RS184	YKL83; *yku70Δ:: hphMX rnh1Δ::hphMX4 rnh201Δ::natMX4*	This study
RS028	W303; *lig4Δ::KAN*	This study
RS167	YKL83; *lig4Δ::KAN rnh1Δ::hphMX4 rnh201Δ::natMX4*	This study
RS285	YKL83; *rad52Δ::klLEU*	This study
RS253	YKL83; *rad51Δ:: KAN*	This study
RS254	YKL83; *rad51Δ:: KAN rnh1Δ::hphMX4 rnh201Δ::natMX4*	This study
RS205	YKL83; *exo1Δ:: KAN*	This study
NGY195	YKL83; *exo1Δ:: KAN rnh1Δ::hphMX4 rnh201Δ::natMX4*	This study
RS272	YKL83; *rad59Δ::KAN*	This study
RS244	YKL83; *rad59Δ:: KAN rnh1Δ::hphMX4 rnh201Δ::natMX4*	This study
RS292	YKL83; *mus81Δ::KAN*	This study
RS124	YKL83; *mus81Δ:: KAN rnh1Δ::hphMX4 rnh201Δ::natMX4*	This study
RS021	W303; *mre11Δ:: hphMX4*	This study
YNL250W	BY; *rad50Δ:: KAN*	Euroscarf
YDR369C	BY; *xrs2Δ:: KAN*	Euroscarf
RS152	YKL83; *srs2Δ:: natMX4*	This study
RS237	YKL83; *srs2Δ::natMX4 rnh1Δ::hphMX4 rnh201Δ::natMX4*	This study
RS151	YKL83; *sgs1Δ::natMX4*	This study
RS238	YKL83; *sgs1Δ::natMX4 rnh1Δ::hphMX4 rnh201Δ::natMX4*	This study
RS388	YKL83; *top3Δ::KAN*	This study
RS389	YKL83; *top3Δ:: KAN rnh1Δ::hphMX4 rnh201Δ::natMX4*	This study
RS160	YKL83; *sae2Δ::KAN*	This study
RS125	YKL83; *sae2Δ:: KAN rnh1Δ::hphMX4 rnh201Δ::natMX4*	This study
RS390	YKL83; *siz1Δ::KAN*	This study
RS391	YKL83; *siz1Δ:: KAN rnh1Δ::hphMX4 rnh201Δ::natMX4*	This study
RS401	YKL83; *sic1Δ::KAN*	This study
NGY157	YKL83; *clb5Δ: hphMX4*	This study
RS358	YKL83; *clb5Δ::hphMX4 rnh1Δ::hphMX4 rnh201Δ::natMX4*	This study

PP544	W303-1A; *cdc7-4 RAD5*	(334)
RS321	YKL83;*cdc7-4 rnh1Δ::hphMX4 rnh201Δ::natMX4*	This study
RSY727	*cdc7Δ::HIS3 mcm5-bob1 his6 leu2 ura3 lys2 cyh2*	R. Sclafani
RS346	YKL83; *cdc7Δ::HIS3 mcm5-bob1 rnh1Δ::hphMX4 rnh201Δ::natMX4*	This study
NGY132	W303; *swe1Δ::KAN*	This study
RS122	YKL83; *swe1Δ::KAN rnh1Δ::hphMX4 rnh201Δ::natMX4*	This study
RS161	YKL83; *mad1Δ::HIS*	This study
RS159	YKL83; *mad1Δ::HIS rnh1Δ::hphMX4 rnh201Δ::natMX4*	This study
P350	W303 *mad1Δ::MAD1-YEGFP*	F. Monje
RS264	YKL83; *mrc1Δ::kanMX4*	This study
RS265	YKL83; *mrc1Δ::kanMX4 rnh1Δ::hphMX4 rnh201Δ::natMX4*	This study
RS279	YKL83; $mrc1^{AQ}$*::HIS*	This study
RS255	YKL83; *mrc1-c14::KAN*	This study
RS280	YKL83; *mrc1AQ:: HIS rnh1Δ::hphMX rnh201Δ::natMX4*	This study
RS256	YKL83; *mrc1-c14:: KAN rnh1Δ::hphMX rnh201Δ:natMX4*	This study
RS258	YKL83; *csm3Δ::kanMX4*	This study
RS261	YKL83; *tof1Δ::kanMX4*	This study
RS259	YKL83; *csm3Δ::kanMX4 rnh1Δ::hphMX4 rnh201Δ::natMX4*	This study
RS262	YKL83; *tof1Δ::kanMX4 rnh1Δ::hphMX4rnh201Δ::natMX4*	This study
F665	W303-1A; *cdc14::3HA-CDC14*	(335)
RS325	*cdc14::3HA-CDC14 rnh1Δ::hphMX4 rnh201Δ::natMX4*	This study

Table 3. List of plasmids used in this study.

Plasmid	Description	Reference
pAG25-natMX4	DEL-MARKER-SET plasmid with *nat1* gene that confers resistance to nourseothricin (NAT)	Euroscarf
pAG32-hphMX4	DEL-MARKER-SET plasmid with *hph* gene that confers resistance to hygromycin B (HYG)	Euroscarf
pFA6a-*kanMX6*	DEL-MARKER-SET plasmid with the *kanMX* cassette that confers resistance to geneticin G418 (KAN)	Euroscarf
pFA6a-*klLEU2MX6*	DEL-MARKER-SET plasmid with the *LEU2* gene that allows growth of yeast on selective medium lacking leucine	Euroscarf
pBJ6	*CEN, URA3, RAD5*	(336)
pCM184- LAUR	*CEN, URA3, tetp:: lacZ::URA3*	(134)
pDML5	*CEN, URA3, GAL1p::RAD52*	(337)
pKan–AID*–9myc	IAA17 (71–114)-9myc *kanMX4* in pSM409	(320)
pPL092	*SSD1-v* (JK9-3da allele) in pRS316 (*URA3*)	(338)
pPL093	*SSD1-d* (W303 allele) in pRS316 (*URA3*)	(338)
pRS314LB	*CEN6, TRP1, LEU2* coding sequence interrupted by 31bp	(326)
pWJ1344	*CEN, LEU2, RAD52::YFP*	R.Rothstein
3317	CEN, *LEU2, RPL25-GFP, mRFP-Nop1*	(331)
p316-R52-YFP	CEN, *URA3, RAD52-YFP*	F. Prado

8. ANNEXES

ANNEX I - Drugs and Reagents

Alpha factor (1mg/ml stock solution, dissolved in DMSO, Biomedal) was added to a final concentration of 1μg/ml for *BAR1+* or 0.3μg/ml for *bar1Δ* strains. The alpha factor pheromone arrests yeast in the G1 phase of the cell cycle.

Ampicillin (Amp) (80mg/ml stock solution, dissolved in water, Sigma) was added to solid or liquid LB at a final concentration of 80μg/ml. The Beta-lactame antibiotic was used to select bacterial strains transformed with a plasmid of interest.

Benomyl (10mg/ml stock solution, dissolved in DMSO, Sigma) was added to a final concentration of 5, 10 or 20μg/ml. The appropriate amount of stock solution was added to warm agar with constant stirring and gentle heating to aid dissolution. Benomyl binds to microtubules, acting as a spindle-depolymerizing drug.

Calcofluor white (CFW) (1mg/ml stock solution, dissolved in water, Sigma; CFW sold as "Fluorescent Brightener 28") was added to a final concentration of 5μg/ml. CFW binds to chitin in the yeast cell wall and negatively affects normal cell wall assembly.

Camptothecin (CPT) (5mg/ml stock solution in 1% DMSO, Santa Cruz) was added to a final concentration of 5μg/ml for plates, or 10μg/ml for liquid cultures, unless otherwise stated.

Canavanine sulphate (Can) (Sigma) was added to a final concentration of 60μg/ml, directly to warm agar. Used to determine nuclear mutation rates.

Ethidium bromide (EtBr) (10mg/ml stock solution dissolved in water, Sigma) was added to a final concentration of 0.4mg per 1 litre of agarose.

FITC-VAD-FMK (5mM stock solution dissolved in DMSO, Promega) was used at a final concentration of 1μM. Used as an indicator to detect activated caspases.

5-fluororotic acid (FOA) (Melford) was added to a final concentration of 500mg/ml.

G418 disulphate (GEN) (200mg/ml stock solution, Melford) was added to a final concentration of 200μg/ml. Used to select yeast that carry gene for resistance to kanamycin/geneticin.

H_2DCFDA (5mM stock solution dissolved in DMSO, Life Technologies) was used at a final concentration of 5μM. Used as an indicator to detect the generation of ROS in cells.

Hydroxyurea (HU) (USBiological) was added to a final concentration of 100mM, directly to warm agar.

Hygromycin (Hyg) (Applichem, 46KU/ml) was added to a final concentration of 0.3mg/ml. Used to select yeast that carry gene for resistance to hygromycin.

Indole-3-acetic acid (IAA) (500mM stock solution dissolved in ethanol, Sigma) was added at a final concentration of 500μM.

Methylene blue (10mM stock solution, diluted in water, Sigma) was added to a final concentration of 20μM. Used to determine the viability of *yeast cells.*

Methyl methanesulphonate (MMS) (250M stock solution, Fluka) was added to a final concentration of 25mM or as specified, directly to warm agar.

Nocodazole (Noc) (10mg/ml stock solution, dissolved in DMSO, Sigma) was added to a final concentration of 15μg/ml.

Nourseotricine (NAT) (Werner BioAgents, Germany; NAT sold as "clonNAT") was added to a final concentration of 100μg/ml. Used to select yeast that carry gene for resistance to NAT.

Pronase (50mg/ml stock solution, dissolved in 50% glycerol, Sigma; pronase sold as "protease from *Streptococcus griseus*") was added to a final concentration of 1μg/ml. Used to digest alpha factor, following G1 synchronization of *bar1Δ* yeast strains.

Propidium iodide (5mg/ml stock solution, dissolved in water, Sigma) was added to a final concentration of 5μg/ml.

ANNEX II – Composition of buffers and solutions

Cocktail gently buffer	50mM Tris-HCl pH8, 20mM EDTA pH8
Coomassie stain	0.1% *Coomassie* Blue (w/w), 50% methanol, 1% acetic acid
Coomassie destain	5% methanol, 7.5% acetic acid
CPE	40mM citric acid pH6, 120mM sodium phosphate pH6, 20mM EDTA-Na pH8
CPES	40mM citric acid pH6, 120mM sodium phosphate pH6, 20mM EDTA-Na pH8, 1.2M D-sorbitol, 1mg/ml zymolyase 20T
CTAB II	1% w/v CTAB (cetyl-trimethyl-ammonium-bromide), 50mM Tris-HCl pH 7.6, 10mM EDTA pH8
CTAB III	1.4M NaCl, 10mM Tris-HCl pH7.6, 1mM EDTA pH8
Denaturation buffer	1.5M NaCl, 0.5M NaOH
G2 solution	800mM guanidine HCl, 30mM Tris-HCl pH8, 30mM EDTA pH8, 5% Tween-20, 0.5% Triton X-100
Hybridization solution	0.25M Na_2HPO_4, 7% SDS, 1mM EDTA pH7.2
Laemmli buffer 2x	4% SDS, 20% glycerol, 10% β-mercaptoethanol, 0.004% bromophenol blue, 0.125 M Tris HCl
Neutralization buffer	1M Tris-HCl, 1.5M NaCl, adjusted to pH7.5.
PBS 10x	1,37 M NaCl, 27mM KCl, 81mM Na_2HPO_4, 14.7mM KH_2PO_4
Ponceau	Ponceau S 0.1% w/v, 5% acetic acid
Running buffer (Western)	50mM Tris Base, 192mM glycine pH8.3, 0.1% SDS
Sorbitol-citrate	1.2 M sorbitol in 0.12 M K_2HPO_4, 0.033 M citric acid, pH 5.9
Spheroplasting buffer	1M sorbitol, 100mM EDTA pH8, 2mM Tris-HCl pH8, 0.1% v/v β-mercaptoethanol, 15U zymolyase/ml
Stripping solution (hybridization)	0.1% SDS, 0.1X SSPE
SSC 20x	3M NaCl, 0.3M trisodium citrate, adjusted to pH7

TAE 50x	2M Tris, 1M acetic acid, and 10mM EDTA.
TBE 5x	0.45M Tris borate, 10mM EDTA-Na, adjusted to pH8
TBS	20 mM Tris-HCl pH8, 0.13M NaCl
TBS-Tween	20 mM Tris-HCl pH 8, 0.13M NaCl, 1% Tween-20, 5% milk powder
TESP	10mM Tris-HCl pH8, 450mM EDTA-Na pH8, 1% SDS, with 1mg/ml freshly prepared proteinase K
Transfer buffer (Western)	50mM Tris Base, 192mM glycine pH8.3, 0.01% SDS, 20% methanol
Wash solution (hybridization)	0.1X SSPE, 0.5mM EDTA, 0.5% SDS

ANNEX III – Published articles

STUCKEY R, Díaz de la Loza MC and Wellinger RE.

Cellular responses to mitochondrial DNA damage in yeast.

In: Mitochondria: Structure, Functions and Dysfunctions; Pp: 709-729, Ed. Ed. O. Svensson,

Nova Science Publishers NY; ISBN 978-1-61761-490-3 (2010).

9. BIBLIOGRAPHY

1. Mechali, M. (2010) Eukaryotic DNA replication origins: many choices for appropriate answers. *Nat Rev Mol Cell Biol*, **11**, 728-738.
2. Lundblad, L. and Struhl, K. (eds.) (2010) *Yeast. Current Protocols in Molecular Biology. 13.0.1-13.0.4*.
3. Diffley, J.F., Cocker, J.H., Dowell, S.J. and Rowley, A. (1994) Two steps in the assembly of complexes at yeast replication origins in vivo. *Cell*, **78**, 303-316.
4. Bousset, K. and Diffley, J.F. (1998) The Cdc7 protein kinase is required for origin firing during S phase. *Genes Dev*, **12**, 480-490.
5. Kearsey, S.E. and Cotterill, S. (2003) Enigmatic variations: divergent modes of regulating eukaryotic DNA replication. *Mol Cell*, **12**, 1067-1075.
6. Pursell, Z.F., Isoz, I., Lundstrom, E.B., Johansson, E. and Kunkel, T.A. (2007) Yeast DNA polymerase epsilon participates in leading-strand DNA replication. *Science*, **317**, 127-130.
7. Crouse, G.F. (2010) An end for mismatch repair. *Proc Natl Acad Sci U S A*, **107**, 20851-20852.
8. Reaban, M.E., Lebowitz, J. and Griffin, J.A. (1994) Transcription induces the formation of a stable RNA.DNA hybrid in the immunoglobulin alpha switch region. *J Biol Chem*, **269**, 21850-21857.
9. Drolet, M., Bi, X. and Liu, L.F. (1994) Hypernegative supercoiling of the DNA template during transcription elongation in vitro. *J Biol Chem*, **269**, 2068-2074.
10. Roy, D. and Lieber, M.R. (2009) G clustering is important for the initiation of transcription-induced R-loops in vitro, whereas high G density without clustering is sufficient thereafter. *Mol Cell Biol*, **29**, 3124-3133.
11. Reddy, K., Tam, M., Bowater, R.P., Barber, M., Tomlinson, M., Nichol Edamura, K., Wang, Y.H. and Pearson, C.E. (2011) Determinants of R-loop formation at convergent bidirectionally transcribed trinucleotide repeats. *Nucleic Acids Res*, **39**, 1749-1762.
12. Cerritelli, S.M. and Crouch, R.J. (2009) Ribonuclease H: the enzymes in eukaryotes. *FEBS J*, **276**, 1494-1505.
13. Jeong, H.S., Backlund, P.S., Chen, H.C., Karavanov, A.A. and Crouch, R.J. (2004) RNase H2 of Saccharomyces cerevisiae is a complex of three proteins. *Nucleic Acids Res*, **32**, 407-414.
14. Kim, N., Huang, S.N., Williams, J.S., Li, Y.C., Clark, A.B., Cho, J.E., Kunkel, T.A., Pommier, Y. and Jinks-Robertson, S. (2011) Mutagenic processing of ribonucleotides in DNA by yeast topoisomerase I. *Science*, **332**, 1561-1564.
15. Nick McElhinny, S.A., Watts, B.E., Kumar, D., Watt, D.L., Lundstrom, E.B., Burgers, P.M., Johansson, E., Chabes, A. and Kunkel, T.A. (2010) Abundant ribonucleotide incorporation into DNA by yeast replicative polymerases. *Proc Natl Acad Sci U S A*, **107**, 4949-4954.
16. Aguilera, A. and Garcia-Muse, T. (2012) R loops: from transcription byproducts to threats to genome stability. *Mol Cell*, **46**, 115-124.
17. Beletskii, A. and Bhagwat, A.S. (1996) Transcription-induced mutations: increase in C to T mutations in the nontranscribed strand during transcription in Escherichia coli. *Proc Natl Acad Sci U S A*, **93**, 13919-13924.
18. Helmrich, A., Ballarino, M., Nudler, E. and Tora, L. (2013) Transcription-replication encounters, consequences and genomic instability. *Nat Struct Mol Biol*, **20**, 412-418.
19. Huertas, P. and Aguilera, A. (2003) Cotranscriptionally formed DNA:RNA hybrids mediate transcription elongation impairment and transcription-associated recombination. *Mol Cell*, **12**, 711-721.
20. Li, X. and Manley, J.L. (2005) Inactivation of the SR protein splicing factor ASF/SF2 results in genomic instability. *Cell*, **122**, 365-378.

21. Wahba, L., Amon, J.D., Koshland, D. and Vuica-Ross, M. (2011) RNase H and multiple RNA biogenesis factors cooperate to prevent RNA:DNA hybrids from generating genome instability. *Mol Cell*, **44**, 978-988.
22. Stirling, P.C., Chan, Y.A., Minaker, S.W., Aristizabal, M.J., Barrett, I., Sipahimalani, P., Kobor, M.S. and Hieter, P. (2012) R-loop-mediated genome instability in mRNA cleavage and polyadenylation mutants. *Genes Dev*, **26**, 163-175.
23. Luna, R., Jimeno, S., Marin, M., Huertas, P., Garcia-Rubio, M. and Aguilera, A. (2005) Interdependence between transcription and mRNP processing and export, and its impact on genetic stability. *Mol Cell*, **18**, 711-722.
24. Baaklini, I., Hraiky, C., Rallu, F., Tse-Dinh, Y.C. and Drolet, M. (2004) RNase HI overproduction is required for efficient full-length RNA synthesis in the absence of topoisomerase I in Escherichia coli. *Mol Microbiol*, **54**, 198-211.
25. Wellinger, R.E., Prado, F. and Aguilera, A. (2006) Replication fork progression is impaired by transcription in hyperrecombinant yeast cells lacking a functional THO complex. *Mol Cell Biol*, **26**, 3327-3334.
26. Gan, W., Guan, Z., Liu, J., Gui, T., Shen, K., Manley, J.L. and Li, X. (2011) R-loop-mediated genomic instability is caused by impairment of replication fork progression. *Genes Dev*, **25**, 2041-2056.
27. McIvor, E.I., Polak, U. and Napierala, M. (2010) New insights into repeat instability: role of RNA*DNA hybrids. *RNA Biol*, **7**, 551-558.
28. Lin, Y., Dent, S.Y., Wilson, J.H., Wells, R.D. and Napierala, M. (2010) R loops stimulate genetic instability of CTG.CAG repeats. *Proc Natl Acad Sci U S A*, **107**, 692-697.
29. Skourti-Stathaki, K., Proudfoot, N.J. and Gromak, N. (2011) Human senataxin resolves RNA/DNA hybrids formed at transcriptional pause sites to promote Xrn2-dependent termination. *Mol Cell*, **42**, 794-805.
30. Yu, K., Chedin, F., Hsieh, C.L., Wilson, T.E. and Lieber, M.R. (2003) R-loops at immunoglobulin class switch regions in the chromosomes of stimulated B cells. *Nat Immunol*, **4**, 442-451.
31. Muramatsu, M., Kinoshita, K., Fagarasan, S., Yamada, S., Shinkai, Y. and Honjo, T. (2000) Class switch recombination and hypermutation require activation-induced cytidine deaminase (AID), a potential RNA editing enzyme. *Cell*, **102**, 553-563.
32. Zarrin, A.A., Del Vecchio, C., Tseng, E., Gleason, M., Zarin, P., Tian, M. and Alt, F.W. (2007) Antibody class switching mediated by yeast endonuclease-generated DNA breaks. *Science*, **315**, 377-381.
33. Ginno, P.A., Lott, P.L., Christensen, H.C., Korf, I. and Chedin, F. (2012) R-loop formation is a distinctive characteristic of unmethylated human CpG island promoters. *Mol Cell*, **45**, 814-825.
34. Deng, W. (2010) AID in reprogramming: quick and efficient: identification of a key enzyme called AID, and its activity in DNA demethylation, may help to overcome a pivotal epigenetic barrier in reprogramming somatic cells toward pluripotency. *Bioessays*, **32**, 385-387.
35. Bhutani, N., Brady, J.J., Damian, M., Sacco, A., Corbel, S.Y. and Blau, H.M. (2010) Reprogramming towards pluripotency requires AID-dependent DNA demethylation. *Nature*, **463**, 1042-1047.
36. Dunn, K. and Griffith, J.D. (1980) The presence of RNA in a double helix inhibits its interaction with histone protein. *Nucleic Acids Res*, **8**, 555-566.
37. Castellano-Pozo, M., Santos-Pereira, J.M., Rondon, A.G., Barroso, S., Andujar, E., Perez-Alegre, M., Garcia-Muse, T. and Aguilera, A. (2013) R loops are linked to histone H3 S10 phosphorylation and chromatin condensation. *Mol Cell*, **52**, 583-590.
38. Fuller, C.W. and Richardson, C.C. (1985) Initiation of DNA replication at the primary origin of bacteriophage T7 by purified proteins. Site and direction of initial DNA synthesis. *J Biol Chem*, **260**, 3185-3196.
39. Itoh, T. and Tomizawa, J. (1980) Formation of an RNA primer for initiation of replication of ColE1 DNA by ribonuclease H *PNAS*, **77**, 2450-2454

40. Kasiviswanathan, R., Collins, T.R. and Copeland, W.C. (2012) The interface of transcription and DNA replication in the mitochondria. *Biochim Biophys Acta*, **1819**, 970-978.
41. Chang, D.D., Hauswirth, W.W. and Clayton, D.A. (1985) Replication priming and transcription initiate from precisely the same site in mouse mitochondrial DNA. *EMBO J*, **4**, 1559-1567.
42. Xu, B. and Clayton, D.A. (1996) RNA-DNA hybrid formation at the human mitochondrial heavy-strand origin ceases at replication start sites: an implication for RNA-DNA hybrids serving as primers. *EMBO J*, **15**, 3135–3143.
43. Lee, D.Y. and Clayton, D.A. (1997) RNase mitochondrial RNA processing correctly cleaves a novel R loop at the mitochondrial DNA leading-strand origin of replication. *Genes Dev*, **11**, 582-592.
44. Kogoma, T. and Lark, K.G. (1970) DNA replication in Escherihia coli: replication in absence of protein synthesis after replication inhibition. *J Mol Biol*, **52**, 143-164.
45. Ogawa, T., Pickett, G., Kogoma, T. and Kornberg, A. (1984) RNase H confers specificity in the dnaA-dependent initiation of replication at the unique origin of the Escherichia coli chromosome in vivo and in vitro. *Proc Natl Acad Sci U S A*, **81**, 1040-1044.
46. Sandler, S.J. (2005) Requirements for replication restart proteins during constitutive stable DNA replication in Escherichia coli K-12. *Genetics*, **169**, 1799-1806.
47. Lindahl, T. (1993) Instability and decay of the primary structure of DNA. *Nature*, **362**, 709-715.
48. Vengrova, S. and Dalgaard, J.Z. (2006) The wild-type Schizosaccharomyces pombe mat1 imprint consists of two ribonucleotides. *EMBO Rep*, **7**, 59-65.
49. Nick McElhinny, S.A., Kumar, D., Clark, A.B., Watt, D.L., Watts, B.E., Lundstrom, E.B., Johansson, E., Chabes, A. and Kunkel, T.A. (2010) Genome instability due to ribonucleotide incorporation into DNA. *Nat Chem Biol*, **6**, 774-781.
50. Cerritelli, S.M., Frolova, E.G., Feng, C., Grinberg, A., Love, P.E. and Crouch, R.J. (2003) Failure to produce mitochondrial DNA results in embryonic lethality in Rnaseh1 null mice. *Mol Cell*, **11**, 807-815.
51. Reijns, M.A., Rabe, B., Rigby, R.E., Mill, P., Astell, K.R., Lettice, L.A., Boyle, S., Leitch, A., Keighren, M., Kilanowski, F. *et al.* (2012) Enzymatic removal of ribonucleotides from DNA is essential for mammalian genome integrity and development. *Cell*, **149**, 1008-1022.
52. Crow, Y.J., Leitch, A., Hayward, B.E., Garner, A., Parmar, R., Griffith, E., Ali, M., Semple, C., Aicardi, J., Babul-Hirji, R. *et al.* (2006) Mutations in genes encoding ribonuclease H2 subunits cause Aicardi-Goutieres syndrome and mimic congenital viral brain infection. *Nat Genet*, **38**, 910-916.
53. Crow, Y.J., Hayward, B.E., Parmar, R., Robins, P., Leitch, A., Ali, M., Black, D.N., van Bokhoven, H., Brunner, H.G., Hamel, B.C. *et al.* (2006) Mutations in the gene encoding the 3'-5' DNA exonuclease TREX1 cause Aicardi-Goutieres syndrome at the AGS1 locus. *Nat Genet*, **38**, 917-920.
54. Rigby, R.E., Leitch, A. and Jackson, A.P. (2008) Nucleic acid-mediated inflammatory diseases. *Bioessays*, **30**, 833-842.
55. Prinz, M. and Knobeloch, K.P. (2012) Type I interferons as ambiguous modulators of chronic inflammation in the central nervous system. *Front Immunol*, **3**, 67.
56. Crow, Y.J. and Rehwinkel, J. (2009) Aicardi-Goutieres syndrome and related phenotypes: linking nucleic acid metabolism with autoimmunity. *Hum Mol Genet*, **18**, R130-136.
57. Boule, J.B. and Zakian, V.A. (2007) The yeast Pif1p DNA helicase preferentially unwinds RNA DNA substrates. *Nucleic Acids Res*, **35**, 5809-5818.
58. Mischo, H.E., Gomez-Gonzalez, B., Grzechnik, P., Rondon, A.G., Wei, W., Steinmetz, L., Aguilera, A. and Proudfoot, N.J. (2011) Yeast Sen1 helicase protects the genome from transcription-associated instability. *Mol Cell*, **41**, 21-32.

59. Drolet, M. (2006) Growth inhibition mediated by excess negative supercoiling: the interplay between transcription elongation, R-loop formation and DNA topology. *Mol Microbiol*, **59**, 723-730.
60. El Hage, A., French, S.L., Beyer, A.L. and Tollervey, D. (2010) Loss of Topoisomerase I leads to R-loop-mediated transcriptional blocks during ribosomal RNA synthesis. *Genes Dev*, **24**, 1546-1558.
61. Wang, J.C. (2002) Cellular roles of DNA topoisomerases: a molecular perspective. *Nat Rev Mol Cell Biol*, **3**, 430-440.
62. Pourquier, P., Pilon, A.A., Kohlhagen, G., Mazumder, A., Sharma, A. and Pommier, Y. (1997) Trapping of mammalian topoisomerase I and recombinations induced by damaged DNA containing nicks or gaps. Importance of DNA end phosphorylation and camptothecin effects. *J Biol Chem*, **272**, 26441-26447.
63. Staker, B.L., Hjerrild, K., Feese, M.D., Behnke, C.A., Burgin, A.B., Jr. and Stewart, L. (2002) The mechanism of topoisomerase I poisoning by a camptothecin analog. *Proc Natl Acad Sci U S A*, **99**, 15387-15392.
64. Pommier, Y. (2006) Topoisomerase I inhibitors: camptothecins and beyond. *Nat Rev Cancer*, **6**, 789-802.
65. Pouliot, J.J., Yao, K.C., Robertson, C.A. and Nash, H.A. (1999) Yeast gene for a Tyr-DNA phosphodiesterase that repairs topoisomerase I complexes. *Science*, **286**, 552-555.
66. Vance, J.R. and Wilson, T.E. (2002) Yeast Tdp1 and Rad1-Rad10 function as redundant pathways for repairing Top1 replicative damage. *Proc Natl Acad Sci U S A*, **99**, 13669-13674.
67. Deng, C., Brown, J.A., You, D. and Brown, J.M. (2005) Multiple endonucleases function to repair covalent topoisomerase I complexes in Saccharomyces cerevisiae. *Genetics*, **170**, 591-600.
68. Warner, J.R. (1999) The economics of ribosome biosynthesis in yeast. *Trends Biochem Sci*, **24**, 437-440.
69. Staub, E., Mackowiak, S. and Vingron, M. (2006) An inventory of yeast proteins associated with nucleolar and ribosomal components. *Genome Biol*, **7**, R98.
70. Mandal, R.K. (1984) The organization and transcription of eukaryotic ribosomal RNA genes. *Prog Nucleic Acid Res Mol Biol*, **31**, 115-160.
71. Brewer, B.J. and Fangman, W.L. (1988) A replication fork barrier at the 3' end of yeast ribosomal RNA genes. *Cell*, **55**, 637-643.
72. Little, R.D., Platt, T.H. and Schildkraut, C.L. (1993) Initiation and termination of DNA replication in human rRNA genes. *Mol Cell Biol*, **13**, 6600-6613.
73. Laloraya, S., Guacci, V. and Koshland, D. (2000) Chromosomal addresses of the cohesin component Mcd1p. *J Cell Biol*, **151**, 1047-1056.
74. Nicklas, R.B. (1997) How cells get the right chromosomes. *Science*, **275**, 632-637.
75. Ide, S., Miyazaki, T., Maki, H. and Kobayashi, T. (2010) Abundance of ribosomal RNA gene copies maintains genome integrity. *Science*, **327**, 693-696.
76. Liu, B. and Alberts, B.M. (1995) Head-on collision between a DNA replication apparatus and RNA polymerase transcription complex. *Science*, **267**, 1131-1137.
77. Prado, F. and Aguilera, A. (2005) Impairment of replication fork progression mediates RNA polII transcription-associated recombination. *EMBO J*, **24**, 1267-1276.
78. Brewer, B.J. (1988) When polymerases collide: replication and the transcriptional organization of the E. coli chromosome. *Cell*, **53**, 679-686.
79. Pomerantz, R.T. and O'Donnell, M. (2010) What happens when replication and transcription complexes collide? *Cell Cycle*, **9**, 2537-2543.
80. Pomerantz, R.T. and O'Donnell, M. (2008) The replisome uses mRNA as a primer after colliding with RNA polymerase. *Nature*, **456**, 762-766.
81. Linskens, M.H. and Huberman, J.A. (1988) Organization of replication of ribosomal DNA in Saccharomyces cerevisiae. *Mol Cell Biol*, **8**, 4927-4935.
82. Deshpande, A.M. and Newlon, C.S. (1996) DNA replication fork pause sites dependent on transcription. *Science*, **272**, 1030-1033.

83. Bermejo, R., Lai, M.S. and Foiani, M. (2012) Preventing replication stress to maintain genome stability: resolving conflicts between replication and transcription. *Mol Cell*, **45**, 710-718.
84. Branzei, D. and Foiani, M. (2008) Regulation of DNA repair throughout the cell cycle. *Nat Rev Mol Cell Biol*, **9**, 297-308.
85. Clark, J.M. and Beardsley, G.P. (1986) Thymine glycol lesions terminate chain elongation by DNA polymerase I in vitro. *Nucleic Acids Res*, **14**, 737-749.
86. Tornaletti, S., Maeda, L.S., Lloyd, D.R., Reines, D. and Hanawalt, P.C. (2001) Effect of thymine glycol on transcription elongation by T7 RNA polymerase and mammalian RNA polymerase II. *J Biol Chem*, **276**, 45367-45371.
87. Lu, A.L., Li, X., Gu, Y., Wright, P.M. and Chang, D.Y. (2001) Repair of oxidative DNA damage: mechanisms and functions. *Cell Biochem Biophys*, **35**, 141-170.
88. Shuck, S.C., Short, E.A. and Turchi, J.J. (2008) Eukaryotic nucleotide excision repair: from understanding mechanisms to influencing biology. *Cell Res*, **18**, 64-72.
89. Gaillard, H. and Aguilera, A. (2012) Transcription coupled repair at the interface between transcription elongation and mRNP biogenesis. *Biochim Biophys Acta*, **1829**, 141-150.
90. Lieber, M.R. (2008) The mechanism of human nonhomologous DNA end joining. *J Biol Chem*, **283**, 1-5.
91. Barlow, J.H., Lisby, M. and Rothstein, R. (2008) Differential regulation of the cellular response to DNA double-strand breaks in G1. *Mol Cell*, **30**, 73-85.
92. Symington, L.S. and Gautier, J. (2011) Double-strand break end resection and repair pathway choice. *Annu Rev Genet*, **45**, 247-271.
93. Wiltzius, J.J., Hohl, M., Fleming, J.C. and Petrini, J.H. (2005) The Rad50 hook domain is a critical determinant of Mre11 complex functions. *Nat Struct Mol Biol*, **12**, 403-407.
94. Paques, F. and Haber, J.E. (1999) Multiple pathways of recombination induced by double-strand breaks in Saccharomyces cerevisiae. *Microbiol Mol Biol Rev*, **63**, 349-404.
95. Prakash, L. (1981) Characterization of postreplication repair in Saccharomyces cerevisiae and effects of rad6, rad18, rev3 and rad52 mutations. *Mol Gen Genet*, **184**, 471-478.
96. Bailly, V., Lauder, S., Prakash, S. and Prakash, L. (1997) Yeast DNA repair proteins Rad6 and Rad18 form a heterodimer that has ubiquitin conjugating, DNA binding, and ATP hydrolytic activities. *J Biol Chem*, **272**, 23360-23365.
97. Woodgate, R. (1999) A plethora of lesion-replicating DNA polymerases. *Genes Dev*, **13**, 2191-2195.
98. Zhang, H. and Lawrence, C.W. (2005) The error-free component of the RAD6/RAD18 DNA damage tolerance pathway of budding yeast employs sister-strand recombination. *Proc Natl Acad Sci U S A*, **102**, 15954-15959.
99. Lazzaro, F., Novarina, D., Amara, F., Watt, D.L., Stone, J.E., Costanzo, V., Burgers, P.M., Kunkel, T.A., Plevani, P. and Muzi-Falconi, M. (2012) RNase H and postreplication repair protect cells from ribonucleotides incorporated in DNA. *Mol Cell*, **45**, 99-110.
100. Hartwell, L.H. and Weinert, T.A. (1989) Checkpoints: controls that ensure the order of cell cycle events. *Science*, **246**, 629-634.
101. Zhou, B.B. and Elledge, S.J. (2000) The DNA damage response: putting checkpoints in perspective. *Nature*, **408**, 433-439.
102. Hartwell, L.H. and Kastan, M.B. (1994) Cell cycle control and cancer. *Science*, **266**, 1821-1828.
103. Elledge, S.J. (1996) Cell cycle checkpoints: preventing an identity crisis. *Science*, **274**, 1664-1672.
104. Hanahan, D. and Weinberg, R.A. (2011) Hallmarks of cancer: the next generation. *Cell*, **144**, 646-674.
105. Sherlock, G. and Rosamond, J. (1993) Starting to cycle: G1 controls regulating cell division in budding yeast. *J Gen Microbiol*, **139**, 2531-2541.

106. Gerald, J.N., Benjamin, J.M. and Kron, S.J. (2002) Robust G1 checkpoint arrest in budding yeast: dependence on DNA damage signaling and repair. *J Cell Sci*, **115**, 1749-1757.
107. Branzei, D. and Foiani, M. (2007) Interplay of replication checkpoints and repair proteins at stalled replication forks. *DNA Repair (Amst)*, **6**, 994-1003.
108. Weinert, T.A. and Hartwell, L.H. (1988) The RAD9 gene controls the cell cycle response to DNA damage in Saccharomyces cerevisiae. *Science*, **241**, 317-322.
109. Alcasabas, A.A., Osborn, A.J., Bachant, J., Hu, F., Werler, P.J., Bousset, K., Furuya, K., Diffley, J.F., Carr, A.M. and Elledge, S.J. (2001) Mrc1 transduces signals of DNA replication stress to activate Rad53. *Nat Cell Biol*, **3**, 958-965.
110. Sanchez, Y., Desany, B.A., Jones, W.J., Liu, Q., Wang, B. and Elledge, S.J. (1996) Regulation of RAD53 by the ATM-like kinases MEC1 and TEL1 in yeast cell cycle checkpoint pathways. *Science*, **271**, 357-360.
111. Tercero, J.A. and Diffley, J.F. (2001) Regulation of DNA replication fork progression through damaged DNA by the Mec1/Rad53 checkpoint. *Nature*, **412**, 553-557.
112. Zhou, Z. and Elledge, S.J. (1993) DUN1 encodes a protein kinase that controls the DNA damage response in yeast. *Cell*, **75**, 1119-1127.
113. Santocanale, C. and Diffley, J.F. (1998) A Mec1- and Rad53-dependent checkpoint controls late-firing origins of DNA replication. *Nature*, **395**, 615-618.
114. Weinert, T.A., Kiser, G.L. and Hartwell, L.H. (1994) Mitotic checkpoint genes in budding yeast and the dependence of mitosis on DNA replication and repair. *Genes Dev*, **8**, 652-665.
115. Lew, D.J. (2003) The morphogenesis checkpoint: how yeast cells watch their figures. *Curr Opin Cell Biol*, **15**, 648-653.
116. Musacchio, A. and Salmon, E.D. (2007) The spindle-assembly checkpoint in space and time. *Nat Rev Mol Cell Biol*, **8**, 379-393.
117. Visintin, R., Prinz, S. and Amon, A. (1997) CDC20 and CDH1: a family of substrate-specific activators of APC-dependent proteolysis. *Science*, **278**, 460-463.
118. Cohen-Fix, O., Peters, J.M., Kirschner, M.W. and Koshland, D. (1996) Anaphase initiation in Saccharomyces cerevisiae is controlled by the APC-dependent degradation of the anaphase inhibitor Pds1p. *Genes Dev*, **10**, 3081-3093.
119. Storchova, Z. and Pellman, D. (2004) From polyploidy to aneuploidy, genome instability and cancer. *Nat Rev Mol Cell Biol*, **5**, 45-54.
120. Arudchandran, A., Cerritelli, S., Narimatsu, S., Itaya, M., Shin, D.Y., Shimada, Y. and Crouch, R.J. (2000) The absence of ribonuclease H1 or H2 alters the sensitivity of Saccharomyces cerevisiae to hydroxyurea, caffeine and ethyl methanesulphonate: implications for roles of RNases H in DNA replication and repair. *Genes Cells*, **5**, 789-802.
121. Saavedra, R.A. and Huberman, J.A. (1986) Both DNA topoisomerases I and II relax 2 micron plasmid DNA in living yeast cells. *Cell*, **45**, 65-70.
122. Pommier, Y. (2009) DNA topoisomerase I inhibitors: chemistry, biology, and interfacial inhibition. *Chem Rev*, **109**, 2894-2902.
123. Marinello, J., Chillemi, G., Bueno, S., Manzo, S.G. and Capranico, G. (2013) Antisense transcripts enhanced by camptothecin at divergent CpG-island promoters associated with bursts of topoisomerase I-DNA cleavage complex and R-loop formation. *Nucleic Acids Res*, **41**, 10110-10123.
124. Labib, K., Tercero, J.A. and Diffley, J.F. (2000) Uninterrupted MCM2-7 function required for DNA replication fork progression. *Science*, **288**, 1643-1647.
125. Fan, H.Y., Cheng, K.K. and Klein, H.L. (1996) Mutations in the RNA polymerase II transcription machinery suppress the hyperrecombination mutant hpr1 delta of Saccharomyces cerevisiae. *Genetics*, **142**, 749-759.
126. Kaeberlein, M. and Guarente, L. (2002) Saccharomyces cerevisiae MPT5 and SSD1 function in parallel pathways to promote cell wall integrity. *Genetics*, **160**, 83-95.

127. Devasahayam, G., Ritz, D., Helliwell, S.B., Burke, D.J. and Sturgill, T.W. (2006) Pmr1, a Golgi Ca2+/Mn2+-ATPase, is a regulator of the target of rapamycin (TOR) signaling pathway in yeast. *Proc Natl Acad Sci U S A*, **103**, 17840-17845.
128. Pommier, Y., Pourquier, P., Fan, Y. and Strumberg, D. (1998) Mechanism of action of eukaryotic DNA topoisomerase I and drugs targeted to the enzyme. *Biochim Biophys Acta*, **1400**, 83-105.
129. Pourquier, P. and Pommier, Y. (2001) Topoisomerase I-mediated DNA damage. *Adv Cancer Res*, **80**, 189-216.
130. Beroukhim, R., Lin, M., Park, Y., Hao, K., Zhao, X., Garraway, L.A., Fox, E.A., Hochberg, E.P., Mellinghoff, I.K., Hofer, M.D. *et al.* (2006) Inferring loss-of-heterozygosity from unpaired tumors using high-density oligonucleotide SNP arrays. *PLoS Comput Biol*, **2**, e41.
131. Lasko, D., Cavenee, W. and Nordenskjold, M. (1991) Loss of constitutional heterozygosity in human cancer. *Annu Rev Genet*, **25**, 281-314.
132. Yuen, K.W., Warren, C.D., Chen, O., Kwok, T., Hieter, P. and Spencer, F.A. (2007) Systematic genome instability screens in yeast and their potential relevance to cancer. *Proc Natl Acad Sci U S A*, **104**, 3925-3930.
133. Herskowitz, I. (1988) Life cycle of the budding yeast Saccharomyces cerevisiae. *Microbiol Rev*, **52**, 536-553.
134. Jimeno, S., Rondon, A.G., Luna, R. and Aguilera, A. (2002) The yeast THO complex and mRNA export factors link RNA metabolism with transcription and genome instability. *EMBO J*, **21**, 3526-3535.
135. Lisby, M., Rothstein, R. and Mortensen, U.H. (2001) Rad52 forms DNA repair and recombination centers during S phase. *Proc Natl Acad Sci U S A*, **98**, 8276-8282.
136. Hsiang, Y.H., Lihou, M.G. and Liu, L.F. (1989) Arrest of replication forks by drug-stabilized topoisomerase I-DNA cleavable complexes as a mechanism of cell killing by camptothecin. *Cancer Res*, **49**, 5077-5082.
137. Strumberg, D., Pilon, A.A., Smith, M., Hickey, R., Malkas, L. and Pommier, Y. (2000) Conversion of topoisomerase I cleavage complexes on the leading strand of ribosomal DNA into 5'-phosphorylated DNA double-strand breaks by replication runoff. *Mol Cell Biol*, **20**, 3977-3987.
138. Torres-Rosell, J., Sunjevaric, I., De Piccoli, G., Sacher, M., Eckert-Boulet, N., Reid, R., Jentsch, S., Rothstein, R., Aragon, L. and Lisby, M. (2007) The Smc5-Smc6 complex and SUMO modification of Rad52 regulates recombinational repair at the ribosomal gene locus. *Nat Cell Biol*, **9**, 923-931.
139. Benguria, A., Hernandez, P., Krimer, D.B. and Schvartzman, J.B. (2003) Sir2p suppresses recombination of replication forks stalled at the replication fork barrier of ribosomal DNA in Saccharomyces cerevisiae. *Nucleic Acids Res*, **31**, 893-898.
140. Kobayashi, T., Heck, D.J., Nomura, M. and Horiuchi, T. (1998) Expansion and contraction of ribosomal DNA repeats in Saccharomyces cerevisiae: requirement of replication fork blocking (Fob1) protein and the role of RNA polymerase I. *Genes Dev*, **12**, 3821-3830.
141. Mayan-Santos, M.D., Martinez-Robles, M.L., Hernandez, P., Schvartzman, J.B. and Krimer, D.B. (2008) A redundancy of processes that cause replication fork stalling enhances recombination at two distinct sites in yeast rDNA. *Mol Microbiol*, **69**, 361-375.
142. Ganley, A.R., Ide, S., Saka, K. and Kobayashi, T. (2009) The effect of replication initiation on gene amplification in the rDNA and its relationship to aging. *Mol Cell*, **35**, 683-693.
143. Takeuchi, Y., Horiuchi, T. and Kobayashi, T. (2003) Transcription-dependent recombination and the role of fork collision in yeast rDNA. *Genes Dev*, **17**, 1497-1506.
144. Rochaix, J.D. and Bird, A.P. (1975) Circular ribosomal DNA and ribosomal DNA: replication in somatic amphibian cells. *Chromosoma*, **52**, 317-327.
145. Sinclair, D.A. and Guarente, L. (1997) Extrachromosomal rDNA circles--a cause of aging in yeast. *Cell*, **91**, 1033-1042.
146. Keil, R.L. and Roeder, G.S. (1984) Cis-acting, recombination-stimulating activity in a fragment of the ribosomal DNA of S. cerevisiae. *Cell*, **39**, 377-386.

147. Ivessa, A.S., Zhou, J.Q. and Zakian, V.A. (2000) The Saccharomyces Pif1p DNA helicase and the highly related Rrm3p have opposite effects on replication fork progression in ribosomal DNA. *Cell*, **100**, 479-489.
148. Vengrova, S. and Dalgaard, J.Z. (2004) RNase-sensitive DNA modification(s) initiates S. pombe mating-type switching. *Genes Dev*, **18**, 794-804.
149. Dalgaard, J.Z. (2012) Causes and consequences of ribonucleotide incorporation into nuclear DNA. *Trends Genet*, **28**, 592-597.
150. Pohjoismaki, J.L., Holmes, J.B., Wood, S.R., Yang, M.Y., Yasukawa, T., Reyes, A., Bailey, L.J., Cluett, T.J., Goffart, S., Willcox, S. *et al.* (2010) Mammalian mitochondrial DNA replication intermediates are essentially duplex but contain extensive tracts of RNA/DNA hybrid. *J Mol Biol*, **397**, 1144-1155.
151. Ganley, A.R., Hayashi, K., Horiuchi, T. and Kobayashi, T. (2005) Identifying gene-independent noncoding functional elements in the yeast ribosomal DNA by phylogenetic footprinting. *Proc Natl Acad Sci U S A*, **102**, 11787-11792.
152. Santangelo, G.M., Tornow, J., McLaughlin, C.S. and Moldave, K. (1988) Properties of promoters cloned randomly from the Saccharomyces cerevisiae genome. *Mol Cell Biol*, **8**, 4217-4224.
153. Torres, J.Z., Bessler, J.B. and Zakian, V.A. (2004) Local chromatin structure at the ribosomal DNA causes replication fork pausing and genome instability in the absence of the S. cerevisiae DNA helicase Rrm3p. *Genes Dev*, **18**, 498-503.
154. Wellinger, R.E., Schar, P. and Sogo, J.M. (2003) Rad52-independent accumulation of joint circular minichromosomes during S phase in Saccharomyces cerevisiae. *Mol Cell Biol*, **23**, 6363-6372.
155. Nishimura, K., Fukagawa, T., Takisawa, H., Kakimoto, T. and Kanemaki, M. (2009) An auxin-based degron system for the rapid depletion of proteins in nonplant cells. *Nat Methods*, **6**, 917-922.
156. Boguslawski, S.J., Smith, D.E., Michalak, M.A., Mickelson, K.E., Yehle, C.O., Patterson, W.L. and Carrico, R.J. (1986) Characterization of monoclonal antibody to DNA.RNA and its application to immunodetection of hybrids. *J Immunol Methods*, **89**, 123-130.
157. Wittekind, M., Dodd, J., Vu, L., Kolb, J.M., Buhler, J.M., Sentenac, A. and Nomura, M. (1988) Isolation and characterization of temperature-sensitive mutations in RPA190, the gene encoding the largest subunit of RNA polymerase I from Saccharomyces cerevisiae. *Mol Cell Biol*, **8**, 3997-4008.
158. Bell, S.P. and Dutta, A. (2002) DNA replication in eukaryotic cells. *Annu Rev Biochem*, **71**, 333-374.
159. Bramhill, D. and Kornberg, A. (1988) Duplex opening by dnaA protein at novel sequences in initiation of replication at the origin of the E. coli chromosome. *Cell*, **52**, 743-755.
160. Itoh, T. and Tomizawa, J. (1980) Formation of an RNA primer for initiation of replication of ColE1 DNA by ribonuclease H. *Proc Natl Acad Sci U S A*, **77**, 2450-2454.
161. Mouron, S., Rodriguez-Acebes, S., Martinez-Jimenez, M.I., Garcia-Gomez, S., Chocron, S., Blanco, L. and Mendez, J. (2013) Repriming of DNA synthesis at stalled replication forks by human PrimPol. *Nat Struct Mol Biol*, **20**, 1383-1389.
162. Garcia-Gomez, S., Reyes, A., Martinez-Jimenez, M.I., Chocron, E.S., Mouron, S., Terrados, G., Powell, C., Salido, E., Mendez, J., Holt, I.J. *et al.* (2013) PrimPol, an archaic primase/polymerase operating in human cells. *Mol Cell*, **52**, 541-553.
163. Kim, R.A. and Wang, J.C. (1989) A subthreshold level of DNA topoisomerases leads to the excision of yeast rDNA as extrachromosomal rings. *Cell*, **57**, 975-985.
164. Kobayashi, T. (2006) Strategies to maintain the stability of the ribosomal RNA gene repeats--collaboration of recombination, cohesion, and condensation. *Genes Genet Syst*, **81**, 155-161.
165. Merker, R.J. and Klein, H.L. (2002) hpr1Delta affects ribosomal DNA recombination and cell life span in Saccharomyces cerevisiae. *Mol Cell Biol*, **22**, 421-429.

166. Mehta, I.S., Figgitt, M., Clements, C.S., Kill, I.R. and Bridger, J.M. (2007) Alterations to nuclear architecture and genome behavior in senescent cells. *Ann N Y Acad Sci*, **1100**, 250-263.
167. Campisi, J. and d'Adda di Fagagna, F. (2007) Cellular senescence: when bad things happen to good cells. *Nat Rev Mol Cell Biol*, **8**, 729-740.
168. Cavanaugh, A.H., Hempel, W.M., Taylor, L.J., Rogalsky, V., Todorov, G. and Rothblum, L.I. (1995) Activity of RNA polymerase I transcription factor UBF blocked by Rb gene product. *Nature*, **374**, 177-180.
169. Hannan, K.M., Hannan, R.D., Smith, S.D., Jefferson, L.S., Lun, M. and Rothblum, L.I. (2000) Rb and p130 regulate RNA polymerase I transcription: Rb disrupts the interaction between UBF and SL-1. *Oncogene*, **19**, 4988-4999.
170. Krawczyk, C., Dion, V., Schar, P. and Fritsch, O. (2014) Reversible Top1 cleavage complexes are stabilized strand-specifically at the ribosomal replication fork barrier and contribute to ribosomal DNA stability. *Nucleic Acids Res*.
171. Vogelauer, M. and Camilloni, G. (1999) Site-specific in vivo cleavages by DNA topoisomerase I in the regulatory regions of the 35 S rRNA in Saccharomyces cerevisiae are transcription independent. *J Mol Biol*, **293**, 19-28.
172. Gan, W., Guan, Z., Liu, J., Gui, T., Shen, K., Manley, J.L. and Li, X. R-loop-mediated genomic instability is caused by impairment of replication fork progression. *Genes Dev*, **25**, 2041-2056.
173. Coelho, P.S., Bryan, A.C., Kumar, A., Shadel, G.S. and Snyder, M. (2002) A novel mitochondrial protein, Tar1p, is encoded on the antisense strand of the nuclear 25S rDNA. *Genes Dev*, **16**, 2755-2760.
174. White, R.J. (2005) RNA polymerases I and III, growth control and cancer. *Nat Rev Mol Cell Biol*, **6**, 69-78.
175. ten Asbroek, A.L., van Groenigen, M., Nooij, M. and Baas, F. (2002) The involvement of human ribonucleases H1 and H2 in the variation of response of cells to antisense phosphorothioate oligonucleotides. *Eur J Biochem*, **269**, 583-592.
176. Teeter, L.D., Atsumi, S., Sen, S. and Kuo, T. (1986) DNA amplification in multidrug, cross-resistant Chinese hamster ovary cells: molecular characterization and cytogenetic localization of the amplified DNA. *J Cell Biol*, **103**, 1159-1166.
177. Schwab, M. (1998) Amplification of oncogenes in human cancer cells. *Bioessays*, **20**, 473-479.
178. Kuo, M.T., Sen, S., Hittelman, W.N. and Hsu, T.C. (1998) Chromosomal fragile sites and DNA amplification in drug-resistant cells. *Biochem Pharmacol*, **56**, 7-13.
179. Elliott, K.T., Cuff, L.E. and Neidle, E.L. (2013) Copy number change: evolving views on gene amplification. *Future Microbiol*, **8**, 887-899.
180. Spradling, A.C. (1981) The organization and amplification of two chromosomal domains containing Drosophila chorion genes. *Cell*, **27**, 193-201.
181. Spradling, A.C. (ed.) (1993) *Developmental genetics of oogenesis.* . Cold Spring Harbor Laboratory Press, Cold Spring Harbor, NY.
182. Qiu, J., Qian, Y., Frank, P., Wintersberger, U. and Shen, B. (1999) Saccharomyces cerevisiae RNase H(35) functions in RNA primer removal during lagging-strand DNA synthesis, most efficiently in cooperation with Rad27 nuclease. *Mol Cell Biol*, **19**, 8361-8371.
183. Dornfeld, K.J. and Livingston, D.M. (1991) Effects of controlled RAD52 expression on repair and recombination in Saccharomyces cerevisiae. *Mol Cell Biol*, **11**, 2013-2017.
184. Symington, L.S. (2002) Role of RAD52 epistasis group genes in homologous recombination and double-strand break repair. *Microbiol Mol Biol Rev*, **66**, 630-670, table of contents.
185. Malkova, A., Ivanov, E.L. and Haber, J.E. (1996) Double-strand break repair in the absence of RAD51 in yeast: a possible role for break-induced DNA replication. *Proc Natl Acad Sci U S A*, **93**, 7131-7136.

186. Krejci, L., Van Komen, S., Li, Y., Villemain, J., Reddy, M.S., Klein, H., Ellenberger, T. and Sung, P. (2003) DNA helicase Srs2 disrupts the Rad51 presynaptic filament. *Nature*, **423**, 305-309.
187. Veaute, X., Jeusset, J., Soustelle, C., Kowalczykowski, S.C., Le Cam, E. and Fabre, F. (2003) The Srs2 helicase prevents recombination by disrupting Rad51 nucleoprotein filaments. *Nature*, **423**, 309-312.
188. Bertuch, A.A. and Lundblad, V. (2003) Which end: dissecting Ku's function at telomeres and double-strand breaks. *Genes Dev*, **17**, 2347-2350.
189. Llorente, B. and Symington, L.S. (2004) The Mre11 nuclease is not required for 5' to 3' resection at multiple HO-induced double-strand breaks. *Mol Cell Biol*, **24**, 9682-9694.
190. Hamilton, N.K. and Maizels, N. (2010) MRE11 function in response to topoisomerase poisons is independent of its function in double-strand break repair in Saccharomyces cerevisiae. *PLoS One*, **5**, e15387.
191. Lengsfeld, B.M., Rattray, A.J., Bhaskara, V., Ghirlando, R. and Paull, T.T. (2007) Sae2 is an endonuclease that processes hairpin DNA cooperatively with the Mre11/Rad50/Xrs2 complex. *Mol Cell*, **28**, 638-651.
192. Huertas, P., Cortes-Ledesma, F., Sartori, A.A., Aguilera, A. and Jackson, S.P. (2008) CDK targets Sae2 to control DNA-end resection and homologous recombination. *Nature*, **455**, 689-692.
193. Zhu, Z., Chung, W.H., Shim, E.Y., Lee, S.E. and Ira, G. (2008) Sgs1 helicase and two nucleases Dna2 and Exo1 resect DNA double-strand break ends. *Cell*, **134**, 981-994.
194. Mimitou, E.P. and Symington, L.S. (2008) Sae2, Exo1 and Sgs1 collaborate in DNA double-strand break processing. *Nature*, **455**, 770-774.
195. Nicolette, M.L., Lee, K., Guo, Z., Rani, M., Chow, J.M., Lee, S.E. and Paull, T.T. (2010) Mre11-Rad50-Xrs2 and Sae2 promote 5' strand resection of DNA double-strand breaks. *Nat Struct Mol Biol*, **17**, 1478-1485.
196. Torres-Ramos, C.A., Yoder, B.L., Burgers, P.M., Prakash, S. and Prakash, L. (1996) Requirement of proliferating cell nuclear antigen in RAD6-dependent postreplicational DNA repair. *Proc Natl Acad Sci U S A*, **93**, 9676-9681.
197. Cassier-Chauvat, C. and Fabre, F. (1991) A similar defect in UV-induced mutagenesis conferred by the rad6 and rad18 mutations of Saccharomyces cerevisiae. *Mutat Res*, **254**, 247-253.
198. Andersen, P.L., Xu, F. and Xiao, W. (2008) Eukaryotic DNA damage tolerance and translesion synthesis through covalent modifications of PCNA. *Cell Res*, **18**, 162-173.
199. Kraus, E., Leung, W.Y. and Haber, J.E. (2001) Break-induced replication: a review and an example in budding yeast. *Proc Natl Acad Sci U S A*, **98**, 8255-8262.
200. Lydeard, J.R., Jain, S., Yamaguchi, M. and Haber, J.E. (2007) Break-induced replication and telomerase-independent telomere maintenance require Pol32. *Nature*, **448**, 820-823.
201. Conconi, A., Bespalov, V.A. and Smerdon, M.J. (2002) Transcription-coupled repair in RNA polymerase I-transcribed genes of yeast. *Proc Natl Acad Sci U S A*, **99**, 649-654.
202. Lin, Y. and Wilson, J.H. (2007) Transcription-induced CAG repeat contraction in human cells is mediated in part by transcription-coupled nucleotide excision repair. *Mol Cell Biol*, **27**, 6209-6217.
203. Tian, M. and Alt, F.W. (2000) Transcription-induced cleavage of immunoglobulin switch regions by nucleotide excision repair nucleases in vitro. *J Biol Chem*, **275**, 24163-24172.
204. Nomura, M. (ed.) (1998) *Transcriptional factors used by Saccharomyces cerevisiae RNA polymerase I and the mechanism of initiation*. Springer-Verlag and R.G. Landes Co., Austin, TX.
205. Beckouet, F., Labarre-Mariotte, S., Albert, B., Imazawa, Y., Werner, M., Gadal, O., Nogi, Y. and Thuriaux, P. (2008) Two RNA polymerase I subunits control the binding and release of Rrn3 during transcription. *Mol Cell Biol*, **28**, 1596-1605.

206. Dammann, R., Lucchini, R., Koller, T. and Sogo, J.M. (1993) Chromatin structures and transcription of rDNA in yeast Saccharomyces cerevisiae. *Nucleic Acids Res*, **21**, 2331-2338.
207. Hall, D.B., Wade, J.T. and Struhl, K. (2006) An HMG protein, Hmo1, associates with promoters of many ribosomal protein genes and throughout the rRNA gene locus in Saccharomyces cerevisiae. *Mol Cell Biol*, **26**, 3672-3679.
208. Conconi, A., Widmer, R.M., Koller, T. and Sogo, J.M. (1989) Two different chromatin structures coexist in ribosomal RNA genes throughout the cell cycle. *Cell*, **57**, 753-761.
209. French, S.L., Osheim, Y.N., Cioci, F., Nomura, M. and Beyer, A.L. (2003) In exponentially growing Saccharomyces cerevisiae cells, rRNA synthesis is determined by the summed RNA polymerase I loading rate rather than by the number of active genes. *Mol Cell Biol*, **23**, 1558-1568.
210. Merz, K., Hondele, M., Goetze, H., Gmelch, K., Stoeckl, U. and Griesenbeck, J. (2008) Actively transcribed rRNA genes in S. cerevisiae are organized in a specialized chromatin associated with the high-mobility group protein Hmo1 and are largely devoid of histone molecules. *Genes Dev*, **22**, 1190-1204.
211. Jones, H.S., Kawauchi, J., Braglia, P., Alen, C.M., Kent, N.A. and Proudfoot, N.J. (2007) RNA polymerase I in yeast transcribes dynamic nucleosomal rDNA. *Nat Struct Mol Biol*, **14**, 123-130.
212. Hagstrom, K.A. and Meyer, B.J. (2003) Condensin and cohesin: more than chromosome compactor and glue. *Nat Rev Genet*, **4**, 520-534.
213. Ii, M., Ii, T. and Brill, S.J. (2007) Mus81 functions in the quality control of replication forks at the rDNA and is involved in the maintenance of rDNA repeat number in Saccharomyces cerevisiae. *Mutat Res*, **625**, 1-19.
214. Sun, H., Bennett, R.J. and Maizels, N. (1999) The Saccharomyces cerevisiae Sgs1 helicase efficiently unwinds G-G paired DNAs. *Nucleic Acids Res*, **27**, 1978-1984.
215. Gangloff, S., McDonald, J.P., Bendixen, C., Arthur, L. and Rothstein, R. (1994) The yeast type I topoisomerase Top3 interacts with Sgs1, a DNA helicase homolog: a potential eukaryotic reverse gyrase. *Mol Cell Biol*, **14**, 8391-8398.
216. Dammann, R., Lucchini, R., Koller, T. and Sogo, J.M. (1995) Transcription in the yeast rRNA gene locus: distribution of the active gene copies and chromatin structure of their flanking regulatory sequences. *Mol Cell Biol*, **15**, 5294-5303.
217. Woolford, J.L., Jr. (ed.) (1991) *The ribosome and its synthesis*. Cold Spring Harbour Laboratory Press, Cold Spring Harbour, N.Y.
218. Bi, X., Yu, Q., Sandmeier, J.J. and Elizondo, S. (2004) Regulation of transcriptional silencing in yeast by growth temperature. *J Mol Biol*, **344**, 893-905.
219. Sung, P. (1994) Catalysis of ATP-dependent homologous DNA pairing and strand exchange by yeast RAD51 protein. *Science*, **265**, 1241-1243.
220. Lydeard, J.R., Lipkin-Moore, Z., Sheu, Y.J., Stillman, B., Burgers, P.M. and Haber, J.E. (2010) Break-induced replication requires all essential DNA replication factors except those specific for pre-RC assembly. *Genes Dev*, **24**, 1133-1144.
221. Kogoma, T. (1997) Stable DNA replication: interplay between DNA replication, homologous recombination, and transcription. *Microbiol Mol Biol Rev*, **61**, 212-238.
222. Aguilera, A. (2001) Double-strand break repair: are Rad51/RecA--DNA joints barriers to DNA replication? *Trends Genet*, **17**, 318-321.
223. Davis, A.P. and Symington, L.S. (2004) RAD51-dependent break-induced replication in yeast. *Mol Cell Biol*, **24**, 2344-2351.
224. Katou, Y., Kanoh, Y., Bando, M., Noguchi, H., Tanaka, H., Ashikari, T., Sugimoto, K. and Shirahige, K. (2003) S-phase checkpoint proteins Tof1 and Mrc1 form a stable replication-pausing complex. *Nature*, **424**, 1078-1083.
225. Lebel, M., Spillare, E.A., Harris, C.C. and Leder, P. (1999) The Werner syndrome gene product co-purifies with the DNA replication complex and interacts with PCNA and topoisomerase I. *J Biol Chem*, **274**, 37795-37799.

226. Hegnauer, A.M., Hustedt, N., Shimada, K., Pike, B.L., Vogel, M., Amsler, P., Rubin, S.M., van Leeuwen, F., Guenole, A., van Attikum, H. *et al.* (2012) An N-terminal acidic region of Sgs1 interacts with Rpa70 and recruits Rad53 kinase to stalled forks. *EMBO J*, **31**, 3768-3783.
227. Wilson, M.A., Kwon, Y., Xu, Y., Chung, W.H., Chi, P., Niu, H., Mayle, R., Chen, X., Malkova, A., Sung, P. *et al.* (2013) Pif1 helicase and Poldelta promote recombination-coupled DNA synthesis via bubble migration. *Nature*, **502**, 393-396.
228. Houseley, J. and Tollervey, D. (2011) Repeat expansion in the budding yeast ribosomal DNA can occur independently of the canonical homologous recombination machinery. *Nucleic Acids Res*, **39**, 8778-8791.
229. Chon, H., Sparks, J.L., Rychlik, M., Nowotny, M., Burgers, P.M., Crouch, R.J. and Cerritelli, S.M. (2013) RNase H2 roles in genome integrity revealed by unlinking its activities. *Nucleic Acids Res*, **41**, 3130-3143.
230. Maga, G. and Hubscher, U. (2003) Proliferating cell nuclear antigen (PCNA): a dancer with many partners. *J Cell Sci*, **116**, 3051-3060.
231. Hoege, C., Pfander, B., Moldovan, G.L., Pyrowolakis, G. and Jentsch, S. (2002) RAD6-dependent DNA repair is linked to modification of PCNA by ubiquitin and SUMO. *Nature*, **419**, 135-141.
232. Shivji, K.K., Kenny, M.K. and Wood, R.D. (1992) Proliferating cell nuclear antigen is required for DNA excision repair. *Cell*, **69**, 367-374.
233. Moldovan, G.L., Pfander, B. and Jentsch, S. (2006) PCNA controls establishment of sister chromatid cohesion during S phase. *Mol Cell*, **23**, 723-732.
234. Pfander, B., Moldovan, G.L., Sacher, M., Hoege, C. and Jentsch, S. (2005) SUMO-modified PCNA recruits Srs2 to prevent recombination during S phase. *Nature*, **436**, 428-433.
235. Mendenhall, M.D. and Hodge, A.E. (1998) Regulation of Cdc28 cyclin-dependent protein kinase activity during the cell cycle of the yeast Saccharomyces cerevisiae. *Microbiol Mol Biol Rev*, **62**, 1191-1243.
236. Verma, R., Annan, R.S., Huddleston, M.J., Carr, S.A., Reynard, G. and Deshaies, R.J. (1997) Phosphorylation of Sic1p by G1 Cdk required for its degradation and entry into S phase. *Science*, **278**, 455-460.
237. Mendenhall, M.D. (1993) An inhibitor of p34CDC28 protein kinase activity from Saccharomyces cerevisiae. *Science*, **259**, 216-219.
238. Schwob, E. and Nasmyth, K. (1993) CLB5 and CLB6, a new pair of B cyclins involved in DNA replication in Saccharomyces cerevisiae. *Genes Dev*, **7**, 1160-1175.
239. Cocker, J.H., Piatti, S., Santocanale, C., Nasmyth, K. and Diffley, J.F. (1996) An essential role for the Cdc6 protein in forming the pre-replicative complexes of budding yeast. *Nature*, **379**, 180-182.
240. Tanaka, T., Knapp, D. and Nasmyth, K. (1997) Loading of an Mcm protein onto DNA replication origins is regulated by Cdc6p and CDKs. *Cell*, **90**, 649-660.
241. Sato, N., Arai, K. and Masai, H. (1997) Human and Xenopus cDNAs encoding budding yeast Cdc7-related kinases: in vitro phosphorylation of MCM subunits by a putative human homologue of Cdc7. *EMBO J*, **16**, 4340-4351.
242. Tanaka, S., Halter, D., Livingstone-Zatchej, M., Reszel, B. and Thoma, F. (1994) Transcription through the yeast origin of replication ARS1 ends at the ABFI binding site and affects extrachromosomal maintenance of minichromosomes. *Nucleic Acids Res*, **22**, 3904-3910.
243. Pessoa-Brandao, L. and Sclafani, R.A. (2004) CDC7/DBF4 functions in the translesion synthesis branch of the RAD6 epistasis group in Saccharomyces cerevisiae. *Genetics*, **167**, 1597-1610.
244. Hollingsworth, R.E., Jr., Ostroff, R.M., Klein, M.B., Niswander, L.A. and Sclafani, R.A. (1992) Molecular genetic studies of the Cdc7 protein kinase and induced mutagenesis in yeast. *Genetics*, **132**, 53-62.

245. Hardy, C.F., Dryga, O., Seematter, S., Pahl, P.M. and Sclafani, R.A. (1997) mcm5/cdc46-bob1 bypasses the requirement for the S phase activator Cdc7p. *Proc Natl Acad Sci U S A*, **94**, 3151-3155.
246. Sclafani, R.A., Tecklenburg, M. and Pierce, A. (2002) The mcm5-bob1 bypass of Cdc7p/Dbf4p in DNA replication depends on both Cdk1-independent and Cdk1-dependent steps in Saccharomyces cerevisiae. *Genetics*, **161**, 47-57.
247. Tourriere, H., Versini, G., Cordon-Preciado, V., Alabert, C. and Pasero, P. (2005) Mrc1 and Tof1 promote replication fork progression and recovery independently of Rad53. *Mol Cell*, **19**, 699-706.
248. Osborn, A.J. and Elledge, S.J. (2003) Mrc1 is a replication fork component whose phosphorylation in response to DNA replication stress activates Rad53. *Genes Dev*, **17**, 1755-1767.
249. Naylor, M.L., Li, J.M., Osborn, A.J. and Elledge, S.J. (2009) Mrc1 phosphorylation in response to DNA replication stress is required for Mec1 accumulation at the stalled fork. *Proc Natl Acad Sci U S A*, **106**, 12765-12770.
250. Duch, A., Felipe-Abrio, I., Barroso, S., Yaakov, G., Garcia-Rubio, M., Aguilera, A., de Nadal, E. and Posas, F. (2012) Coordinated control of replication and transcription by a SAPK protects genomic integrity. *Nature*, **493**, 116-119.
251. Booher, R.N., Deshaies, R.J. and Kirschner, M.W. (1993) Properties of Saccharomyces cerevisiae wee1 and its differential regulation of p34CDC28 in response to G1 and G2 cyclins. *EMBO J*, **12**, 3417-3426.
252. Sia, R.A., Bardes, E.S. and Lew, D.J. (1998) Control of Swe1p degradation by the morphogenesis checkpoint. *EMBO J*, **17**, 6678-6688.
253. Harvey, S.L. and Kellogg, D.R. (2003) Conservation of mechanisms controlling entry into mitosis: budding yeast wee1 delays entry into mitosis and is required for cell size control. *Curr Biol*, **13**, 264-275.
254. Zhao, X., Muller, E.G. and Rothstein, R. (1998) A suppressor of two essential checkpoint genes identifies a novel protein that negatively affects dNTP pools. *Mol Cell*, **2**, 329-340.
255. Zhao, X. and Rothstein, R. (2002) The Dun1 checkpoint kinase phosphorylates and regulates the ribonucleotide reductase inhibitor Sml1. *Proc Natl Acad Sci U S A*, **99**, 3746-3751.
256. Redon, C., Pilch, D.R., Rogakou, E.P., Orr, A.H., Lowndes, N.F. and Bonner, W.M. (2003) Yeast histone 2A serine 129 is essential for the efficient repair of checkpoint-blind DNA damage. *EMBO Rep*, **4**, 678-684.
257. Pellicioli, A., Lucca, C., Liberi, G., Marini, F., Lopes, M., Plevani, P., Romano, A., Di Fiore, P.P. and Foiani, M. (1999) Activation of Rad53 kinase in response to DNA damage and its effect in modulating phosphorylation of the lagging strand DNA polymerase. *EMBO J*, **18**, 6561-6572.
258. Bloom, J. and Cross, F.R. (2007) Multiple levels of cyclin specificity in cell-cycle control. *Nat Rev Mol Cell Biol*, **8**, 149-160.
259. Wasch, R. and Cross, F.R. (2002) APC-dependent proteolysis of the mitotic cyclin Clb2 is essential for mitotic exit. *Nature*, **418**, 556-562.
260. Straight, A.F. and Murray, A.W. (1997) The spindle assembly checkpoint in budding yeast. *Methods Enzymol*, **283**, 425-440.
261. Schwab, M., Lutum, A.S. and Seufert, W. (1997) Yeast Hct1 is a regulator of Clb2 cyclin proteolysis. *Cell*, **90**, 683-693.
262. King, R.W., Deshaies, R.J., Peters, J.M. and Kirschner, M.W. (1996) How proteolysis drives the cell cycle. *Science*, **274**, 1652-1659.
263. Torres-Rosell, J., Machin, F., Jarmuz, A. and Aragon, L. (2004) Nucleolar segregation lags behind the rest of the genome and requires Cdc14p activation by the FEAR network. *Cell Cycle*, **3**, 496-502.
264. Machin, F., Torres-Rosell, J., Jarmuz, A. and Aragon, L. (2005) Spindle-independent condensation-mediated segregation of yeast ribosomal DNA in late anaphase. *J Cell Biol*, **168**, 209-219.

265. D'Amours, D., Stegmeier, F. and Amon, A. (2004) Cdc14 and condensin control the dissolution of cohesin-independent chromosome linkages at repeated DNA. *Cell*, **117**, 455-469.
266. Visintin, R., Hwang, E.S. and Amon, A. (1999) Cfi1 prevents premature exit from mitosis by anchoring Cdc14 phosphatase in the nucleolus. *Nature*, **398**, 818-823.
267. Bloom, J. and Cross, F.R. (2007) Novel role for Cdc14 sequestration: Cdc14 dephosphorylates factors that promote DNA replication. *Mol Cell Biol*, **27**, 842-853.
268. Foley, E.A. and Kapoor, T.M. (2013) Microtubule attachment and spindle assembly checkpoint signalling at the kinetochore. *Nat Rev Mol Cell Biol*, **14**, 25-37.
269. Taylor, S.S. (1999) Chromosome segregation: dual control ensures fidelity. *Curr Biol*, **9**, R562-564.
270. Hoyt, M.A. (2000) Exit from mitosis: spindle pole power. *Cell*, **102**, 267-270.
271. Hennessy, K.M., Lee, A., Chen, E. and Botstein, D. (1991) A group of interacting yeast DNA replication genes. *Genes Dev*, **5**, 958-969.
272. Ide, S. and Kobayashi, T. (2010) Analysis of DNA replication in Saccharomyces cerevisiae by two-dimensional and pulsed-field gel electrophoresis. *Curr Protoc Cell Biol*, **Chapter 22**, Unit 22 14.
273. Calvert, M.E., Lannigan, J.A. and Pemberton, L.F. (2008) Optimization of yeast cell cycle analysis and morphological characterization by multispectral imaging flow cytometry. *Cytometry A*, **73**, 825-833.
274. Germann, S.M., Schramke, V., Pedersen, R.T., Gallina, I., Eckert-Boulet, N., Oestergaard, V.H. and Lisby, M. (2014) TopBP1/Dpb11 binds DNA anaphase bridges to prevent genome instability. *J Cell Biol*, **204**, 45-59.
275. Mendoza, M. and Barral, Y. (2008) Co-ordination of cytokinesis with chromosome segregation. *Biochem Soc Trans*, **36**, 387-390.
276. Nicoletti, I., Migliorati, G., Pagliacci, M.C., Grignani, F. and Riccardi, C. (1991) A rapid and simple method for measuring thymocyte apoptosis by propidium iodide staining and flow cytometry. *J Immunol Methods*, **139**, 271-279.
277. Weinberger, M., Ramachandran, L., Feng, L., Sharma, K., Sun, X., Marchetti, M., Huberman, J.A. and Burhans, W.C. (2005) Apoptosis in budding yeast caused by defects in initiation of DNA replication. *J Cell Sci*, **118**, 3543-3553.
278. Carmody, R.J. and Cotter, T.G. (2001) Signalling apoptosis: a radical approach. *Redox Rep*, **6**, 77-90.
279. Sen, N., Das, B.B., Ganguly, A., Mukherjee, T., Tripathi, G., Bandyopadhyay, S., Rakshit, S., Sen, T. and Majumder, H.K. (2004) Camptothecin induced mitochondrial dysfunction leading to programmed cell death in unicellular hemoflagellate Leishmania donovani. *Cell Death Differ*, **11**, 924-936.
280. Ramirez, R., Carracedo, J., Jimenez, R., Canela, A., Herrera, E., Aljama, P. and Blasco, M.A. (2003) Massive telomere loss is an early event of DNA damage-induced apoptosis. *J Biol Chem*, **278**, 836-842.
281. Li, Y., Rory Goodwin, C., Sang, Y., Rosen, E.M., Laterra, J. and Xia, S. (2009) Camptothecin and Fas receptor agonists synergistically induce medulloblastoma cell death: ROS-dependent mechanisms. *Anticancer Drugs*, **20**, 770-778.
282. Schwob, E., Bohm, T., Mendenhall, M.D. and Nasmyth, K. (1994) The B-type cyclin kinase inhibitor p40SIC1 controls the G1 to S transition in S. cerevisiae. *Cell*, **79**, 233-244.
283. Knapp, D., Bhoite, L., Stillman, D.J. and Nasmyth, K. (1996) The transcription factor Swi5 regulates expression of the cyclin kinase inhibitor p40SIC1. *Mol Cell Biol*, **16**, 5701-5707.
284. Visintin, R., Craig, K., Hwang, E.S., Prinz, S., Tyers, M. and Amon, A. (1998) The phosphatase Cdc14 triggers mitotic exit by reversal of Cdk-dependent phosphorylation. *Mol Cell*, **2**, 709-718.
285. Shou, W., Seol, J.H., Shevchenko, A., Baskerville, C., Moazed, D., Chen, Z.W., Jang, J., Charbonneau, H. and Deshaies, R.J. (1999) Exit from mitosis is triggered by Tem1-

dependent release of the protein phosphatase Cdc14 from nucleolar RENT complex. *Cell*, **97**, 233-244.
286. Straight, A.F., Shou, W., Dowd, G.J., Turck, C.W., Deshaies, R.J., Johnson, A.D. and Moazed, D. (1999) Net1, a Sir2-associated nucleolar protein required for rDNA silencing and nucleolar integrity. *Cell*, **97**, 245-256.
287. Shou, W., Sakamoto, K.M., Keener, J., Morimoto, K.W., Traverso, E.E., Azzam, R., Hoppe, G.J., Feldman, R.M., DeModena, J., Moazed, D. *et al.* (2001) Net1 stimulates RNA polymerase I transcription and regulates nucleolar structure independently of controlling mitotic exit. *Mol Cell*, **8**, 45-55.
288. Park, H. and Sternglanz, R. (1999) Identification and characterization of the genes for two topoisomerase I-interacting proteins from Saccharomyces cerevisiae. *Yeast*, **15**, 35-41.
289. Sadoff, B.U., Heath-Pagliuso, S., Castano, I.B., Zhu, Y., Kieff, F.S. and Christman, M.F. (1995) Isolation of mutants of Saccharomyces cerevisiae requiring DNA topoisomerase I. *Genetics*, **141**, 465-479.
290. Wang, B.D., Yong-Gonzalez, V. and Strunnikov, A.V. (2004) Cdc14p/FEAR pathway controls segregation of nucleolus in S. cerevisiae by facilitating condensin targeting to rDNA chromatin in anaphase. *Cell Cycle*, **3**, 960-967.
291. Liang, F., Jin, F., Liu, H. and Wang, Y. (2009) The molecular function of the yeast polo-like kinase Cdc5 in Cdc14 release during early anaphase. *Mol Biol Cell*, **20**, 3671-3679.
292. Alexandru, G., Uhlmann, F., Mechtler, K., Poupart, M.A. and Nasmyth, K. (2001) Phosphorylation of the cohesin subunit Scc1 by Polo/Cdc5 kinase regulates sister chromatid separation in yeast. *Cell*, **105**, 459-472.
293. Uhlmann, F., Lottspeich, F. and Nasmyth, K. (1999) Sister-chromatid separation at anaphase onset is promoted by cleavage of the cohesin subunit Scc1. *Nature*, **400**, 37-42.
294. Bermudez-Lopez, M., Ceschia, A., de Piccoli, G., Colomina, N., Pasero, P., Aragon, L. and Torres-Rosell, J. The Smc5/6 complex is required for dissolution of DNA-mediated sister chromatid linkages. *Nucleic Acids Res*, **38**, 6502-6512.
295. Torres-Rosell, J., Machin, F., Farmer, S., Jarmuz, A., Eydmann, T., Dalgaard, J.Z. and Aragon, L. (2005) SMC5 and SMC6 genes are required for the segregation of repetitive chromosome regions. *Nat Cell Biol*, **7**, 412-419.
296. Torres-Rosell, J., De Piccoli, G., Cordon-Preciado, V., Farmer, S., Jarmuz, A., Machin, F., Pasero, P., Lisby, M., Haber, J.E. and Aragon, L. (2007) Anaphase onset before complete DNA replication with intact checkpoint responses. *Science*, **315**, 1411-1415.
297. Peters, J.M. (2006) The anaphase promoting complex/cyclosome: a machine designed to destroy. *Nat Rev Mol Cell Biol*, **7**, 644-656.
298. Christman, M.F., Dietrich, F.S., Levin, N.A., Sadoff, B.U. and Fink, G.R. (1993) The rRNA-encoding DNA array has an altered structure in topoisomerase I mutants of Saccharomyces cerevisiae. *Proc Natl Acad Sci U S A*, **90**, 7637-7641.
299. Machin, F., Torres-Rosell, J., De Piccoli, G., Carballo, J.A., Cha, R.S., Jarmuz, A. and Aragon, L. (2006) Transcription of ribosomal genes can cause nondisjunction. *J Cell Biol*, **173**, 893-903.
300. Tomson, B.N., D'Amours, D., Adamson, B.S., Aragon, L. and Amon, A. (2006) Ribosomal DNA transcription-dependent processes interfere with chromosome segregation. *Mol Cell Biol*, **26**, 6239-6247.
301. Uemura, T. and Tanagida, M. (1986) Mitotic spindle pulls but fails to separate chromosomes in type II DNA topoisomerase mutants: uncoordinated mitosis. *EMBO J*, **5**, 1003-1010.
302. Gisselsson, D., Pettersson, L., Hoglund, M., Heidenblad, M., Gorunova, L., Wiegant, J., Mertens, F., Dal Cin, P., Mitelman, F. and Mandahl, N. (2000) Chromosomal breakage-fusion-bridge events cause genetic intratumor heterogeneity. *Proc Natl Acad Sci U S A*, **97**, 5357-5362.

303. Hoffelder, D.R., Luo, L., Burke, N.A., Watkins, S.C., Gollin, S.M. and Saunders, W.S. (2004) Resolution of anaphase bridges in cancer cells. *Chromosoma*, **112**, 389-397.
304. Ho, Y., Gruhler, A., Heilbut, A., Bader, G.D., Moore, L., Adams, S.L., Millar, A., Taylor, P., Bennett, K., Boutilier, K. *et al.* (2002) Systematic identification of protein complexes in Saccharomyces cerevisiae by mass spectrometry. *Nature*, **415**, 180-183.
305. Norden, C., Mendoza, M., Dobbelaere, J., Kotwaliwale, C.V., Biggins, S. and Barral, Y. (2006) The NoCut pathway links completion of cytokinesis to spindle midzone function to prevent chromosome breakage. *Cell*, **125**, 85-98.
306. Funabiki, H. (2011) To Cut or NoCut in mitosis. *Nat Rev Mol Cell Biol*, **12**, 463.
307. Sordet, O., Khan, Q.A., Kohn, K.W. and Pommier, Y. (2003) Apoptosis induced by topoisomerase inhibitors. *Curr Med Chem Anticancer Agents*, **3**, 271-290.
308. Foiani, M., Liberi, G., Lucchini, G. and Plevani, P. (1995) Cell cycle-dependent phosphorylation and dephosphorylation of the yeast DNA polymerase alpha-primase B subunit. *Mol Cell Biol*, **15**, 883-891.
309. Marini, F., Pellicioli, A., Paciotti, V., Lucchini, G., Plevani, P., Stern, D.F. and Foiani, M. (1997) A role for DNA primase in coupling DNA replication to DNA damage response. *EMBO J*, **16**, 639-650.
310. Mayer, M.L., Gygi, S.P., Aebersold, R. and Hieter, P. (2001) Identification of RFC(Ctf18p, Ctf8p, Dcc1p): an alternative RFC complex required for sister chromatid cohesion in S. cerevisiae. *Mol Cell*, **7**, 959-970.
311. Leman, A.R., Noguchi, C., Lee, C.Y. and Noguchi, E. (2010) Human Timeless and Tipin stabilize replication forks and facilitate sister-chromatid cohesion. *J Cell Sci*, **123**, 660-670.
312. Chan, R.C., Chan, A., Jeon, M., Wu, T.F., Pasqualone, D., Rougvie, A.E. and Meyer, B.J. (2003) Chromosome cohesion is regulated by a clock gene paralogue TIM-1. *Nature*, **423**, 1002-1009.
313. Krings, G. and Bastia, D. (2004) swi1- and swi3-dependent and independent replication fork arrest at the ribosomal DNA of Schizosaccharomyces pombe. *Proc Natl Acad Sci U S A*, **101**, 14085-14090.
314. Gomez-Gonzalez, B., Felipe-Abrio, I. and Aguilera, A. (2009) The S-phase checkpoint is required to respond to R-loops accumulated in THO mutants. *Mol Cell Biol*, **29**, 5203-5213.
315. Kops, G.J., Weaver, B.A. and Cleveland, D.W. (2005) On the road to cancer: aneuploidy and the mitotic checkpoint. *Nat Rev Cancer*, **5**, 773-785.
316. Sherman, F., Fink, G.R. and Hicks, J.B. (1986) *Methods in yeast genetics : a Cold Spring Harbor Laboratory course manual*. Cold Spring Harbor, N.Y.
317. Hanahan, D. (1983) Studies on transformation of Escherichia coli with plasmids. *J Mol Biol*, **166**, 557-580.
318. Longtine, M.S., McKenzie, A., 3rd, Demarini, D.J., Shah, N.G., Wach, A., Brachat, A., Philippsen, P. and Pringle, J.R. (1998) Additional modules for versatile and economical PCR-based gene deletion and modification in Saccharomyces cerevisiae. *Yeast*, **14**, 953-961.
319. Deshaies, R.J. (1999) SCF and Cullin/Ring H2-based ubiquitin ligases. *Annu Rev Cell Dev Biol*, **15**, 435-467.
320. Morawska, M. and Ulrich, H.D. (2013) An expanded tool kit for the auxin-inducible degron system in budding yeast. *Yeast*, **30**, 341-351.
321. Inoue, H., Nojima, H. and Okayama, H. (1990) High efficiency transformation of Escherichia coli with plasmids. *Gene*, **96**, 23-28.
322. Ito, H., Fukuda, Y., Murata, K. and Kimura, A. (1983) Transformation of intact yeast cells treated with alkali cations. *J Bacteriol*, **153**, 163-168.
323. Gietz, R.D., Schiestl, R.H., Willems, A.R. and Woods, R.A. (1995) Studies on the transformation of intact yeast cells by the LiAc/SS-DNA/PEG procedure. *Yeast*, **11**, 355-360.

324. Holmes, D.S. and Quigley, M. (1981) A rapid boiling method for the preparation of bacterial plasmids. *Anal Biochem*, **114**, 193-197.
325. Amberg, D.C., Burke, D. and Strathern, J.N. (2005) *Methods in yeast genetics : a Cold Spring Harbor Laboratory course manual*. Cold Spring Harbor, N.Y.
326. Prado, F. and Aguilera, A. (1995) Role of reciprocal exchange, one-ended invasion crossover and single-strand annealing on inverted and direct repeat recombination in yeast: different requirements for the RAD1, RAD10, and RAD52 genes. *Genetics*, **139**, 109-123.
327. Ide, S. and Kobayashi, T. Analysis of DNA replication in Saccharomyces cerevisiae by two-dimensional and pulsed-field gel electrophoresis. *Curr Protoc Cell Biol*, **Chapter 22**, Unit 22 14.
328. Matsui, A., Kamada, Y. and Matsuura, A. (2013) The role of autophagy in genome stability through suppression of abnormal mitosis under starvation. *PLoS Genet*, **9**, e1003245.
329. Laco, G.S. and Pommier, Y. (2008) Role of a tryptophan anchor in human topoisomerase I structure, function and inhibition. *Biochem J*, **411**, 523-530.
330. Naumov, G.I., Naumova, E.S., Lantto, R.A., Louis, E.J. and Korhola, M. (1992) Genetic homology between Saccharomyces cerevisiae and its sibling species S. paradoxus and S. bayanus: electrophoretic karyotypes. *Yeast*, **8**, 599-612.
331. Ulbrich, C., Diepholz, M., Bassler, J., Kressler, D., Pertschy, B., Galani, K., Bottcher, B. and Hurt, E. (2009) Mechanochemical removal of ribosome biogenesis factors from nascent 60S ribosomal subunits. *Cell*, **138**, 911-922.
332. Foiani, M., Marini, F., Gamba, D., Lucchini, G. and Plevani, P. (1994) The B subunit of the DNA polymerase alpha-primase complex in Saccharomyces cerevisiae executes an essential function at the initial stage of DNA replication. *Mol Cell Biol*, **14**, 923-933.
333. Kanellis, P., Agyei, R. and Durocher, D. (2003) Elg1 forms an alternative PCNA-interacting RFC complex required to maintain genome stability. *Curr Biol*, **13**, 1583-1595.
334. Alabert, C., Bianco, J.N. and Pasero, P. (2009) Differential regulation of homologous recombination at DNA breaks and replication forks by the Mrc1 branch of the S-phase checkpoint. *EMBO J*, **28**, 1131-1141.
335. Valerio-Santiago, M. and Monje-Casas, F. (2011) Tem1 localization to the spindle pole bodies is essential for mitotic exit and impairs spindle checkpoint function. *J Cell Biol*, **192**, 599-614.
336. Johnson, R.E., Henderson, S.T., Petes, T.D., Prakash, S., Bankmann, M. and Prakash, L. (1992) Saccharomyces cerevisiae RAD5-encoded DNA repair protein contains DNA helicase and zinc-binding sequence motifs and affects the stability of simple repetitive sequences in the genome. *Mol Cell Biol*, **12**, 3807-3818.
337. Domfield, K.J. and Livingstone, D.M. (1991) Effects of Controlled RAD52 Expression on Repair and Recombination in Saccharomyces cerevisiae. *Mol Cell Biol*, **11**, 2013-2017.
338. Reinke, A., Anderson, S., McCaffery, J.M., Yates, J., 3rd, Aronova, S., Chu, S., Fairclough, S., Iverson, C., Wedaman, K.P. and Powers, T. (2004) TOR complex 1 includes a novel component, Tco89p (YPL180w), and cooperates with Ssd1p to maintain cellular integrity in Saccharomyces cerevisiae. *J Biol Chem*, **279**, 14752-14762.